PROPAGATION AND GENERATION OF WAVES IN SOLAR ATMOSPHERE

by

SWATI ROUTH

Presented to the Faculty of the Graduate School of

The University of Texas at Arlington in Partial Fulfillment

of the Requirements

for the Degree of

DOCTOR OF PHILOSOPHY

THE UNIVERSITY OF TEXAS AT ARLINGTON

December 2009

ACKNOWLEDGEMENTS

ABSTRACT

PROPAGATION AND GENERATION OF WAVES IN SOLAR ATMOSPHERE

SWATI ROUTH, Ph.D.

The University of Texas at Arlington, 2009

Supervising Professor: Zdzislaw Musielak

The fact that the temperature increases with height in the solar atmosphere has been known for many years. To maintain this temperature increase, sources of heating must be present in the atmosphere. One of the most important, and still unsolved, problems in solar physics is to identify the basic physical processes that are responsible for this heating, and explain solar activities caused by the heating. It is also observationally well-established that the solar atmosphere shows a broad range of oscillations that are different in magnetic and non-magnetic regions of the atmosphere. The oscillations are driven by propagating waves, which cause the atmosphere to oscillate at its natural (cutoff) frequency. Since different waves have different cutoff frequencies, it is important to have a method that would allow determining such cutoffs for the solar atmosphere.

In this PhD dissertation, the concept of cutoff frequency is extended to inhomogeneous atmospheres, and a general method to determine the cutoff frequency is presented. The method leads to new forms of wave equations obtained for all wave variables, and allows deriving the cutoff frequency without formally solving the wave equations. The main result is that the derived cutoff frequency is a local quantity

and that its value at a given atmospheric height determines the frequency that waves must have in order to be propagating at this height. The developed method is general enough, so that it can be used to establish theoretical bases for studying the propagation and generation of different waves in the solar atmosphere.

Acoustic waves play an important role in the heating of magnetic-free regions of the solar atmosphere. To determine the propagation conditions for these waves in the non-isothermal solar atmosphere, the method is used to obtain the resulting acoustic cutoff frequency. This new cutoff frequency is a local quantity and it generalizes Lamb's acoustic cutoff frequency that was obtained for an isothermal atmosphere. The method is also used to extend Lighthill's theory of sound generated by turbulent motions, which was originally developed for a uniform medium, to the case when the background medium has a special temperature distribution. Basic equations describing the efficiency of the acoustic wave generation are derived and specific results are presented.

Magnetic regions of the solar atmosphere, identified here with magnetic flux tubes, are heated by longitudinal, transverse and torsional waves. If the tubes are isothermal, then the propagation of longitudinal and transverse tube waves is restricted to frequencies that are higher than the corresponding cutoff frequency for each wave. However, no such cutoff frequency exists for torsional tube waves. The results obtained in this PhD dissertation demonstrate that temperature gradients and other inhomogeneities of solar magnetic flux tubes lead to a significant modification of the cutoff frequency for transverse tube waves and to the origin of a new cutoff frequency for torsional tube waves. This new cutoff is used to determine conditions for the wave propagation in the solar atmosphere, and the obtained results are compared to the recent observational data that support the existence of torsional tube waves on the Sun.

TABLE OF CONTENTS

LIST OF FIGURES

CHAPTER 1

INTRODUCTION

The Sun is an average main-sequence star whose interior can be divided into three regions: the core, where the solar energy is produced, radiative zone, where the solar energy is transported mainly by radiation, and convection zone, where the energy transport is dominated by vigorous convective motions (see Fig. 1.1). The temperature reaches maximum in the core and then decreases gradually towards the solar photosphere, which is located above the solar convection zone and is the source of most of the solar energy needed to sustain life on the Earth. The temperature reaches minimum in the solar photosphere and then increases through the solar atmospheric layers called chromosphere, transition region and corona.

The solar chromosphere is a source of the prominent calcium and magnesium emission lines. There are also strong ultraviolet lines, which are formed in the solar transition region, and intense X-rays and the solar winds that originate in the solar corona. Moreover, each atmospheric layer supports oscillations of different periods and amplitudes. Despite the vast amount of solar data collected during numerous ground and space observations, and significant theoretical efforts, it is still unclear how different regions of the solar atmosphere are heated and why these regions support different atmospheric oscillations. Studies of the wave propagation and generation in the solar atmosphere presented in this PhD dissertation shed a new light on both the atmospheric heating problem and the existence of solar atmospheric oscillations.

The two spectral lines that dominate in the solar chromosphere are Ca II H+K and Mg II h+k emission lines and they are typically used to measure the level of
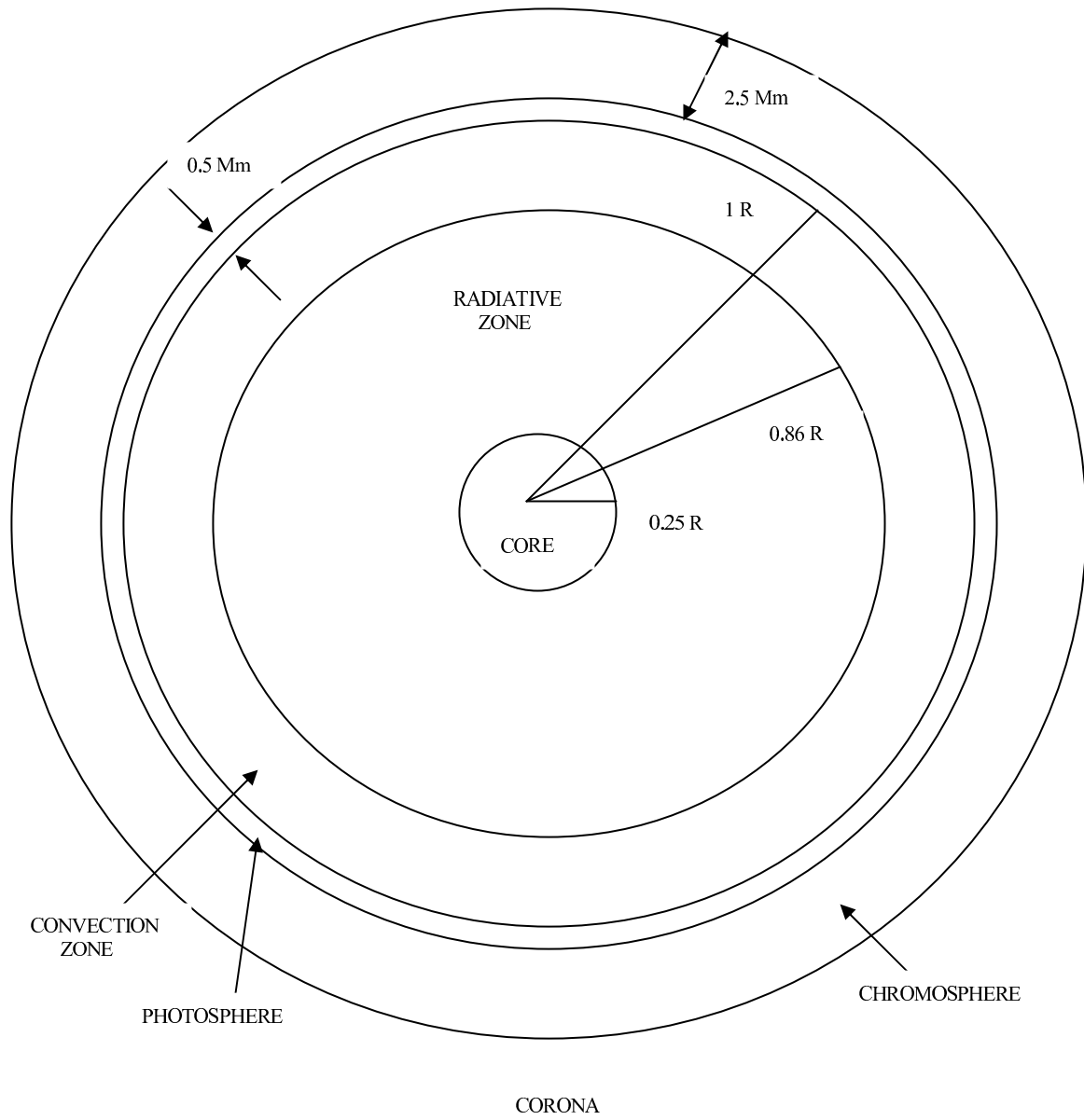
Figure 1.1. The overall structure of the Sun.

chromospheric activity (e.g., [1], [2]). Observations also show many UV lines that originate in the solar transition region and these lines are typically used to determine the level of transition region activity (e.g., [3], [2]). The solar corona is a source of X-ray emission, which is associated with coronal loops, and the solar wind that originates in solar coronal holes (e.g., [4], [5], [6]); the so-called coronal activity is identified with the observed level of X-ray emission.

To account for the observed emissions, a significant amount of non-radiative energy is needed to heat different regions of the solar atmosphere. A heat input of the order 2 x 10^7 ergs / cm^2 s and 1 x 10^6 ergs / cm^2 s is required for the solar chromosphere and transition region, respectively (e.g., [7], [1], [8]). The solar data also shows that the observed emission from magnetically active regions can be 10 (or more) times higher than that observed in quiet (weak magnetic field) regions (e.g., [1], [9], [2], [6]).

Observations have also demonstrated that the solar atmosphere is highly in-homogeneous and that the solar magnetic field plays dominate role in forming these inhomogeneities. The most prominent magnetic structures in the solar photosphere are sunspots and magnetic flux tubes (e.g., [10], [11], [12], [13], [14] , [6], [15]); these structures are often called active regions. In addition, there are also regions of weak (or no) magnetic fields and they are called quiet regions (e.g., [2]).

According to traditional view, the most prominent source of non-radiative energy needed to heat the solar atmosphere is the solar convection zone, where different waves are generated. These waves carry their energy through the photosphere and dissipate in the overlying atmosphere (e.g., [2], [6]). In magnetic-free regions, acoustic waves are likely to be responsible for the heating, however, in magnetic regions, where magnetic flux tubes dominate, longitudinal, transverse and torsional tube waves may significantly contribute to the heating (e.g., [16], [17], [18]).

To identify heating mechanisms in different parts of the solar atmosphere, theoretical and time-dependent models of the solar chromosphere were constructed ([19], [20], [21], [22], [23]). In these models acoustic waves were identified as sources of the heating of non-magnetic regions, and longitudinal and transverse tube waves as sources of the heating of magnetic flux tubes. The models were used to compute the resulting emissions in the Ca II and Mg II lines and the obtained results were compared to the observed level of chromospheric activity in late-type stars, including the Sun. Based on this comparison, it was concluded that acoustic and magnetic tube waves alone could not supply enough energy (¨heating gaps¨) to explain the observed Ca II and Mg II emissions in the upper layers of the solar atmosphere and in active solar-type stars. Clearly, additional sources of energy are needed.

One possibility is to account for the energy carried by torsional tube waves, which were not included in the above theoretical models. There is recent observational evidence for the existence of these waves on the Sun (e.g., [24], [25], [26]) and according to the authors, the amount of energy carried by the waves is sufficient to heat the solar corona. Another way of heating the solar atmosphere is by small magnetic loops that are being perpetually generated and then they very quickly disappear by releasing their energy through magnetic reconnection. These short-lived loops were detected by SOHO observations ([27], [9], [28]) and their energy content seems to be sufficient to heat the solar corona.

The main oscillations of the solar chromosphere are typically identified with 3-min oscillations. Observations of Ca II H and K, Hα, and the Ca II infrared triplet lines show that the 3-min chromospheric oscillations range from 2 to 5 min inside non-magnetic or weak magnetic regions (supergranulation cells), however, in magnetic regions located at the boundaries of supergranules (the magnetic network), the oscillations range from 6 to 15 min ([29], [30], [31], [32], [33], [34]). Detection of

oscillations in the solar transition region, coronal loops and coronal holes has provided evidence for the existence of waves in the upper regions of the solar atmosphere (e.g., [29], [35], [36], [37], [38], [39], [40], [34], [36], [41]). Recently, Jess et al. ([25]) detected oscillations in the solar atmosphere with periods ranging from 126 s to 700 s, and identified these oscillations as a signature of torsional waves propagating along expanding magnetic flux tubes.

It was first showed by [42], who used original Lamb's work ([43]), that the 3-min chromospheric oscillations could be explained as a response of the solar atmosphere to the propagating acoustic waves; the result is that the atmosphere oscillates at its natural (the acoustic cutoff) period (see also [44]). Acoustic waves with these periods are observed at all heights in the cell interior (e.g., [45], [46], [47]). In magnetic regions, the observed periods are typically interpreted as cutoff periods of waves propagating along magnetic flux tubes. Responses of magnetic flux tubes to the propagating longitudinal tube waves and pulses ([48]) and to the propagating transverse tube waves and pulses ([49], [50]) were also investigated.

Based on the above observational and theoretical results, there is an urgent need to establish theoretical bases for studying the propagation and generation of different waves in the solar atmosphere. Therefore, the main goal of this PhD dissertation is to develop a general theory to determine cutoff frequencies for different waves propagating in inhomogeneous media, and apply this theory to different wave motions observed in the solar atmosphere. Specific goals include calculating cutoff frequencies for acoustic waves propagating in the non-isothermal solar atmosphere (described by the VAL C model - see [51]) and for torsional and transverse waves propagating along non-isothermal (thin and thick) magnetic flux tubes, and extension of the original Lighthill theory of sound generation ([52], [53], [18]) to account for the temperature gradient effects. The results obtained in this PhD dissertation shed a new light

on the problem of heating and excitation of oscillations in the inhomogeneous solar atmosphere.

CHAPTER 2

WAVES IN THE SOLAR ATMOSPHERE: AN OVERVIEW

2.1 Propagation of Acoustic Wave

More than 100 years ago, Lamb ([43]) introduced a cutoff frequency for linear acoustic waves propagating in an isothermal and stratified medium, which he called an isothermal atmosphere. The cutoff frequency, defined as the ratio of sound speed to twice density (pressure) scale height, was obtained by solving the acoustic wave equation for the vertical displacement. The fact that the background medium is isothermal makes the cutoff frequency a global quantity that is the same in the entire medium. The cutoff is now known as the acoustic (or Lamb's) cutoff frequency; in this PhD dissertation, we shall refer to this cutoff as the global acoustic cutoff frequency.

The physical meaning of this cutoff is that the wave propagation is affected by the density gradient only when the wavelength is equal to, or longer than, the density scale height. Otherwise, the waves propagate freely in the medium because the cutoff frequency is global (the same in the entire medium) and, therefore, its effect on the wave propagation is the same at each atmospheric height. Lamb ([43]) also demonstrated that the waves are propagating only when their frequencies are higher than the cutoff, otherwise they are evanescent, and that the cutoff is the natural frequency of the atmosphere ([54]); the latter simply means that any acoustic disturbance imposed on the atmosphere would trigger an atmospheric response at the cutoff frequency ([55]).

Lamb ([43]) also considered a non-isothermal atmosphere with the temperature decreasing linearly with height, and studied the effects of this uniform temperature

7

gradient on the acoustic cutoff frequency. He was able to obtain analytical solutions
and determine the conditions for the acoustic wave propagation in the atmosphere.
Lamb's treatment of acoustic waves was extended to two dimensions (vertical and
horizontal) with a uniform vertical temperature gradient. The obtained analytical
solutions were used to establish the range of frequencies corresponding to the propa-
gating acoustic waves in this model ([54]).

In numerous studies of propagation of acoustic waves that followed Lamb's work,
different aspects of the wave propagation were investigated by using methods based
on either global and local dispersion relations, or the WKB approximation, or finding
analytical or numerical solutions to acoustic wave equations. The global dispersion
relation for acoustic waves can only be obtained when the background medium is
homogeneous ([56]) , or when gradients of the physical parameters of the medium do
not directly affect the speed of sound, like in Lamb's isothermal atmosphere (Sum-
mers 1976; Thomas 1983; Morse and Ingard 1986; Salomons 2002). There were also
attempts to justify the so-called local dispersion relation approach, which requires the
acoustic wavelength to be shorter than the characteristic scales over which the basic
physical parameters in the medium vary (e.g., Whitman 1974; Thomas 1983). The
latter requirement is known as the WKB approximation and many studies of acoustic
(and other) waves were performed by taking this approximation into account.

Analytical and numerical solutions of acoustic wave equations were obtained
for many different physical situations and the solutions were used to determine the
wave propagation conditions (Whitman 1974; Thomas 1983; Campos 1986). The
fact that the propagation conditions for acoustic waves in an isothermal atmosphere
can be determined by using the acoustic cutoff frequency was originally shown by

Lamb (1908, 1932). He also demonstrated that the cutoff is the natural frequency of the atmosphere, which means that propagating acoustic waves excite atmospheric oscillations with the frequency equal to the natural frequency (e.g., Schmitz and Fleck 1992, 1998).

The acoustic cutoff frequency plays an important role in helioseismology, which uses solar oscillations to determine the internal structure of the Sun (e.g., Brown et al. 1987), and in asteroseismology, which deals with oscillations of different stars (e.g., Hansen et al. 1985; Musielak et al. 2005). The cutoff has also been used to study free atmospheric oscillations of the Earth (Suda et al. 1998; Rhie and Romanowicz 2004) and other planets (Kobayashi and Nishida 1998), and acoustic oscillations of Jupiter (Deming et al. 1989; Lee 1993). Since planetary and stellar atmospheres are not isothermal, the acoustic cutoff frequency being a global quantity cannot formally be calculated for the entire atmosphere. Therefore, a typical approach is to evaluate the cutoff at each atmospheric height by using the local value of the temperature (e.g., Brown et al. 1987). This is rather a crude approximation, especially if there are steep temperature gradients in the atmosphere.

A method to determine the cutoff frequency for linear and adiabatic acoustic waves propagating in non-isothermal media without gravity was developed by Musielak et al. (2006). The method is based on transformations of wave variables that lead to standard wave equations, and it uses the oscillation theorem to determine the turning point frequencies. Then, physical arguments are used to select the largest of these frequencies as the acoustic cutoff frequency. In this PhD dissertation, the method is modified and extended to acoustic waves propagating in an non-isothermal atmosphere and other wave motions observed in the solar atmosphere.

2.1.1   Lamb's acoustic cutoff frequency

In his original work [1908,1910,1930], Lamb considered acoustic waves propagating in the z-direction in the background medium with the gravity $\vec{g} = -g\hat{z}$ and the density gradient $\rho_0(z) = \rho_{00}\exp(-z/2H)$, where ρ_{00} is the gas density at the height $z = 0$ and $H = c_s^2\gamma g$ is the density scale height, with γ being the ratio of specific heats and c_s being the speed of sound. In his model, the background gas pressure p_0 varies with height z, however, the temperature T_0 remains constant. As a result, $H = \text{const}$ and $c_s = \text{const}$. This stratified but otherwise isothermal medium is often referred to as an isothermal atmosphere because of its applications to the solar and stellar atmospheres. The waves are described by the following variables: velocity $u_1(t, z)$, pressure $p_1(t, z)$ and density $\rho_1(t, z)$ perturbations . Applying these assumptions to the standard set of linearized hydrodynamic equations [Morse and Ingard 1986], we write the continuity, momentum and energy equations as

$$\frac{\partial \rho_1}{\partial t} + \frac{\partial(\rho_0 u_1)}{\partial z} = 0, \tag{2.1}$$

$$\rho_0 \frac{\partial u_1}{\partial t} + \frac{\partial p_1}{\partial z} = 0, \tag{2.2}$$

$$\frac{\partial p_1}{\partial t} + u\frac{dp_0}{dz} - c_s^2\left(\frac{\partial \rho_1}{\partial t} + u\frac{d\rho_0}{dz}\right) = 0, \tag{2.3}$$

where the speed of sound is $c_s = [\gamma p_0/\rho_0(z)]^{1/2} = [\gamma R T_0(z)/\mu]^{1/2}$, with γ being the ratio of specific heats.

Using the aboe equations the acoustic wave equations for the wave variables $u_1(t, z)$, $p_1(t, z)$ and $\rho_1(t, z)$ become

$$\left[\frac{\partial^2}{\partial t^2} - c_s^2\,\frac{\partial^2}{\partial z^2} + \Omega_{ac}^2\right](u_1, p_1, \rho_1) = 0. \tag{2.4}$$

where the acoustic cutoff freqency $\Omega_{ac} = c_s/2H$. Note that the form of the wave equation is the same for each wave variable.

Since $\Omega_{ac} = $ const, one can make Fourier transforms in time and space and derive the global dispersion relation: $(\omega^2 - \Omega_{ac}^2) = k^2 c_s^2$, where ω is the wave frequency and $k = k_z$ is the wave vector. This shows that the waves are propagating when $\omega > \Omega_{ac}$ and k is real, and they are non-propagating when either $\omega = \Omega_0$ with $k = 0$ or $\omega < \Omega_0$ with k being imaginary; in the latter case, the waves are called evanescent waves.

Extension of Lamb's approach to non-isothermal atmosphere and the resulting new acoustic cutoff frequencies are described in Chapter 4.

2.2 Generation of Acoustic Wave

It is well-known that an unsteady turbulent flow generates pressure fluctuations in order to balance the fluctuations in momentum. Such pressure fluctuations propagate outward from their source as acoustic waves. Studies of these flow-generated acoustic waves have begun with Gutin's theory of propeller noise, which was develoed in 197. Yet, it was not untill 1952, when Lighthill introduced his acoustic analogy to deal with the problem of jet noise, that a general theory began to emerge.

A theory of acoustic wave generation by a turbulent jet embedded in an infinite homogeneous fluid was originally developed by Lighthill (1952, 1960) who showed that Reynolds stresses are sources of quadrupole emission. The theory allows evaluating the wave energy flux far away from a finite region of turbulence by assuming that the backreaction of generated waves on the turbulence is negligible. The main prediction of the theory is the now famous u^8 law of the acoustic power output by the turbulent

jet, where u is the jet velocity. Good agreements between this theoretical prediction and the results of several experiments performed for jets of different diameters have been found by Goldstein (1976). Lighthill's theory was extended to include the effects of solid boundaries by Curle (1955), Powell (1960), Ffowcs Williams and Hall (1970), and the effects of magnetic fields (e.g., Campos 1976, and references therein).

An important result was obtained by Proudman (1952) who described the turbulent motions in a jet by the Heisenberg turbulence energy spectrum (Heisenberg 1947) and derived a general formula for the generated acoustic power output. This Lighthill-Proudman formula was used to evaluate the acoustic wave energy fluxes generated by turbulent motions in the solar (Unno and Kawabata 1955; De Jager and Kuperus 1961; Kuperus 1965) and stellar (DeLoore 1970; Renzini et al. 1977; Böhm and Cassinelli 1971; Arcoragi and Fontaine 1980; Musielak 1982) convection zones, and to discuss the role played by acoustic waves in heating of stellar atmospheres (e.g., Narain and Ulmschneider 1996, and references therein).

As mentioned above, Lighthill's theory concerns only homogeneous media and treats turbulence as isotropic, homogeneous and decaying in time. A significant extension of Lighthill's theory was done by Stein (1967), who followed earlier work of Unno and Kato (1962), Unno (1964) and Moore and Spiegel (1964), and included the effects of stratification. This Lighthill-Stein theory allows calculating the acoustic wave energy spectra and its main result is that stratification is responsible for monopole and dipole sources of acoustic emission (Goldreich and Kumar 1988; Musielak et al. 1994). The theory was formally extended to include magnetic effects and applied to magnetic flux tubes that exist in the solar and stellar atmospheres (Musielak et al. 1989, 1995).

2.2.1 Lighthill's theory of sound generation

To describe the sound generation by a turbulent jet, Lighthill (1952, 1960) derived an inhomogeneous wave equation for a single wave variable by collecting all linear and nonlinear terms on the left-hand side (the propagator) and on the right-hand side (the source function) of the wave equation, respectively, and obtained

$$\hat{L}_s[\rho] = \hat{S}[T_{ij}(u_t)], \tag{2.5}$$

where $\hat{L}_s$ is the acoustic wave propagator given by

$$\hat{L}_s = \frac{\partial^2}{\partial t^2} - c_s^2 \nabla^2, \tag{2.6}$$

and ρ represents density perturbations associated with the waves, c_s is the speed of sound, u_t is the turbulent velocity, and $T_{ij}(u_t) = \rho_o u_{ti} u_{tj} + p_{ij} - c_s^2 \rho \delta_{ij}$ is Lighthill's turbulence stress tensor with i,j = 1,2 and 3, and ρ_o being the density of the background medium. Lighthill assumed that the jet was embedded in an uniform atmosphere, which was also at rest, and considered linear (weak) acoustic waves that produce no backreaction on the turbulent flow. He then showed that $T_{ij} \approx \rho_o u_{ti} u_{tj}$ and that the source function $\hat{S}[T_{ij}(u_t)]$ was given by a double divergence of T_{ij}. The physical meaning of the source function is that the stresses produce equal and opposite forces on opposite sides of a fluid element leading to the distortion of its surface without changing the volume (quadrupole emission). In other words, the fluid motions generating acoustic waves behave as a volume distribution of acoustic quadrupoles, so one may write $\hat{S}[T_{ij}(u_t)] = S_{quadrupole}$.

Proudman (1952) applied Lighthill's theory to the case when the fluctuating fluid motions are represented by the Heisenberg turbulence energy spectrum (Heisen-

berg 1947) and derived a general formula for the generated acoustic power output, P_a. This Lighthill-Proudman formula is usually given in the following form:

$$P_a = \alpha_q \frac{\rho_o u_t^3}{l_o} M_t^5, \tag{2.7}$$

where the emissivity coefficient $\alpha_q \approx 38$, l_o is the characteristic length scale of the turbulence and $M_t = u_t/c_s$ is the turbulent Mach number.

The formula is valid for subsonic turbulence ($M_t << 1$) and it was extensively used in early calculations of acoustic wave energy fluxes generated in the Sun and other stars (e.g., Kuperus 1965; Renzini et al. 1977; Arcoragi and Fontaine 1980). Since the formula does not account for temperature gradients, it was assumed that Eq. (2.7) was satisfied locally in the turbulent region and the total emitted wave energy flux was calculated by performing the integration over the thickness of that region.

In all the above applications of Lighthill's and Lighthill-Stein's theory of sound generation, the background medium was assumed to be isothermal. Therefore, One of the main aims of this dissertation is to extend Lighthill's theory to a non-isothermal medium. The problem is inherently difficult, so a simple temperature model that allows for analytical solutions will only be considered (see Chapter 5).

2.3 Propagation of MHD Waves

2.3.1 Basic MHD equation

Magnetohydrodynamics (MHD) is the study of highly conducting fluids in the presence of magnetic fields. It has broad applications in laboratory plasmas, magnetospheric physics, space physics and astrophysics.

The basic set of MHD equations is derived from conservation laws (i.e., conservation of mass, momentum and energy) in conjunction with Maxwell's equations. The main assumptions of MHD are well summarized by Priest (1982):

- The characteristic length scales are much greater than those of the plasma.
- The characteristic time scales are much greater than the particle collision time scales.
- Plasma properties are isotropic.
- The characteristic speeds are much smaller than the speed of light, so that relativistic effects can be neglected.

We further assume that the fluid is isentropic and isothermal, that the gas pressure is a scalar, and that the displacement currents and electrostatic forces may be neglected; the molecular viscosity and Ohmic diffusion is negligible as long as shock formation does not occur. Our assumption leads to the following perfect fluid, ideal MHD equations (e.g., Parker 1979; Priest 1983):

Continuity equation:

$$\frac{d\rho}{dt} + \rho\nabla \cdot \mathbf{u} = 0, \tag{2.8}$$

Momentum equation:

$$\rho\frac{d\mathbf{u}}{dt} + \nabla p - \rho\mathbf{g} - \frac{1}{4\pi}\left(\nabla \times \mathbf{B}\right) \times \mathbf{B} = 0, \tag{2.9}$$

Induction equation:

$$\frac{\partial \mathbf{B}}{\partial t} - \nabla \times \left(\mathbf{u} \times \mathbf{B}\right) = 0, \tag{2.10}$$

with the solenoidal condition:$\nabla \times B = 0$; where we have used Ohm's law $vecE + \vec{u} \times \vec{B} = 0$. Energy equation:

$$\frac{\partial p}{\partial t} + \mathbf{u} \cdot \nabla p_0 - c_s^2 \left(\frac{\partial \rho}{\partial t} + u\rho_0^{'} \right) = 0, \qquad (2.11)$$

where $\frac{d}{dt} = \frac{\partial}{\partial t} + \vec{u} \cdot \nabla$ and $c_s = \sqrt{\gamma RT/\mu}$ is the speed of sound in the medium. After linearization, these equations describe propagation of MHD fast, slow and Alfvén waves.

2.3.2 MHD Fast, Slow and Alfvén Waves

The behavior of linear MHD waves propagating in a homogeneous medium with a uniform magnetic field of arbitrary direction is presently well-understood. In this case, there are three types of MHD modes: fast, slow and Alfven waves. In general, fast and slow MHD waves (also called magnetoacoustic waves) have both longitudinal and transverse components, however, Alfven waves are associated only with purely transverse motions (e.g., Priest 1982). Analysis of the group velocity of magnetoacoustic waves shows that the energy propagation of fast MHD waves is almost independent of the direction (similar to the phase velocity) and that, in contrast, slow MHD waves have the striking property that the wave energy associated with their propagation is always carried within a small angle with respect to the background magnetic field. For Alfven waves the associated wave energy propagates only along the magnetic field line direction.

Since slow and Alfven MHD waves transfer energy primarily along the magnetic field lines, the waves may be used to explain the observed association between the enhanced local heating of the solar atmosphere and the enhanced magnetic field strength. Extensive discussions of the role played by these MHD waves in the solar

atmosphere can be found in early papers written by Kulsrud (1955), Osterbrock(1961) and Parker (1964), as well as in Priest (1982) and Collins (1989a, b). However, the assumptions of uniform magnetic fields and uniform background media are inconsistent with the solar data (Stenflo 1978; Saar 1987; Solanki 1993) which show highly inhomogeneous structures in the observable part of the solar atmosphere. As a result, a simple wave treatment of MHD waves propagating in uniform media has very limited applications to the solar atmosphere (see Narain and Ulmschneider 1996).

To study the propagation of MHD waves in a stratified and magnetized medium some authors have used a local dispersion relation, in which stratification is introduced via the use of local cutoff frequencies (see Thomas 1983, and Campos 1987, and references therein). In general, this approach can be justified either when the vertical wavelength is much smaller than the atmospheric characteristic scale heights (the WKB approximation) or when a very special distribution of the atmospheric parameters is assumed (Nye and Thomas, 1974). Thomas (1983) and Musielak (1990) discussed some restrictions on the validity of local dispersion relations, and showed that some results previously obtained were outside the range of validity of this approach; in particular, they demonstrated that some cutoff frequencies were incorrectly calculated.

A number of authors have considered the propagation of linear Alfven waves in an inhomogeneous solar atmosphere assuming specific forms of inhomogeneity for which full analytical solutions to the Alfven wave equations can be found (Ferraro and Plumpton 1958; Hollweg 1978; Leroy 1978; Heinemann and Olbert 1980; Rosner, Low and Holzer 1986). For an isothermal, hydrostatic, plane-parallel atmosphere with constant magnetic field, the obtained solutions have been used to demonstrate that Alfven waves are reflected and that the region where reflection is strong can be

determined from the condition that the wave frequency is smaller than the local cutoff frequency for these waves (Rosner, Low and Holzer 1986; An et al. 1989, 1990). A new analytical approach for assessing the reflection of linear Alfven waves in smoothly nonuniform media has been presented by Musielak, Fontenla and Moore (1992); see also Musielak, Musielak and Mobashi (2006).

2.3.3 Solar magnetic flux tubes

The magnetic fields in astrophysical situations are often quite inhomogeneous, due to the fact that they are embedded in highly turbulent fluids. In the case of the solar convection zone observations of the surface show fields ( ) which are essentially discrete, i.e. consisting of individual strands separated by field free fluid. Theoretical calculations of the behavior of fields in turbulent media support the idea that the field gets concentrated into a small fraction of the volume within a few turnover times of the turbulent eddies (Kraichnan ,1976, Spruit, 1981).This is especially the case if the back-reaction of the field on the flow is taken into account(e.g. Peckover and Weiss,1978, Spruit, 1981). To study the behavior of such complicated field, one needs approximations. Weak inhomogeneities can be treated as perturbations of a homogeneous field. The very strong inhomogeneity often encountered suggests an opposite point of view to consider the field as existing of discrete structures separated by field free regions. We will call these structures the "magnetic flux tubes".

Discrete flux tubes are found in many different forms on the Sun. Sunspots are present where a large 3000 Gauss flux tube breaks through the surface, typically in pairs with the tube coming up through one spot and going back down through

$$\Phi_B = \int \vec{B}.d\vec{S}$$
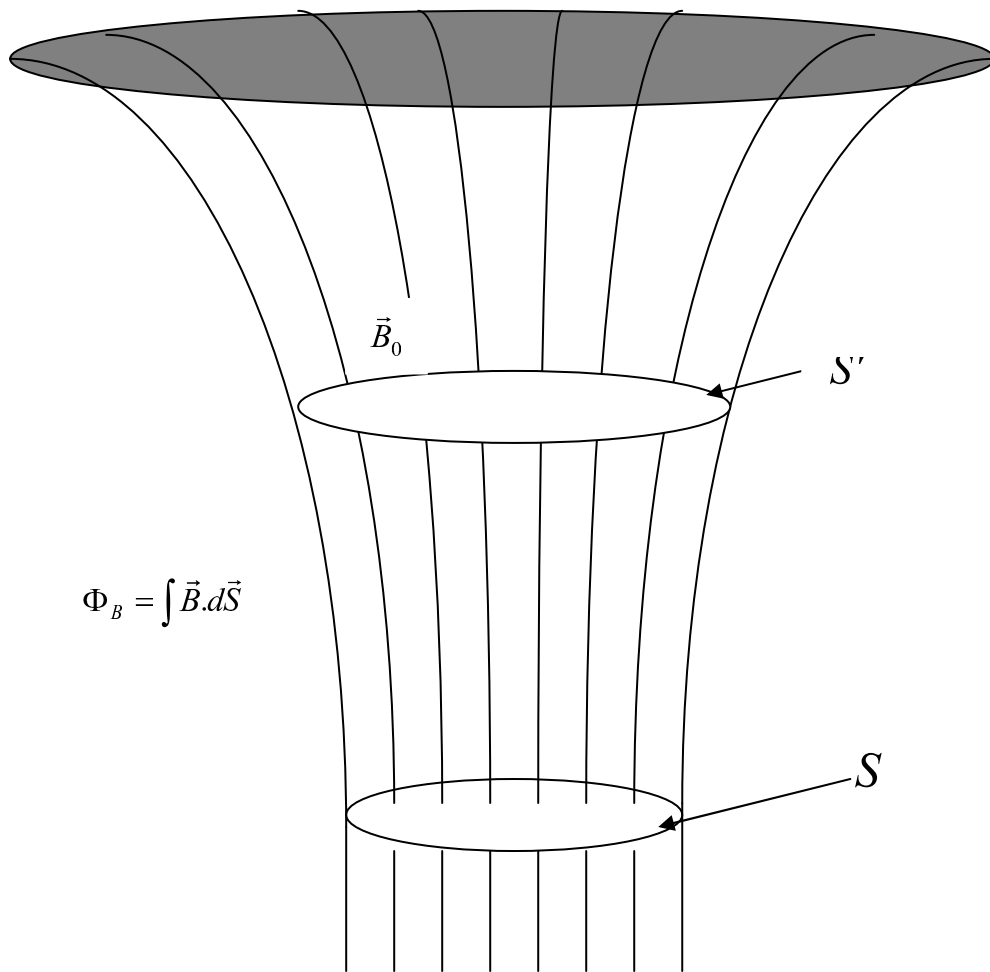
Figure 2.1. The structure of a magnetic flux tube.

the other. Also a spot (of typical diameter 20 Mm) is suggestive that it may itself consist of many smaller tubes. In the chromosphere above a sunspot pair one sees fibril structures joining one spot to the other and presumably outlining the magnetic field. In photospheric magnetic field maps one finds that, outside the active regions surrounding sunspot groups, the solar surface is covered with a fragmentary network structure consisting of many tiny flux tubes at the boundaries of large convection cells (the supergranulation).These tubes are a few hundred kilometers across and have a field strength of about 1500 Gauss.

The solar corona is seen in soft X-rays to consist of myriads of flux loops, both outside active regions and also within an active region. Hot flux loops (10^7 K) may also be created by large solar flares which subsequently cool to give an arcade of cool loops joining the two ribbons which make up the flare in its main phase in the chromosphere. Solar prominences are huge vertical sheets of plasma up in the corona but with a density a factor of a hundred higher and a temperature a factor of a hundred lower than the surrounding coronal plasma. Occasionally they loose equilibrium and erupt outwards when they undergo a metamorphosis and take on the appearance of a large twisted flux tube.

Parker (1955) suggested that an isolated horizontal flux tube in the solar interior would tend to rise by so-called magnetic buoyancy. The argument is very simple. If a tube is in lateral equilibrium with its field-free surroundings having a plasma pressure p_e , then its internal pressure p_0 and magnetic field B_0 satisfy

$$p_0 + B_0^2/2\mu = p_e, \tag{2.12}$$

or if the temperature T is uniform,

$$RT\rho_e = RT\rho_0 + \frac{B_0^2}{2\mu}. \tag{2.13}$$

Thus $\rho_e > \rho_0$ and the plasma in the tube experiences a buoyancy force, which exceeds the magnetic tension if $(\rho_e - \rho_0)g > B_0^2/\mu L$, where L is the length of tube which is curved upwards. After substituting for $(\rho_e - \rho_0)$ from (??) this condition becomes $L > 2H$ where $H = RT/g$ is the scale height.

If such a large flux tube in the interior rises and breaks through the surface it will form a pair of sunspots. In practice, the unbalanced force would make flux tubes rise much faster than a solar cycle period and so it is thought that the flux tubes are created by dynamo action not throughout the convection zone but only at

its base. Most of the flux tubes which penetrate the solar surface are thought to be almost vertical due to magnetic buoyancy. A whole hierarchy of such tubes exists from the tiniest, only one to two hundred kilometers across, to enormous sunspots with a diameter of thirty Megameters (Zwaan, 1978; Roberts, 1989).

A basic problem is to determine the structure of such a tube (its pressure p_0, density ρ_0, field B_0 and radius r) as a function of height (z). As the external pressure and density fall off in value with height, so the internal field strength tends to decrease and the tube spreads out(as the radius r increases). One needs to solve the equilibrium condition

$$-\nabla\left(p_0 + B_0^2/2\mu\right) + (\vec{B_0} \cdot \nabla)\frac{\vec{B_0}}{\mu} + \rho_0\vec{g} = 0 \tag{2.14}$$

inside the tube together with the hydrostatic equilibrium equation $dp_e/dz = \rho_e g$ outside and a pressure matching condition $p_0 + B_0^2/2\mu = p_e$ on the surface S of the tube. For a thin tube with $p_0 \propto p_e \propto e^{z-/H}$ pressure balance gives $B^2 \propto e^{-z/H}$ and so the tube radius expands exponentially like $r \propto e^{z/4H}$.

A very simplified model of the field is obtained, if one assumes that the flux tube is narrow enough. They are supposed to be so thin that they are always in pressure balance with their surroundings, and such that their diameter changes only slowly along their length. This approximation is certainly not valid for sunspots, but it is reasonable for the small elements of which the field outside of sunspots consists. Assuming the internal field is also nearly uniform across the cross section of the tube, the field can then be characterized by one value B, which depends on depth only. As we assume that there are no forces except gravity acting on the gas in the interior, the vertical balance of forces is then given by $dp_0/dz = \rho_0 g$ and the horizontal balance by$p_0 + B_0^2/2\mu = p_e$. It is also assumed that at each depth inside temperature T is

equal to the external temperature T_e .We also assume that viscosity and resistivity are negligible and that the motion is adiabatic (ideal MHD limit).

Three different types of waves can be supported by these flux tubes, namely, longitudinal, transverse and torsional tube waves (see [57], [58]). Longitudinal (sausage) tube waves are similar to slow MHD waves in the low-beta plasma limit. Transverse (kink) tube waves are similar to Alfvén MHD waves. Torsional tube waves have no analogy to MHD waves. Different aspects of the wave propagation and the energy deposition by these tube waves in the solar atmosphere were studied analytically and numerically by many authors (e.g., Hollweg 1978, 1981, 1990, 1992; Spruit 1981, 1982; Ferriz-Mas, Schüssler, and Anton 1989; Ferriz-Mas and Schüssler 1994; Kudoh and Shibata 1999; Saito, Kudoh and Shibata 2001; Hasan et al. 2003; Noble, Musielak and Ulmschneider 2003; Musielak, Routh, and Hammer 2007; Routh, Musielak and Hammer 2007) and discussed in many reviews, including Hollweg (1985), Roberts (1991), Narain & Ulmschneider (1996), Roberts and Ulmschneider (1997), Ulmschneider and Musielak (2003), and Hasan (2008).

2.3.4 Longitudinal Tube Waves

Defouw ([59]) considered an isolated magnetic flux tube embedded in a magnetic field-free compressible and isothermal medium. The tube is assumed to be thin, untwisted, and oriented vertically, with circular cross-section, and in temperature equilibrium with its surroundings. He chose a cartesian coordinate system with z axis along the tube axis and gravity $\vec{g} = -g\hat{z}$, where $\hat{z}$ is the unit vector along the z-axis. Because of the thin tube approximation the magnetic field inside the tube is

given by $\vec{B}_0 = B_0\hat{z}$. Magntic flux conservation and horizontal pressure balance lead to an exponentially spreading tube geometry.

The wave mode considered is similar to a sound wave propagating along the tube. However, the wave differs from an ordinary sound wave because the cross-section of the flow channel provided by the magnetic field varies in response to the pressure fluctuations of the tube wave. To describe the wave or pulse in the tube model, the velocity perturbation $\vec{v} = v_z(z,t)\hat{z}$, the magnetic field perturbation $\vec{b} = b_z(z,t)\hat{z}$, the density perturbation $\rho = \rho(z,t)$, and the pressure perturbation $p = p(z,t)$ have been introduced. Then after linearizing the basic MHD equations and applying the thin flux tube approximation the wave equation for the velocity perturbation was (e.g., Musielak et al. 1989)

$$\frac{\partial^2 v_z}{\partial t^2} - c_T^2 \frac{\partial^2 v_z}{\partial z^2} + \frac{c_T^2}{2H}\frac{\partial v_z}{\partial z} + \frac{c_T^2}{H^2}\left(\frac{1}{2} - \frac{1}{2\gamma} + \frac{c_s^2}{c_A^2}\frac{\gamma-1}{\gamma^2}\right) = 0, \qquad (2.15)$$

where the tube velocity is given by $c_T = \frac{c_s c_A}{\sqrt{c_s^2+c_A^2}}$, and $c_s = \gamma p_0/\rho_0$ is the sound speed, $c_A = B_0/\sqrt{4\pi\rho_0}$ the Alfven velocity and H is the pressure scale height. The tube velocity c_T is constant and the form of the wave equation is same for every wave variable.

To cast the above wave equation in the form of a Klein-Gordon equation, introduce $v_z(z,t) = v(z,t)\sqrt{B_0/\rho_0}$ and obtain (Musielak et al.,2003)

$$\left[\frac{\partial^2}{\partial t^2} - c_T^2\frac{\partial^2}{\partial z^2} + \Omega_T^2\right]v(z,t) = 0, \qquad (2.16)$$

where Ω_T is the cutoff frequency for longitudinal tube waves (Defow 1976):

$$\Omega_T = \frac{c_T}{H}\left(\frac{9}{16} - \frac{1}{2\gamma} + \frac{c_s^2}{c_A^2}\frac{\gamma-1}{\gamma^2}\right)^{1/2}, \qquad (2.17)$$

which is the frequency of the free atmospheric oscillation inside the magnetic flux tube. Longitudinal waves are propagating if their frequency $\omega > \Omega_T$, otherwise

they are evanescent. The method described above was origianlly introduced by ([60] and Musielak et al. ([61]), who demonstrated that the wave equation for these waves can be transformed into its standard form (also referred to as the Klein-Gordon equation), which directly displays the global cutoff frequency.

The role played by these waves in the heating of different parts of the solar and stellar atmospheres was discussed by Narain and Ulmschneider ([16]) and Ulmschneider and Musielak ([17]). The energy carried by sausage waves was used as the input to the theoretical models of stellar chromospheres constructed by Cuntz et al. ([20]) and Fawzy et al. ([22], [23]).

2.3.5 Transverse Tube Waves

The fact that the propagation of transverse waves along a thin and isothermal magnetic flux tube is affected by a cutoff frequency was originally shown by Spruit ([57], [58]); as a result, we refer to this cutoff as Spruit's cutoff frequency.

Here we show an alternative approach to derive Spruit cutoff. In the limit of a thin and isothermal magnetic flux tube for which $c_k = $ const and $H = $ const, the wave equation for wave variables v and $b$can be written as

$$\frac{\partial^2 v}{\partial t^2} - c_k^2 \frac{\partial^2 v}{\partial z^2} + \frac{c_k^2}{2H} \frac{\partial v}{\partial z} = 0, \tag{2.18}$$

and

$$\frac{\partial^2 b}{\partial t^2} - c_k^2 \frac{\partial^2 b}{\partial z^2} - \frac{c_k^2}{2H} \frac{\partial b}{\partial z} = 0, \tag{2.19}$$

where $c_k = B_0 / \sqrt{4\pi(\rho_0 + \rho_e)}$ is the transverse wave velocity. Since the wave equations for v and b are different, two different transformations are needed to remove the terms with the first-order derivatives from these equations. The transformations are

$v(z,t) = \tilde{v}(z,t)\rho_0^{-1/4}(z)$ and $b_x(z,t) = b(\tilde{z},t)\rho_0^{1/4}(z)$, and the resulting wave equations become

$$\left[\frac{\partial^2}{\partial t^2} - c_k^2 \frac{\partial^2}{\partial z^2} + \Omega_S^2\right] [\tilde{v}(z,t), \tilde{b}(z,t)] = 0, \tag{2.20}$$

where $\Omega_S = \frac{c_k}{4H}$.

Since the critical frequency Ω_S is independent of z, there is no need to use the oscillation theorem and determine the turning-point frequency (see Sec. 3 and 4). The cutoff frequency is simply given by $\Omega_{cut} = \Omega_S = $ const.

Having $c_k = $ const and $\Omega_{cut} = $ const, we can make Fourier transforms in time and space and derive the global dispersion relation: $(\omega^2 - \Omega_{cut}^2) = k^2 c_k^2$, where ω is the wave frequency and $k = k_z$ is the wave vector along the tube axis. Using this dispersion relation, it is easy to show that Ω_{cut} is the global cutoff frequency for transverse tube waves. According to the dispersion relation, the waves are propagating when $\omega > \Omega_{cut}$ and k is real, and that they are non-propagating when either $\omega = \Omega_{cut}$ with $k = 0$ or $\omega < \Omega_{cut}$ with k being imaginary; in the latter case, the waves are called evanescent waves. Studies of transverse tube waves performed in this PhD dissertation and new obtained results are presented in Chapter 7.

2.3.6 Torsional Tube Waves

Propagation of torsional Alfvén waves along solar and stellar magnetic flux tubes was extensively studied in the literature (e.g., [10], [11], [9],[62], [63], [64], [65], [66], [39], [66], [67]). Two different approaches were considered and different sets of wave variables were used. In the first approach, the propagation of the waves was described in a global coordinate system (e.g., [64], [67]), while in the second

approach a local coordinate system was used ([68], [69], [62]). The momentum and induction equations derived by Ferriz-Mas et al. ([64]) were adopted by Ploner and Solanki (1999) in their studies of the influence of torsional tube waves on spectral lines formed in the solar atmosphere. In numerical studies of torsional tube waves performed by Kudoh and Shibata ([36]) and Saito, Kudoh, and Shibata ([40]), the basic equations originally derived by Hollweg were extended to more than one dimension and nonlinear terms were included.

The specific problem of the existence or non-existence of a cutoff frequency for torsional Alfvén waves propagating along thin and isothermal magnetic flux tubes has not been discussed in the literature. An exception is the paper by Noble et al.([67]), who studied the generation rate of torsional tube waves in the solar convection zone and introduced the cutoff frequency, defined as the ratio of the Alfvén velocity to four times the pressure (or density) scale height, for these waves. In chapter 6, we revisit the problem by deriving new wave equations that describe the propagation of torsional tube waves and demonstrating that this propagation is cutoff-free. We also show that the cutoff-free propagation is independent of different choices of wave variables and coordinate systems used by Ferriz-Mas et al. ([22], [23]) and Hollweg ([68], [69], [62], [63], [70]). Torsional tube waves are extensively studied in this PhD dissertation and new obtained results are presented in Chapter 6.

CHAPTER 3

A GENERAL METHOD TO DETERMINE CUTOFF

FREQUENCIES IN INHOMOGENEOUS MEDIA

3.1 Introduction

The fact that global cutoff frequencies play an important role in establishing criteria for propagation of different waves in media with such gradients of physical parameters that do not affect the characteristic speeds of the waves has been well-known. Among the cases discussed in Chapter 2, the global cutoff frequencies derived for acoustic waves by Lamb (1908), and for longitudinal and transverse tube waves by Defouw (1976) and Spruit (1981), respectively, are very relevant to studies of the waves in the isothermal solar atmosphere. The behavior of torsional waves is different as their propagation along a thin and isothermal flux tube is cutoff-free, which has important implications for the required heating of the solar atmosphere (Musielak, Routh and Hammer 2007).

In the realistic solar atmosphere, gradients of temperature, density and magnetic field are present and they strongly affect the wave propagation. The global cutoff frequencies previously obtained with the assumption of the isothermal atmosphere must be replaced by new (local) cutoff frequencies that correctly account for the gradients in the solar atmosphere. A method that allows deriving such local cutoff frequencies was originally introduced by Musielak et al. (2006). The method is based on integral transformations that are used to transform wave equations into their standard forms (also known as Klein-Gordon equations), uses the oscillation and

turning-point theorems to determine the turning-point frequencies, and shows how to uniquely obtain the cutoff frequency.

Although Klein-Gordon equations, first introduced to solar physics by Roberts (1981), were used to study the propagation of longitudinal (Rae and Roberts 1982), transverse (Musielak and Ulmschneider 2001) and torsional (Noble et al. 2003) tube waves, and the oscillation theorem was first used by Schmitz and Fleck (1998) in their studies of the acoustic wave propagation in the solar atmosphere, none of these approaches can be considered as a general method to determine cutoff frequencies in inhomogeneous media. As already mentioned above, first such method was introduced by Musielak et al. (2006) and applied to acoustic waves propagating in an non-isothermal medium. In this PhD dissertation, the method is generalized so it can be applied to any linear waves propagating in an inhomogeneous media, which include different wave motions observed in the non-isothermal solar atmosphere.

3.2   Wave equation

A wave equation describing linear waves propagating in a medium, which is inhomogeneous in the z-direction, can be written in the following general form:

$$\frac{\partial^2 \psi}{\partial t^2} - V^2(z)\frac{\partial^2 \psi}{\partial z^2} + P(z)\frac{\partial \psi}{\partial z} + Q(z)\psi = 0 \ , \tag{3.1}$$

where V is the wave velocity and P and Q are given in terms of wave speeds and atmospheric scale heights, and their derivatives.

3.3   Transformed wave equation

Let us begin with the begin the transformation $d\tau = dz/V$ and write the above wave equation as

$$\left[\frac{\partial^2}{\partial t^2} - \frac{\partial^2}{\partial \tau^2} + \left(\frac{p}{V} + \frac{V'}{V}\right)\frac{\partial}{\partial \tau} + q\right]\psi(\tau,t) = 0 \ , \tag{3.2}$$

where $V' = dV/d\tau$.

To remove the first order derivatives with respect to τ from this wave equation, we use

$$\psi(\tau,t) = \phi(\tau,t)\exp\left[\frac{1}{2}\int^\tau\left(\frac{p}{V} + \frac{V'}{V}\right)d\tilde{\tau}\right] \ , \tag{3.3}$$

and obtain the following Klein-Gordon equation

$$\left[\frac{\partial^2}{\partial t^2} - \frac{\partial^2}{\partial \tau^2} + \Omega_{cr}^2(\tau)\right]\phi(\tau,t) = 0 \ , \tag{3.4}$$

where

$$\Omega_{cr}^2(\tau) = \frac{3}{4}\left(\frac{V'}{V}\right)^2 - \frac{1}{2}\frac{V''}{V} + \frac{1}{4}p^2V^2 + \frac{pV'}{V^2} - \frac{p'}{2V} + q \ , \tag{3.5}$$

with $V'' = d^2V/d\tau^2$. Ω_{cr} is the critical frequency (Musielak, Fontenla, & Moore, 1992; Musielak et al. 2006; Routh et al. 2007).

Making the Fourier transform in time (but not in space because the coefficients are not constant in space) $[v(\tau,t), b(\tau,t)] = [\tilde{v}(\tau), \tilde{b}(\tau)]e^{-i\omega t}$, where ω is the wave frequency, we obtain

$$\left[\frac{\partial^2}{\partial \tau^2} + \omega^2 - \Omega_{cr}^2(\tau)\right]\tilde{\phi}(\tau) = 0 \ . \tag{3.6}$$

The next step of the method is to apply the oscillation and turning-point theorems. In the following, we state these theorems without proofs.

3.4 Oscillation and turning point theorems

Oscillation theorem: Consider an ordinary differential equation of the form:

$$\frac{d^2y_1}{dx^2} + A(x)\, y_1 \ = \ 0 \ , \tag{3.7}$$

which is known to have all of its solutions to be oscillatory. Assume that there is another equation of the form:

$$\frac{d^2 y_2}{dx^2} + B(x)\, y_2 \;=\; 0\;,\tag{3.8}$$

where $B(x) > A(x)$ for all x. Then, all of the solutions of Eq. (3.8) are also oscillatory. The proof of this powerful theorem that gives a condition for the existence of oscillatory solutions is simple and available in the literature (e.g., Kahn 1990).

Turning-point theorem: Consider an ordinary differential equation of the form:

$$\frac{d^2 y_1}{dx^2} + A(x)\, y_1 \;=\; 0\;,\tag{3.9}$$

which is known to have a turning point that separates the oscillatory and non-oscillatory solutions. If there is another equation of the form:

$$\frac{d^2 y_2}{dx^2} + B(x)\, y_2 \;=\; 0\;.\tag{3.10}$$

then a turning point of this equation can be determined from the condition $B(x) = A(x)$.

The proof is trivial since the condition requires that the equations are the same.

3.5   Euler's equation and its turning point

In general, Euler's equation (e.g., Murphy 1960) can be written as

$$\frac{d^2 y}{dx^2} + \frac{C_E}{4x^2} y = 0\;,\tag{3.11}$$

where C_E is a constant whose value determines the form of the solution. For $C_E > 1$, the equation has oscillatory solutions, however, the solutions become non-oscillatory when $C_E < 1$, and finally for $C_E = 1$ there is a turning point, which separates these two distinct types of solutions.

After making the Fourier transform in time, we obtain

$$\frac{d^2 Y_i}{dx^2} + \left[\omega^2 - \Omega_i^2(x)\right] Y_i = 0 \ , \tag{3.12}$$

where the form of the critical frequencies $\Omega_i^2(x)$, with $i = 1$ and 2, may be different for different wave variables and for different models.

Comparing Eqs (3.11) and (3.12), and using the oscillation theorem, it can be shown that the wave equations given by Eq. (3.12) have oscillatory wave solutions when the condition $[\omega^2 - \Omega_i^2(x)] > 1/4x^2$ is valid for all x.

The turning point theorem can also be used to show that the wave equations have turning points when the condition $[\omega^2 - \Omega_i^2(x)] = 1/4x^2$ is satisfied for all x.

3.6 Turning-point frequencies

Applying the oscillation and turning-point theorems, the following turning-point frequencies are obtained

$$\Omega_{tp,\tau}^2(\tau) = \Omega_{cr}^2(\tau) + \frac{1}{4\tau^2} \ , \tag{3.13}$$

where

$$\tau(z) = \int^z \frac{d\tilde{z}}{V(\tilde{z})} + \tau_C \ , \tag{3.14}$$

with τ_C being an integration constant to be evaluated when models are specified (see Chapters 5-7. According to Eq. (7.101), the variable $\tau(z)$ is the actual wave travel time $t_w(z)$ from the base of a model to a given height z.

3.7 The cutoff frequency

The turning-point frequencies separate the solutions into propagating and non-propagating (evanescent) waves. Since there is a turning-point frequency for each

wave variable, only one of them can be the cutoff frequency. We follow Musielak et al. (2006) and Routh et. al. (2007), and identify the largest turning-point frequency as the cutoff frequency. The choice is physically justified by the fact that in order to have propagating waves at a given height z, the wave frequency ω must always be higher than any turning-point frequency at this height; note that as a result of this choice both wave variables are always described by the propagating wave solutions.

The main result of the method is the cutoff frequency, which is a local quantity and its value at a given atmospheric height determines the frequency that waves must have in order to be propagating at this height. The developed method is general enough, so that it can be used to establish theoretical bases for studying the propagation and generation of different waves in the solar atmosphere.

CHAPTER 4
PROPAGATION OF ACOUSTIC WAVES
IN NON-ISOTHERMAL ATMOSPHERE

As already discussed in Chapter 2, the acoustic cutoff frequency was originally introduced by Lamb (1908), who studied propagation of acoustic waves in an isothermal atmosphere and defined the cutoff as the ratio of sound speed to twice density (pressure) scale height. In Lamb's approach, the cutoff is a global quantity (the same in the entire medium) and its value determines the range of frequencies for which the waves are either propagating or evanescent. Lamb (1908) also considered a non-isothermal atmosphere with the temperature decreasing linearly with height, and studied the effects of this uniform temperature gradient on the acoustic cutoff frequency. He was able to obtain analytical solutions and determine the conditions for the acoustic wave propagation in the atmosphere

In many studies that followed Lamb's work (see Chapter 2), the authors either used the WKB approximation or considered an non-isothermal atmosphere and evaluated the global cutoff frequency at each atmospheric height by using the local value of the temperature. This is rather a crude approximation, especially if there are steep temperature gradients in the atmosphere. We now use the method described in Chapter 3 to generalize Lamb's results and obtain the local acoustic cutoff frequency that properly describes the propagation of acoustic waves in the non-isothermal atmosphere.

4.1 Acoustic wave equations

Let us consider a one-dimensional atmospheric model in which gradients of density, temperature and pressure occur along the z-axis that is also the direction of the wave propagation. Propagation of linear and adiabatic acoustic waves in this model is described by the standard set of linearized and one-dimensional hydrodynamic equations written as

$$\frac{\partial \rho}{\partial t} + \frac{\partial (\rho_0 u)}{\partial z} = 0 , \tag{4.1}$$

$$\rho_0 \frac{\partial u}{\partial t} + \frac{\partial p}{\partial z} + \rho g = 0 , \tag{4.2}$$

$$\frac{\partial p}{\partial t} + u\frac{dp_0}{dz} - c_s^2 \left(\frac{\partial \rho}{\partial t} + u\frac{d\rho_0}{dz} \right) = 0 , \tag{4.3}$$

where u, p and ρ represent the perturbed velocity, pressure and density, respectively. In addition, $\vec{g} = -g\hat{z}$ is gravity, c_s is the speed of sound, and ρ_0 and p_0 are the background gas density and pressure, respectively. The background medium is assumed to be in hydrostatic equilibrium, which means that $dp_0/dz = -\rho_0 g$. The sound speed is given by $c_s = [\gamma p_0/\rho_0]^{1/2} = [\gamma R T_0/\mu]^{1/2}$, where γ being the ratio of specific heats, R is the universal gas constant, μ is the mean molecular weight, and T_0 is the background temperature.

In a stratified and non-isothermal medium, $T_0 = T_0(z)$, $c_s = c_s(z)$, and both density, H_ρ, and pressure, H_p scale heights are also functions of z. Introducing q_i, where $i = 1$, 2 and 3, and $q_1 = u$, $q_2 = p$ and $q_3 = \rho$, and combining Eqs (4.1), (4.2) and (4.3), we obtain the following acoustic wave equations

$$\hat{L}_i \left[\frac{\partial^2}{\partial t^2} - c_s^2(z) \frac{\partial^2}{\partial z^2} + \frac{c_s^2(z)}{H_i(z)} \frac{\partial}{\partial z} \right] \hat{L}_i^{-1} q_i = 0 , \tag{4.4}$$

where $\hat{L}_1 = \hat{1}$,

$$\hat{L}_2 = \hat{1} - g \left(\frac{\partial}{\partial t} \right)^{-2} \frac{\partial}{\partial z} \quad \text{and} \quad \hat{L}_3 = \frac{\partial^2}{\partial z^2} . \tag{4.5}$$

In addition, $H_1(z) = H_p(z)$ and $H_2(z) = H_3(z) = -H_\rho(z)$ with

$$H_p(z) = \frac{1}{p_0(z)} \frac{dp_0(z)}{dz} \quad \text{and} \quad H_\rho(z) = \frac{1}{\rho_0(z)} \frac{d\rho_0(z)}{dz} \,, \tag{4.6}$$

and $H_\rho(z) \neq H_p(z)$ but $\frac{1}{H_\rho} = \frac{1}{H_p} + \frac{H_{p'}}{H_p}$.

The wave equations given by Eq. (4.4) describe one-dimensional (along the z-axis) propagation of linear and adiabatic acoustic waves in a non-isothermal atmosphere, and their specific forms clearly show that the behavior of the wave variables u, p and ρ is not the same.

When we transform $q_i = \hat{L}_i q_{1i}$, Eq. (4.4) becomes

$$\left[\frac{\partial^2}{\partial t^2} - c_s^2(z) \frac{\partial^2}{\partial z^2} + \frac{c_s^2(z)}{H_i(z)} \frac{\partial}{\partial z} \right] q_{1i} = 0 \,, \tag{4.7}$$

4.2 Local acoustic cutoff frequency

We begin with the transformation

$$d\tau = \frac{dz}{c_s(z)} \,, \tag{4.8}$$

and apply it to the wave equations for u_1 and p_1; since rho_1 and p_1 have the same behavior, we consider only the latter one. Introducing $u_2(\tau, t)$ and $p_2(\tau, t)$, we obtain

$$\frac{\partial^2 u_2}{\partial t^2} - \frac{\partial^2 u_2}{\partial \tau^2} + \left(\frac{c_s'}{c_s} + \frac{c_s}{H_p} \right) \frac{\partial u_2}{\partial \tau} = 0 \,, \tag{4.9}$$

and

$$\frac{\partial^2 p_2}{\partial t^2} - \frac{\partial^2 p_2}{\partial \tau^2} + \left(\frac{c_s'}{c_s} - \frac{c_s}{H_\rho} \right) \frac{\partial p_2}{\partial \tau} = 0 \,. \tag{4.10}$$

To cast the above wave equations in their standard (or Klein-Gordon) forms, we need to remove the first order terms from the above equations. To do so, we use the following transformations: $u_2 = \tilde{u}(t, \tau) \exp \left[1/2 \int_{\tau_0}^\tau (c_s'/c_s + c_s/H_p) \right]$ and $p_2 = \tilde{p}(t, \tau) \exp \left[1/2 \int_{\tau_0}^\tau (c_s'/c_s - c_s/H_\rho) \right]$.

This gives

$$\left[\frac{\partial^2}{\partial t^2} - \frac{\partial^2}{\partial \tau^2} + \Omega_{cr,u}^2(\tau) \right] \tilde{u}(\tau, t) = 0 \; , \tag{4.11}$$

and

$$\left[\frac{\partial^2}{\partial t^2} - \frac{\partial^2}{\partial \tau^2} + \Omega_{cr,p}^2(\tau) \right] \tilde{p}(\tau, t) = 0 \; , \tag{4.12}$$

where

$$\Omega_{cr,u}^2(\tau) = \frac{3}{4} \left(\frac{c_s'}{c_s} \right)^2 - \frac{1}{2} \frac{c_s''}{c_s} + \frac{1}{4} \left(\frac{c_s}{H_p} \right)^2 + \frac{1}{2} \frac{c_s H_p'}{H_p^2} \; , \tag{4.13}$$

and

$$\Omega_{cr,p}^2(\tau) = \frac{3}{4} \left(\frac{c_s'}{c_s} \right)^2 - \frac{1}{2} \frac{c_s''}{c_s} + \frac{1}{4} \left(\frac{c_s}{H_\rho} \right)^2 - \frac{1}{2} \frac{c_s H_\rho'}{H_\rho^2} \; , \tag{4.14}$$

with $c_s'' = d^2 c_s / d\tau^2$. Note that $\Omega_{cr,u}$ and $\Omega_{cr,p}$ are known as the critical frequencies (Musielak, Fontenla, & Moore, 1992; Musielak et al. 2006; Routh et al. 2007).

We make the Fourier transform in time $[\tilde{u}(\tau, t), \tilde{p}(\tau, t)] = [\tilde{\tilde{u}}(\tau), \tilde{\tilde{p}}(\tau)] e^{-i\omega t}$, where ω is the wave frequency. Then, Eqs (4.12) and (4.13) become

$$\left[\frac{\partial^2}{\partial \tau^2} + \omega^2 - \Omega_{cr,u}^2(\tau) \right] \tilde{\tilde{u}}(\tau) = 0 \; , \tag{4.15}$$

and

$$\left[\frac{\partial^2}{\partial \tau^2} + \omega^2 - \Omega_{cr,p}^2(\tau) \right] \tilde{\tilde{p}}(\tau) = 0 \; . \tag{4.16}$$

Applying the oscillation and turning-point theorems (see chapter 3) we obtain the following turning-point frequencies

$$\Omega_{tp,u}^2(\tau) = \Omega_{cr,u}^2(\tau) + \frac{1}{4\tau^2} \; , \tag{4.17}$$

and

$$\Omega_{tp,p}^2(\tau) = \Omega_{cr,p}^2(\tau) + \frac{1}{4\tau^2} \; , \tag{4.18}$$

where

$$\tau(z) = \int^z \frac{d\tilde{z}}{c_s(\tilde{z})} + \tau_C \; , \tag{4.19}$$

with τ_C being an integration constant to be evaluated when atmosphere models are specified.

The turning-point frequencies separate the solutions into propagating and non-propagating (evanescent) waves. Since there is a turning-point frequency for each wave variable, only one of them can be the cutoff frequency. We follow Musielak et al. (2006) and Routh et. al. (2007), and identify the largest turning-point frequency as the cutoff frequency. The choice is physically justified by the fact that in order to have propagating torsional tube waves at a given height z, the wave frequency ω must always be higher than any turning-point frequency at this height; note that as a result of this choice both wave variables are always described by the propagating wave solutions. Thus, we can write

$$\Omega_{cut,\tau}(\tau) = \max[\Omega_{tp,u}(\tau), \Omega_{tp,p}(\tau)] \, , \tag{4.20}$$

and use it to determine the cutoff frequency for each τ.

According to Eq. (4.19), the variables τ and z are related to each other. Hence, we may use

$$c_s \frac{dc_s}{d\tau} = \frac{dc_s}{dz} \, , \tag{4.21}$$

and

$$\frac{1}{c_s} \frac{d^2 c_s}{d\tau^2} = c_s \frac{d^2 c_s}{dz^2} + \left(\frac{dc_s}{dz} \right)^2 \, , \tag{4.22}$$

to express the critical frequencies $\Omega_{cr,u}^2(\tau)$ and $\Omega_{cr,p}^2(\tau)$ in terms of z

$$\Omega_{cr,u}^2(z) = (\omega_{ac} + \omega_{as})^2 + 2\omega_{ac}\omega_{as} - c_s\omega_{as}' \, , \tag{4.23}$$

and

$$\Omega_{cr,p}^2(z) = (\omega_{ac} + \omega_{as})^2 - 2\omega_{ac}\omega_{as} + c_s\omega_{as}' \, . \tag{4.24}$$

where $\omega_{ac} = \frac{\gamma g}{2c_s} = \frac{c_s}{2H}$ represents the original Lamb acoustic cutoff frequency and $\omega_{as} = \frac{1}{2}\frac{dc_s}{dz}$. Note that in an isothermal atmosphere both the critical frequencies reduce to Lamb's cutoff $\omega_a c$.

The same conversion can be applied to the turning-point frequencies $\Omega^2_{tp,u}(\tau)$ and $\Omega^2_{tp,p}(\tau)$, and the results are

$$\Omega^2_{tp,u}(z) = \Omega^2_{cr,u}(z) + \frac{1}{4}\left[\int^z \frac{d\tilde{z}}{c_s(\tilde{z})} + \tau_C\right]^{-2} , \tag{4.25}$$

and

$$\Omega^2_{tp,p}(z) = \Omega^2_{cr,p}(z) + \frac{1}{4}\left[\int^z \frac{d\tilde{z}}{c_s(\tilde{z})} + \tau_C\right]^{-2} , \tag{4.26}$$

with the cutoff frequency given by

$$\Omega_{cut,}(z) = \max[\Omega_{tp,u}(z), \Omega_{tp,p}(z)] . \tag{4.27}$$

The main result is that the derived cutoff frequency is a local quantity and that its value at a given atmospheric height determines the frequency that acoustic waves must have in order to be propagating at this height.

4.3   Application: power-law models

We now consider the atmospheric model with the following temperature distribution

$$T_0(z) = T_{00}\xi^m , \tag{4.28}$$

where $\xi = z/z_0$ is the distance ratio, with z_0 being a fixed height in the model, and m can be any real number. We define T_{00} to be the temperature at z_0 and take $T_{00} = 5000$ K for all considered models. The resulting temperature distributions are shown in Fig. 4.1

We consider two special cases of $m = 1$ and $m = 2$, and one general case of $m > 2$. For each model, we calculate the critical frequencies by using Eqs (4.23) and
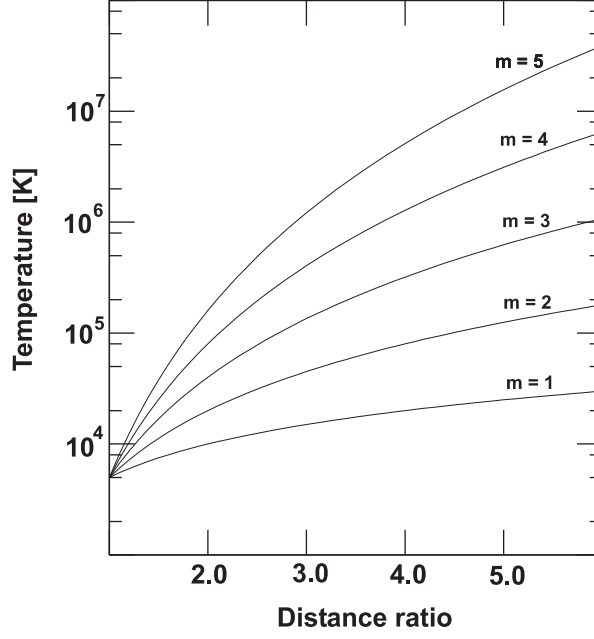
Figure 4.1. Temperature vs. the distance ratio z/z_0.

(4.24), the turning-point frequencies by using Eqs (4.25) and (4.26), and determine the cutoff frequency $\Omega_{cut}(\xi)$ from the condition given by Eq. (4.27). The calculations of the turning-point frequencies require evaluation of the variable τ, which represents the wave travel time t_w. This is done by using Eq. (4.19) in which the integration constant τ_C is evaluated by taking $\tau(\xi = 1) = \tau_0 = z_0/c_{s0}$, where c_{s0} is the value of $c - s$ at z_0; Note that the integration constant is evaluated in the same way for all considered power-law models.

4.3.1 Linear temperature models

For this model $T_0(\xi) = T_{00}\xi$ (see Fig. 4.1), which gives $c_s(\xi) = c_{s0}\xi^{1/2}$. In this case, the turning-point frequency $\Omega_{tp,u}$ is always larger than $\Omega_{tp,p}$, and the cutoff frequency is

$$\Omega_{cut}(\xi) = \Omega_0 \left[\left(\frac{\gamma^2 g^2}{c_{s0}^4} + \frac{2\gamma g z_0}{c_{s0}^2} + \frac{3}{4} \right) + \frac{\xi}{(2\xi^{1/2} - 1)^2} \right]^{1/2} \xi^{-1/2} , \tag{4.29}$$
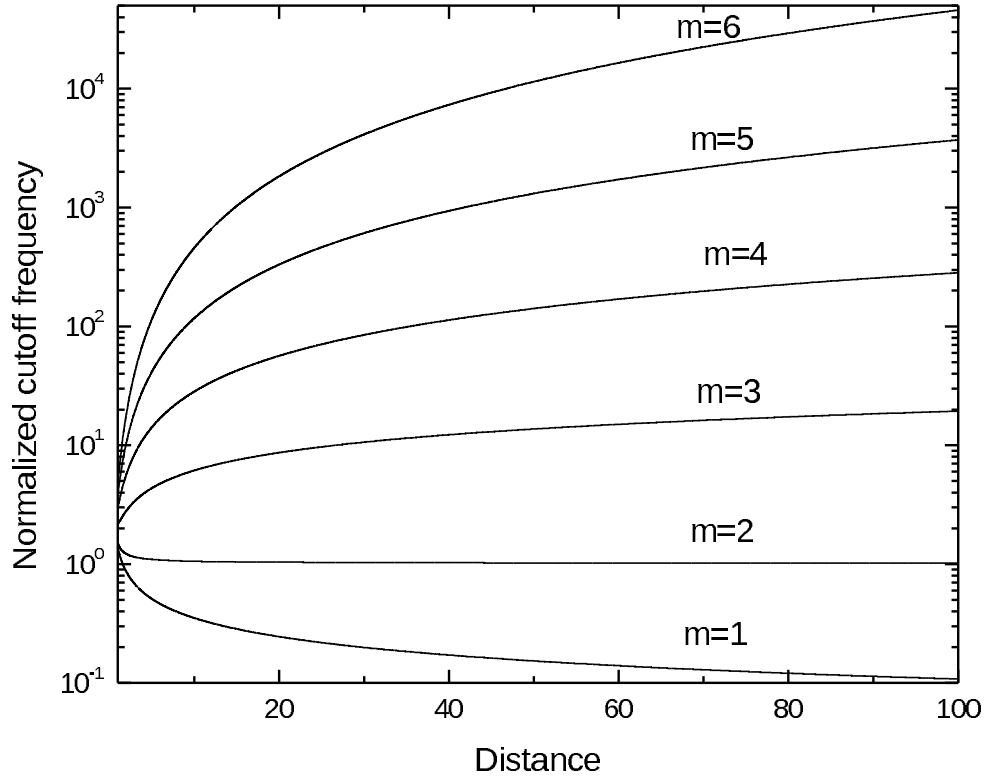
Figure 4.2. The normalized cutoff frequency Ω_{cut}/Ω_0 vs. the distance ratio z/z_0.

where $\Omega_0 = c_{s0}/2z_0$ has a fixed value at z_o. The plot of the normalized cutoff frequency $[\Omega_{cut}(\xi)/\Omega_0]$ versus ξ is shown in Fig. 4.2.

4.3.2 Quadratic temperature models

With $T_0(\xi) = T_{00}\xi^2$, we find $c_s(\xi) = c_{s0}\xi$, and $\Omega_{tp,u}$ as the larger turning-point frequency and so the cutoff frequency can be written as

$$\Omega_{cut}(\xi) = \Omega_0 \left[1 + \frac{4\gamma g z_0}{c_{s0}^2} \frac{1}{\xi} + \frac{\gamma^2 g^2 z_0^2}{c_{s0}^4} \frac{1}{\xi^2} + \frac{1}{(1 + ln\xi)^2} \right]^{1/2} . \qquad (4.30)$$

4.3.3 Other power-law temperature models

We now consider the general case of $T_0(\xi) = T_{00}\xi^m$, where $m > 2$. This gives $c_s(\xi) = c_{s0}\xi^{m/2}$, and among the two turning-point frequencies $\Omega_{tp,p}$ is always larger than $\Omega_{tp,u}$. Hence, the cutoff frequency is

$$\Omega_{cut}(\xi) = \Omega_0 \left[\frac{m(3m-4)}{4}\xi^{m-2} + \frac{\gamma^2 g^2 z_0^2}{c_{s0}^4}\xi^{-m} + \frac{(m-2)^2}{(m-2\xi^{(2-m)/2})^2} \right]^{1/2} . \qquad (4.31)$$

The results presented in Fig. 4.2 show that the values of the cutoffs rapidly increase when steeper temperature gradients are considered. For $m = 1$ and $m = 2$, the cutoffs are determined by $\Omega_{tp,u}$ as the critical frequencies of u are larger than those of p. For $m > 2$ the cutoffs are determined by $\Omega_{tp,p}$ as the critical frequencies derived for the wave variable p are larger than those obtained for u.

CHAPTER 5

EXTENSION OF LIGHTHILL'S THEORY OF SOUND

GENERATION TO NON-ISOTHERMAL MEDIUM

As already discussed in Chapter 2, the original Lighthill theory of sound genera-
tion was developed for an uniform medium (Lighthill 1952). The theory was extended
to an isothermal atmosphere by Stein (1967) and modified by Musielak et al. (1994).
However, to the best of our knowledge, the effects of temperature gradients on the
rate of the acoustic wave generation have not been investigated. Such studies can now
be performed by using the method described in Chapter 3. Therefore, the main goal
of this chapter is to extend Lighthill's theory to a non-isothermal medium. The model
of this medium is assumed to be simple enough so that that analytical solutions can
be obtained. The solutions are then used to study the effects caused by one specific
temperature gradient on the wave generation and propagation. The obtained results
show that a temperature gradient in the region of wave generation leads to monopole
and dipole sources of acoustic emission, and that the gradient is responsible for the
acoustic cutoff frequency, which affects the wave propagation.

5.1 Basic equations

Let us consider a compact region of turbulent flow embedded in a very large
volume of an ideal gas and assume that both the turbulent region and the surrounding
medium are non-uniform because of the existence of a temperature gradient. To
simplify the problem so that analytical solutions can be obtained, we neglect gravity

and consider a model in which the gas pressure $p_0 = $ const, however, the background temperature T_0, density ρ_0 and speed of sound c_s vary with height in the model.

To describe the generation and propagation of acoustic waves in this model, we consider a set of hydrodynamic equations and assume that the turbulent flow is subsonic and the waves are linear. In general, the waves propagate in all three (x, y and z) directions, however, their propagation in the z-direction is affected by the gradient. We introduce x_i, with i = 1, 2 and 3, and define $x_1 = x$, $x_2 = y$ and $x_3 = z$. The waves are described by using the velocity $u_i(t, x_i)$, density $\rho(t, x_i)$ and pressure $p(t, x_i)$ perturbations. We further assume that the effects of viscosity and heat conduction can be neglected. Based on these assumptions, we linearize the hydrodynamic equations and follow Lighthill (1952) to separate the linear and nonlinear terms. This gives [1]

$$\frac{\partial \rho}{\partial t} + \frac{\partial (\rho_0 u_i)}{\partial x_i} = -\frac{\partial (\rho u_i)}{\partial x_i} \, , \tag{5.1}$$

$$\rho_0 \frac{\partial u_i}{\partial t} + \frac{\partial p}{\partial x_i} = -\frac{\partial \rho u_i}{\partial t} - \frac{\partial (\rho_0 u_i u_j)}{\partial x_j} \, , \tag{5.2}$$

and

$$\frac{\partial p}{\partial t} + \rho_0 c_s^2 \frac{\partial u_i}{\partial x_i} = -u_i \frac{\partial p}{\partial x_i} - c_s^2 \rho \frac{\partial u_i}{\partial x_i} \, , \tag{5.3}$$

where, in general, $c_s = c_s(x_i)$ in our nonisothermal model.

5.2 Wave equation and source function

We derive an inhomogeneous wave equation for the pressure perturbation p associated with the waves by eliminating the other wave variables, and obtain

$$\frac{\partial^2 p}{\partial t^2} - \frac{\partial}{\partial x_i} \left[c_s^2(x_i) \, \frac{\partial p}{\partial x_i} \right] = S(t, x_i) \, , \tag{5.4}$$

---

[1] We have used subscript notation for the Cartesian components of vectors and tensors, and any substript repeated in a single term is to be summed from 1 to 3.

where the source function $S(t, x_i)$ is given by

$$S(t, x_i) = \frac{\partial}{\partial x_i} \left[c_s^2 \frac{\partial(\rho u_i)}{\partial t} \right] + \frac{\partial}{\partial x_i} \left[c_s^2 \frac{\partial(\rho_0 u_i u_j)}{\partial x_j} \right] - \frac{\partial}{\partial t} \left(u_i \frac{\partial p}{\partial x_i} \right) + c_s^2 \frac{\partial}{\partial t} \left(\rho \frac{\partial u_i}{\partial x_i} \right) \quad (5.5)$$

It must be noted that in our model the inhomogeneous wave equations for the wave velocity u_i and density ρ are of different forms. The fact that is an important issue when acoustic cutoff frequencies are calculated (Musielak & Musielak 2005) and will be discussed in Sec. 3.5 of the paper.

We now follow Lighthill (1952) and treat the source function as being fully determined by a known turbulent flow. To emphasize this point, we label the source function as $S_{turb}(t, x_i)$. Since the turbulent flow considered in this paper is subsonic, we make a Mach-number expansion of the source function and retain only the lowest order terms; the procedure is discussed in great details by Stein (1967) and Musielak et al. (1994), and will not be repeated here. This allows us to write

$$S_{turb}(t, x_i) \approx \frac{\partial}{\partial x_i} \left[c_s^2 \frac{\partial(\rho_0 u_i u_j)}{\partial x_j} \right]_{turb} . \quad (5.6)$$

which is consistent with Lighthill's results described in Sec. 2 in case of $c_s = $ const.

Hence, the inhomogeneous acoustic wave equation becomes

$$\frac{\partial^2 p}{\partial t^2} - c_s^2 \frac{\partial^2 p}{\partial x_i^2} - 2 c_s c_s' \frac{\partial p}{\partial x_i} = S_{turb}(t, x_i) , \quad (5.7)$$

where $c_s' = dc_s/dx_3 = dc_s/dz$, and

$$S_{turb}(t, x_i) = c_s^2 \frac{\partial^2}{\partial x_i \partial x_j} \left(\rho_0 u_{ti} u_{tj} \right) + 2 c_s c_s' \frac{\partial}{\partial x_j} \left(\rho_0 u_{ti} u_{tj} \right) , \quad (5.8)$$

with changes in notation and replacing $[u_i]_{turb}$ in the source function S_{turb} by u_{ti}. It must be noted that Eq. (5.7) reduces to Lighthill's inhomogeneous wave equation (see Eq. **??**) in the limit of $c_s = $ const and with $p = c_s^2 \rho$.

5.3 Transformed wave equation

To remove the nonconstant coefficient c_s^2 from the term with the second-order derivative in Eq. (5.7), we introduce the new variable $d\tau_i = dx_i/c_s$ and obtain

$$\frac{\partial^2 p}{\partial t^2} - \frac{\partial^2 p}{\partial \tau_i^2} - \frac{1}{c_s}\left(\frac{\partial c_s}{\partial \tau_i}\right)\frac{\partial p}{\partial \tau_i} = S_{turb}(t, \tau_i) , \tag{5.9}$$

with

$$S_{turb}(t, \tau_i) = \frac{\partial^2}{\partial \tau_i \partial \tau_j}(\rho_0 u_{ti} u_{tj}) + \frac{1}{c_s}\left(\frac{\partial c_s}{\partial \tau_i}\right)\frac{\partial}{\partial \tau_j}(\rho_0 u_{ti} u_{tj}) . \tag{5.10}$$

As the next step, we remove the first order derivative from Eq. (5.9) by using the following transformation:

$$p(t, \tau_i) = p_1(t, \tau_i)e^{-I_c} , \tag{5.11}$$

where

$$I_c = \frac{1}{2}\int_{\tau_{i0}}^{\tau_i} \frac{1}{c_s}\left(\frac{\partial c_s}{\partial \tilde{\tau}_i}\right)\tilde{d}\tau_i . \tag{5.12}$$

This gives

$$\frac{\partial^2 p_1}{\partial t^2} - \frac{\partial^2 p_1}{\partial \tau_i^2} + \Omega_i^2(\tau_i)p_1 = S_{turb}(t, \tau_i) , \tag{5.13}$$

where

$$\Omega_i^2(\tau_i) = \frac{1}{2}\left[\frac{1}{c_s}\left(\frac{\partial^2 c_s}{\partial \tau_i^2}\right) - \frac{1}{2c_s^2}\left(\frac{\partial c_s}{\partial \tau_i}\right)^2\right] , \tag{5.14}$$

and

$$S_{turb}(t, \tau_i) = \left[\frac{\partial^2}{\partial \tau_i \partial \tau_j}(\rho_0 u_{ti} u_{tj}) + \frac{1}{c_s}\left(\frac{\partial c_s}{\partial \tau_i}\right)\frac{\partial}{\partial \tau_j}(\rho_0 u_{ti} u_{tj})\right]e^{I_c} . \tag{5.15}$$

It must be noted that Eq. (5.13) is often referred to as a Klein-Gordon equation (Morse & Feshbach 1953; Musielak et al. 1992). In addition, the form of $S_{turb}(t, \tau_i)$ is interesting as it shows both local $(\partial c_s/\partial x_i)$ and global (I_c) effects determine the source function.

5.4 Solution and acoustic cutoff frequency

To solve Eq. (5.13), we must specify the temperature gradient in our non-isothermal model. Since the gas pressure $p_0 = RT_0\rho_0/\mu$, where R is the universal gas constant and μ is the mean molecular weight, must be constant in our model, the temperature and density variations with height must be related to each other. Let us consider a model in which both T_0 and ρ_0 vary only in one direction, say, the x_3 (or z) direction and assume that $T_0(\xi) = T_{00}\xi^2$, where $\xi = z/z_0$, with z_0 being a given height, and T_{00} is a temperature at this height. For the model to be in hydrostatic equilibrium ($p_0 = $ const), the density ρ_0 must decrease with ξ as $\rho_0 = \rho_{00}\xi^{-2}$. In this model, the speed of sound c_s is a linear function of ξ and we have $c_s(\xi) = c_{s0}\xi$, where c_{s0} is the speed of sound at z_0.

The non-isothermal model requires that $\tau_1 = x_1/c_s$ and $\tau_2 = x_2/c_s$ but $\tau_3 = ln|\xi|/\omega_0$, where $\omega_0 = c_{s0}/z_0$. Hence, we obtain $\xi = e^{\omega_0\tau_3}$ and $c_s(\tau_3) = c_{s0}e^{\omega_0\tau_3}$. We use these results to calculate Ω_i^2 (see Eq. 5.14), which gives $\Omega_1^2 = 0$, $\Omega_2^2 = 0$ and $\Omega_3^2 = \Omega_0^2$ with $\Omega_0^2 = \omega_0^2/4$ or

$$\Omega_0^2 = \frac{c_{s0}^2}{4z_0^2} . \tag{5.16}$$

This allows us to write the inhomogeneous Klein-Gordon equation (see Eq. 5.13) in the following form:

$$\frac{\partial^2 p_1}{\partial t^2} - \frac{\partial^2 p_1}{\partial \tau_i^2} + \Omega_i^2(\tau_i)p_1 = S_{turb}(t, \tau_i) , \tag{5.17}$$

where $\Omega_1^2 = \Omega_2^2 = 0$, $\Omega_3^2 = \Omega_0^2$ and

$$S_{turb}(t, \tau_i) = \left[\frac{\partial^2}{\partial \tau_i \partial \tau_j} (\rho_0 u_{ti} u_{tj}) + 2\Omega_0 \frac{\partial}{\partial \tau_j} (\rho_0 u_{ti} u_{tj}) \right] e^{\Omega_0\tau_3} . \tag{5.18}$$

An interesting result is that Ω_0 is constant in the τ-space (but not in the z-space), so we can formally make Fourier transforms in time and τ-space. Based on the form of Eq. (5.17) and the fact that $\Omega_0 = $ const, we conclude that Ω_0 is the

acoustic cutoff frequency (Lamb 1908, 1910); one must keep in mind that this is true only in the τ-space (see also Musielak at el. 2006).

We make Fourier transforms in time and τ-space

$$p_1(t, \tau_i) = \int \int p_2(\omega, k_i) e^{i(\omega t - k_i \tau_i)} d\omega \ d^3 k_i \ , \tag{5.19}$$

where k_i is a wave vector corresponding to τ_i. This gives

$$\int \int [-\omega^2 + k_i^2 + \Omega_i^2] p_2(k_i, \omega) e^{i(\omega t - k_i \tau_i)} \ d\omega \ d^3 k_i = S_{turb}(t, \tau_i,) \ , \tag{5.20}$$

and

$$p_2(\omega, k_i) = \frac{S_{turb}(\omega, k_i)}{-\omega^2 + k_i^2 + \Omega_i^2} \ , \tag{5.21}$$

with

$$S_{turb}(\omega, k_i) = \frac{1}{(2\pi)^4} \int \int S_{turb}(t, \tau_i) e^{-i(\omega t - k_i \tau_i)} \ dt \ d^3 \tau_i \ . \tag{5.22}$$

Substituting Eq. (5.15) in Eq. (5.22) and integrating by parts results in:

$$S_{turb}(\omega, k_i) = \frac{-1}{(2\pi)^4} \int (\rho_0 u_i u_j) \left(\frac{\partial^2}{\partial \tau_i \partial \tau_j} + \frac{c'_{si}}{c_s} \frac{\partial}{\partial \tau_j} \right) e^{I_c} e^{-i(\omega t - k_i \tau_i)} d^3 \tau_i \ dt$$

$$\tag{5.23}$$

After performing the algebra, $S_{turb}(t, \tau_i)$ was deduced to be: (See Appendix A)

$$S_{turb}(t, \tau_i) = \left\{ k_i k_j - \frac{1}{4} \frac{c'_{si} c'_{sj}}{c_s^2} - \frac{c_{si}''}{2c_s} - \frac{i}{2c_s} \left[\frac{1}{2} c'_{sj} k_i + \frac{3}{2} c'_{si} k_j \right] \right\} (e^{I_c} \rho_0 u_i u_j) \tag{5.24}$$

Taking the first derivative of velocity of sound to be zero for x and y directions, the above equation turns out to be

$$S_{turb}(t, \tau_i) = e^{I_c} \rho_0 \left\{ k_i k_j u_i u_j - \frac{1}{4} \frac{(c'_{sz})^2}{c_s^2} u_3 u_3 - \frac{c_{sz}''}{2c_s} - \frac{i}{2c_s} \left[\frac{1}{2} c'_{sz} u_3 k_i u_i + \frac{3}{2} c'_{sz} u_3 k_j u_j \right] \right\}$$

$$\tag{5.25}$$

5.5   Calculation of the Emitted Acoustic Energy Flux

The mean acoustic energy flux is calculated by using

$$\vec{F} = <pu^*>$$

(5.26)

From the momentum conservation and continuity equation, after ignoring gravity and non linear terms, the velocity of the fluid [2] is expressed in terms of the pressure perturbation, as

$$u_i = -\frac{1}{\rho_0}\left(\frac{\partial}{\partial t}\right)^{-1}\frac{1}{c_s}\frac{\partial p}{\partial \tau_i}.$$

(5.27)

Substituting this relation into the energy flux equation leads to

$$\vec{F} = -<p\frac{1}{\rho_0 c_s}\left(\frac{\partial}{\partial t}\right)^{-1}\frac{\partial p^*}{\partial \tau_i}>$$

(5.28)

And p can be expressed in terms of its Fourier transform,

$$p_2(t,\tau_i) = \int \frac{S_{turb}(\omega,k_i)}{-\omega^2 + k_i^2 + \Omega_i^2}e^{i\omega t - ik_i\tau_i}d^3k_i d\omega$$

(5.29)

$$\vec{F}(\omega,k_i) = \lim_{T\to\infty}\frac{2\pi}{T}\frac{1}{\rho_0 c_s}\int\left(\frac{k_i}{\omega}\right)\frac{S_1(\omega,k_i)S_1^*(\omega,k_i)d^3k_i d^3k_i}{\{-\omega^2 + k_i^2 + \Omega_i^2\}\{-\omega^2 + k_i^2 + \Omega_i^2\}}.$$

(5.30)

5.6   Asymptotic Fourier Transform

Lighthill's (1960) formula for the asymptotic value of Fourier transforms far from the source is

$$\int \frac{F(\vec{k})}{G(\vec{k})}e^{(i\vec{k}\cdot\vec{\tau})}d^3\vec{k} = \frac{4\pi^2}{|\vec{\tau}|}\sum_k \frac{F(\vec{k})e^{i\vec{k}\cdot\vec{\tau}}}{|\Delta_k G|\sqrt{K}}$$

(5.31)

---

[2]See Eq. 54 in Stein, 1967

where G, the denominator in the integral in (5.30), is defined as $G = \vec{k}_i \cdot \vec{k}_i - (\omega^2 - \Omega_i^2)$. K is the Gaussian curvature of the slowness surface [3] on which the direction of normal is defined as $|\hat{\tau}| = \frac{\Delta_k G}{|\Delta_k G|} = \frac{(k_1, k_2, k_3)}{\sqrt{(k_1^2 + k_2^2 + k_3^2)}}$. Referring to (5.29), only those wave numbers and frequencies contribute to the pressure perturbation where the denominator, G, vanishes, i.e, where the dispersion relation (G=0) is satisfied. The sum is over the set $\vec{k}$ on the slowness surface, G=0. The cosine of the angle between the sound propagation (group velocity), $\hat{\tau}$, and the vertical is $\cos\theta = \hat{z} \cdot \hat{\tau} = \frac{k_3}{|k|}$. The cosine of the angle between the wave vector, $\vec{k}$, and the vertical is $\cos\theta_k = \frac{\hat{z} \cdot \vec{k}}{|k|} = \frac{k_3}{|k|}$. Hence in our particular case the direction of the wave vector is the same as the direction of propagation, that is, $\theta_k = \theta$. By applying (5.31) to (5.30), one can produce the acoustic flux at large distances, which is

$$\vec{F}(\omega, k_i) = \lim_{T \to \infty} \frac{8\pi^5}{T} \frac{\hat{\tau}_i}{|\tau_i|^2} \frac{\sqrt{(\omega^2 - \Omega_i^2)}}{\omega \rho_0 c_s} |S_{turb}(\omega, k_i)|^2 \tag{5.32}$$

5.7 Evaluation of Spectral Efficiency

In the absence of generally accepted model of turbulence, the description of turbulent flow is based on two-point, two-time velocity correlation functions which are obtained by considering the source at two points in a turbulent fluid at two different times.

$$S_{turb}^*(\omega, k_i) = \frac{1}{(2\pi)^4} \int S_{turb}^*(t'', \tau_i'') e^{-i(\omega t'' - k_i \tau_i'')} d^3\tau_i'' dt'' \tag{5.33}$$

$$S_{turb}(\omega, k_i) = \frac{1}{(2\pi)^4} \int S_{turb}(t', \tau_i') e^{i(\omega t' - k_i \tau_i')} d^3\tau_i' dt' \tag{5.34}$$

Here primed and double-primed refer to the two turbulent source points. Averaging the position and time, $\vec{\tau}_0$ being the vector to the mean position between the

---

[3]The slowness surface is the surface in wave number space where the dispersion relation is satisfied.

two turbulent source points and $t_0 = 0.5(t'' + t')$ being the mean time between t'' and t', the coordinates in the evaluation of $|S(\vec{k}, \omega)|^2$ are transformed:

$$|S_{turb}(\omega, k_i)|^2 = \frac{1}{(2\pi)^8} \int \int \int \int S_{turb}^*(t_0 + \frac{t}{2}, \tau_{0i} + \frac{\tau_i}{2})$$
$$S_{turb}(t_0 - \frac{t}{2}, \tau_{0i} - \frac{\tau_i}{2})e^{-i\omega t + ik_i\tau_i}d^3\tau_i \, d^3\tau_{0i} \, dt \, dt_0$$

where $\tau_i = \tau_i'' - \tau_i'$ and $t = t'' - t'$ are the space and time intervals between the two points respectively. Performing the integration over t_0 will result in the time averaging of $|S_{turb}(\omega, k_i)|^2$:

$$|S_{turb}(\omega, k_i)|^2 = \frac{T}{(2\pi)^8} \int \int \int \int < S_{turb}^*(t_0 + \frac{t}{2}, \tau_{0i} + \frac{\tau_i}{2})$$
$$S_{turb}(t_0 - \frac{t}{2}, \tau_{0i} - \frac{\tau_i}{2}) > e^{-i\omega t + ik_i\tau_i}d^3\tau_i \, d^3\tau_{0i} \, dt \qquad (5.35)$$

Using subscript i,j and l,m for two different locations and two different times, Eq (21) can be used to calculate $|S_{turb}^*(t_0 + \frac{t}{2}, \tau_{0i} + \frac{\tau_i}{2})S_{turb}(t_0 - \frac{t}{2}, \tau_{0i} - \frac{\tau_i}{2})|$.

$$|S_{turb}^*(t_0 + \frac{t}{2}, \tau_{0i} + \frac{\tau_i}{2})S_{turb}(t_0 - \frac{t}{2}, \tau_{0i} - \frac{\tau_i}{2})| = (\rho_o^2 e^{2I_c})[k_i k_j u_i' u_j'$$
$$-\frac{1}{4}\frac{(c_{sz}')^2}{c_s^2}u_3'u_3' - \frac{c_{sz}''}{2c_s}u_3\prime u_3\prime + \frac{i}{2c_s}(\frac{3}{2}c_{sz}'u_3'k_ju_j' + \frac{1}{2}c_{sz}'u_3'k_iu_i')][k_l k_m u_l'' u_m'' -$$
$$-\frac{1}{4}\frac{(c_{sz}')^2}{c_s^2}u_3'u_3' - \frac{c_{sz}''}{2c_s}u_3\prime u_3\prime - \frac{i}{2c_s}(\frac{3}{2}c_{sz}'u_3'k_ju_j' + \frac{1}{2}c_{sz}'u_3'k_iu_i')]$$

$$(5.36)$$

Spectral efficiency, $\Upsilon(t, \vec{\tau})$, is obtained by expanding the above equation, ignoring the complex part because being an odd function of ω it disappears upon integration over ω.

$$\Upsilon(t,\tau_i) = k_i k_j k_l k_m u_i' u_j' u_l'' u_m'' - \frac{1}{2}\left[\frac{1}{2}\left(\frac{c_{sz}'}{c_s}\right)^2 + \frac{c_{sz}''}{c_s}\right] k_i k_j u_i' u_j' u_3'' u_3'' -$$

$$\frac{1}{2}\left[\frac{1}{2}\left(\frac{c_{sz}'}{c_s}\right)^2 + \frac{c_{sz}''}{c_s}\right] k_l k_m u_l'' u_m'' u_3' u_3' +$$

$$\frac{1}{4}\left[\frac{1}{4}\left(\frac{c_{sz}'}{c_s}\right)^4 + \left(\frac{c_{sz}''}{c_s}\right)^2 + \frac{(c_{sz}')^2 c_{sz}''}{c_s^3}\right] u_3' u_3' u_3'' u_3'' + \left(\frac{c_{sz}'}{c_s}\right)^2 k_j u_j' k_m u_m'' u_3' u_3''\ (5.37)$$

$$|S_{turb}(\omega,k_i)|^2 = \frac{T e^{2I_c}}{(2\pi)^8} \int\int\int \rho_0^2 \Upsilon(t,\tau_i) e^{-i\omega t + i k_i \tau_i} d^3\tau_i d^3\tau_{0i} dt$$

$$\vec{F}(\omega,k_i) = \frac{\pi\hat{\tau}_i}{|2\tau_i|^2}\frac{\sqrt{(\omega^2-\Omega_i^2)}}{\omega} e^{2I_c} \int\int\int \frac{\rho_0(\tau_{0i})}{(4\pi^2)^2 c_s(\tau_{0i})}\Upsilon(\vec{\tau},t) e^{-i\omega t + i k_i \tau_i} d^3\tau_i d^3\tau_{0i} dt$$

Substituting the value of $c_{sz}'/c_s = 2\Omega_0$, Eq. 5.37 is reduced to

$$\Upsilon(t,\tau_i) = < (k_i u_i')^2 (k_i u_i'')^2 > -3\Omega_0^2\{< (k_i u_i')^2 u_3'' u_3'' > + < (k_i u_i'')^2 u_3' u_3' >\}$$

$$+9\Omega_0^4 < u_3' u_3' u_3'' u_3'' > +4\Omega_0^2 < (k_i u_i')(k_i u_i'') u_3' u_3'' >\ (5.38)$$

To reduce the fourth-order velocity correlation to a second-order velocity correlation, we use the formula introduced by Zhou (5.39) in 1954.

$$< u_1 u_2 u_3' u_4' > = < u_1 u_2 >< u_3' u_4' > + < u_1 u_3' >< u_2 u_4' > + < u_1 u_4' >< u_2 u_3' >$$

$$(5.39)$$

$$\Upsilon(t,\tau_i) = 2w^4 < v'v'' >^2 +4\Omega_0^2 w^2 < v'v'' >< u_3' u_3'' > -8\Omega_0^2 w^2 < v' u_3'' >^2$$

$$+18\Omega_0^4 < u_3' u_3'' >^2\ (5.40)$$

5.8 Convolution of the turbulence spectra

Generally, the Fourier transform of the product of the second-order velocity correlations is expressed as

$$\frac{1}{(2\pi)^4} \int d^3\vec{\tau} \int_{-\infty}^{\infty} e^{-i(\omega t - \vec{k}\cdot\vec{\tau})} dt < u_l' u_m'' >< u_n' u_o'' >$$
$$= \int \int \lambda_{lm}(\vec{k} - \vec{p}, \omega - \sigma)\lambda_{no}(\vec{p}, \sigma)d^3\vec{p}\, d\sigma = J_{lmno} \qquad (5.41)$$

where λ_{ij}, the Fourier transform of the velocity correlation $< u_i' u_j'' >$, is defined as:

$$\lambda_{ij} = \frac{1}{(2\pi)^4} \int \int < u_i(\vec{x}, t_0)u_j(\vec{x} + \vec{r}, t_0 + t) > e^{i(\omega t - \vec{k}\cdot\vec{r})}d^3\vec{r}\, dt \qquad (5.42)$$

From the phenomenological treatment of turbulence, the correlations between the instanteous velocity components at two different locations in the turbulent region can be evaluated when a turbulent energy spectrum $E(\vec{k}, \omega)$ is specified. Assuming the turbulence to be isotropic, homogeneous and incompressible, λ_{ij} can be expressed as

$$\lambda_{ij}(\vec{k}, \omega) = \frac{E(\vec{k}, \omega)}{4\pi k^2}(\delta_{ij} - \frac{k_i k_j}{k^2}) \qquad (5.43)$$

Even though the medium is nonisothermal, it can be treated locally as homogeneous and isotropic, hence the application of the above equation. It is further assumed that the turbulence energy spectrum, $E(\vec{k}, \omega)$, can be factored into the frequency independent spatial turbulent energy spectrum E(k) and the turbulent frequency factor $\Delta(\omega, k)$, $E(\vec{k}, \omega) = E(k)\Delta(\omega, k)$, which in turn can be substituted in (5.43) to simplify the calculation of (5.41).

$$\frac{1}{(4\pi)^2} \int \int \frac{E(\vec{k} - \vec{p})}{q^2} \frac{E(\vec{p})}{p^2}\Delta(\omega - \sigma, \vec{k} - \vec{p})\Delta(\sigma, \vec{p})$$
$$(\delta_{lm} - \frac{k_l k_m}{q^2})(\delta_{no} - \frac{k_n k_o}{p^2})d^3\vec{p}\, d\sigma = J_{lmno} \qquad (5.44)$$

where $\vec{q} \equiv \vec{k} - \vec{p}$. The integration of σ, which has the frequency terms only, can be performed separately,

$$g(p, q, \omega) \equiv \int_{-\infty}^{\infty} \Delta(\omega - \sigma, \vec{q})\Delta(\sigma, \vec{p})d\sigma$$

and Eq. (5.44) can be rewritten as

$$\frac{1}{(4\pi)^2} \int \frac{E(\vec{q})}{q^2} \frac{E(\vec{p})}{p^2} g(p, q, \omega)(\delta_{lm} - \frac{k_l k_m}{q^2})(\delta_{no} - \frac{k_n k_o}{p^2})d^3 p = J_{lmno} \qquad (5.45)$$

The integration of $d^3\vec{p}$ is simplified by taking $\vec{k}$ as the axis of the spherical cordinate system, $d^3 p = p^2 dp \sin\theta d\theta d\phi = p^2 dp d\mu d\phi = 2\pi p^2 dp d\mu$ with $\mu = \cos\theta_{pk} = \cos\theta$ and $|q| = \sqrt{(k^2 + p^2 - 2kp\mu)}$. The Fourier transforms of velocity correlations appearing in (5.40) contain four terms, namely J_{kkkk}, J_{kzkz}, J_{kkzz} and J_{zzzz}. Next we substitue J_{kkkk}, J_{kzkz}, J_{kkzz} and J_{zzzz} in (5.40), take $(\frac{1}{8\pi}) \int_0^\infty dp \int_{-1}^{+1} d\mu \frac{E(q)E(p)}{q^2} g(p, q, \omega)$ as common, and define the remaining equation as $f(\omega, \theta, p, q, \mu)$.

$$f(\omega, \theta, p, q, \mu) = f_q + f_d + f_m$$

$$f_q = 2(w)^4 \frac{p^2}{q^2}(1 - \mu^2)^2,$$

$$f_d = -8w^2\Omega_0^2 \left\{ \mu^2 \cos^2\theta_k(1 - \frac{p^2}{q^2}(1 - \mu^2)) + (\frac{p^2}{q^2}\mu^2 - \frac{pk\mu}{q^2})\frac{1}{2}(1 - \mu^2)\sin^2\theta_k \right\}$$
$$+ 4w^2\Omega_0^2 \left\{ \frac{p^2}{q^2}(1 - \mu^2)\{1 - \mu^2 \cos^2\theta_k - \frac{1}{2}(1 - \mu^2)\sin^2\theta_k\} \right\},$$

$$f_m = 18\Omega_0^4 \left\{ 1 - \mu^2 \cos^2\theta_k - \frac{1}{2}(1 - \mu^2)\sin^2\theta_k + \frac{k^2}{q^2}\{ -\cos^2\theta_k + \mu^2\cos^4\theta_k + \frac{1}{2}(1 - \mu^2)\cos^2\theta_k \sin^2\theta_k \} \right.$$

$$+ \frac{p^2}{q^2}\{ -\mu^2\cos^2\theta_k + \mu^4\cos^4\theta_k + 3\mu^2(1 - \mu^2)\cos^2\theta_k \sin^2\theta_k - \frac{1}{2}(1 - \mu^2)\sin^2\theta_k$$

$$\left. + \frac{3}{8}(1 - \mu^2)^2\sin^4\theta_k \} + \frac{2pk\mu}{q^2}\{\cos^2\theta_k - \mu^2\cos^4\theta_k - \frac{3}{2}(1 - \mu^2)\cos^2\theta_k \sin^2\theta_k \} \right\}$$

The emitted acoustic energy flux for a given frequency, calculated in τ space, is:

$$\vec{F}(t, \tau_i) = \frac{1}{16} \frac{\hat{\tau}_i}{|\tau_i|^2} \frac{(\omega^2 - \Omega_i^2)^{1/2}}{\omega} e^{2I_c} \int \frac{\rho_0(\tau_{0i})}{c_s(\tau_{0i})} d^3\tau_{0i}$$
$$\int_0^\infty dp \int_{-1}^{+1} d\mu \frac{E(q)E(p)}{q^2} g(p, q, \omega) f(\omega, k, p, q, \mu) \qquad (5.46)$$

The obtained results show that the temperature gradient leads to monopole and dipole type of emission, which is different than quadrupole emission that dominates in Lighthill's theory of sound generation.

CHAPTER 6

PROPAGATION OF TORSIONAL TUBE WAVES

Propagation of torsional tube waves in various magnetic flux tubes has been extensively discussed in the literature (see Chapter 2). However, it has been recently shown by Musielak, Routh and Hammer (2007) that the propagation of these waves inside a thin and isothermal magnetic flux tube is cutoff-free. Other important results are related to the origin of a cutoff frequency for torsional waves propagating inside a thick but isothermal flux tube (Routh, Musielak and Hammer 2007), and inside a thin but non-isothermal flux tube (Routh, Musielak and Hammer 2009). The results obtained in the above papers are described below.

6.1 Cutoff-Free Propagation of Torsional Waves

6.1.1 Formulation and governing equations

We consider an isolated and vertically oriented magnetic flux tube that is embedded in a magnetic field-free, compressible and isothermal medium. The tube has a circular cross-section and is in temperature equilibrium with the external medium. Let us introduce a global cylindrical coordinate system (r, ϕ, z), with z being the tube axis, and describe the background medium inside the tube by the gas density $\rho_0 = \rho_0(r, z)$, the gas pressure $p_0 = p_0(r, z)$ and the magnetic field $\vec{B}_0 = B_{or}(r, z)\hat{r} + B_{oz}(r, z)\hat{z}$. The physical properties of the external medium are determined by $\rho_e = \rho_e(r, z)$, $p_e = p_e(r, z)$ and $\vec{B}_e = 0$. Moreover, we also have $T_0 = T_e = $ const.

To describe torsional waves, we introduce $\vec{v} = v_\phi(r, z, t)\hat{\phi}$ and $\vec{b} = b_\phi(r, z, t)\hat{\phi}$, and assume that the waves are linear and purely incompressible, which means that both the perturbed density ρ and pressure p can be neglected. As a result of these assumptions, the propagation of the waves is fully described by the momentum and induction equations. The ϕ-component of the momentum equation can be written in the following form

$$\frac{\partial}{\partial t}\left(\frac{v_\phi}{r}\right) - \frac{1}{4\pi\rho_0 r^2}\left[B_{0r}\frac{\partial}{\partial r} + B_{0z}\frac{\partial}{\partial z}\right](rb_\phi) = 0 \ , \tag{6.1}$$

and the ϕ-component of the induction equation becomes

$$\frac{\partial}{\partial t}(rb_\phi) - r^2\left[B_{0r}\frac{\partial}{\partial r} + B_{0z}\frac{\partial}{\partial z}\right]\left(\frac{v_\phi}{r}\right) = 0 \ . \tag{6.2}$$

The derived momentum and induction equations are our basic equations for all the results derived and discussed in this chapter.

6.1.2 Thin flux tube approximation

Solar magnetic flux tubes are considered to be thin if their magnetic field is horizontally uniform, which means that at a given height all magnetic field lines have the same physical properties (e.g., Priest 1982). The essence of the so-called thin flux tube approximation (Roberts & Webb 1978, 1979; Spruit 1981, 1982; Priest 1982; Hollweg 1985; Ferriz-Mas, Schüssler, & Anton, 1989; Ferriz-Mas & Schüssler 1994; Musielak et al. 1995; Roberts & Ulmschneider 1997; Hasan et al. 2003) is that radial expansions around the axis of symmetry can be truncated at a low order. For the radial component of the magnetic field the leading term is of first order,

$$B_{0r}(r, z) = B_{0r}(r, z)|_{r=0} + r\left[\frac{\partial B_{0r}(r, z)}{\partial r}\right]_{r=0} + \ \dots \ , \tag{6.3}$$

since $B_{0r}(r = 0, z) = 0$ at the symmetry axis (cf. Ferriz Mas & Schüssler 1989). Away from the tube axis $B_{0r}(r, z)$ can be expressed in terms of r and $B_{0z}(z)$. Using the solenoidal condition $\nabla \cdot \vec{B}_0 = 0$, we obtain

$$B_{0r}(r, z) = -\frac{r}{2}B'_{0z}(z) \ , \tag{6.4}$$

where $B'_{0z} = dB_{0z}/dz$.

The thin flux tube approximation also requires that $\rho_0 = \rho_0(z)$, $p_0 = p_0(z)$, $B_{0z} = B_{0z}(z)$, $\rho_e = \rho_e(z)$, $p_e = p_e(z)$ and $T_0 = T_e = $ const. In addition, the horizontal pressure balance must be satisfied, $p_0 + B_{0z}^2/8\pi = p_e$ at $r = R_t$, where R_t is the tube radius. The increase of R_t with height is determined by the conservation of the magnetic flux $\pi R_t^2 B_{0z} = $ const. As a result of the above assumptions, the Alfvèn velocity $c_A = B_{0z}/\sqrt{4\pi\rho_0}$ remains constant along the entire length of a thin and isothermal magnetic flux tube, and $B'_{0z} = -B_{0z}/2H$, where the pressure (density) scale height H is also constant. For reasons explained in the next subsection, the wave variables v_ϕ and b_ϕ are considered here to be functions of time and both spatial coordinates r and z.

6.1.3 Wave equations

Using Eq. (6.4) and taking into account the fact that the variables r and z are independent in the global coordinate system, we write Eqs. (6.1) and (6.2) as

$$\frac{\partial v_\phi}{\partial t} + \frac{B'_{0z}}{8\pi\rho_0}\left(r\frac{\partial b_\phi}{\partial r} + b_\phi\right) - \frac{B_{0z}}{4\pi\rho_0}\frac{\partial b_\phi}{\partial z} = 0 \ , \tag{6.5}$$

and

$$\frac{\partial b_\phi}{\partial t} + \frac{B'_{0z}}{2}\left(r\frac{\partial v_\phi}{\partial r} - v_\phi\right) - B_{0z}\frac{\partial v_\phi}{\partial z} = 0 \ . \tag{6.6}$$

We combine the above equations and derive the wave equations for the wave variables $v_\phi(r, z, t)$ and $b_\phi(r, z, t)$

$$\frac{\partial^2 v_\phi}{\partial t^2} - c_A^2 \frac{\partial^2 v_\phi}{\partial z^2} + \frac{c_A^2}{2H} \frac{\partial v_\phi}{\partial z} - \frac{c_A^2}{16H^2} v_\phi$$

$$-c_A^2 \left(\frac{r}{4H}\right) \left[\left(\frac{r}{4H}\right) \frac{\partial^2 v_\phi}{\partial r^2} + 2\frac{\partial^2 v_\phi}{\partial r \partial z} - \frac{1}{4H} \frac{\partial v_\phi}{\partial r}\right] = 0 \ , \qquad (6.7)$$

and

$$\frac{\partial^2 b_\phi}{\partial t^2} - c_A^2 \frac{\partial^2 b_\phi}{\partial z^2} - \frac{c_A^2}{2H} \frac{\partial b_\phi}{\partial z} - \frac{c_A^2}{16H^2} b_\phi$$

$$-c_A^2 \left(\frac{r}{4H}\right) \left[\left(\frac{r}{4H}\right) \frac{\partial^2 b_\phi}{\partial r^2} + 2\frac{\partial^2 b_\phi}{\partial r \partial z} + \frac{3}{4H} \frac{\partial b_\phi}{\partial r}\right] = 0 \ . \qquad (6.8)$$

The derived wave equations show that the value of the parameter $(r/4H)$ determines the contributions of the r-dependence of the wave variables v_ϕ and b_ϕ to the propagation of torsional tube waves. For wide flux tubes, the contributions are important, however, for very thin flux tubes with $(r/4H) << 1$, the contributions become negligible. It must be noted that the limit $(r/4H) \to 0$ is not allowed because $v_\phi(r, z, t)|_{r=0} = 0$ and $b_\phi(r, z, t)|_{r=0} = 0$. From a physical point of view, this means that a flux tube reduced to a single magnetic field line cannot support torsional waves.

Since the derived wave equations have different forms for v_ϕ and b_ϕ, the wave variables behave differently. In the following, we transform these wave equations to new variables that obey the same wave equations.

6.1.4   Transformed wave equations

Using the transformations $v_\phi(r, z, t) = v(r, z, t)\rho^{-1/4}$ and $b_\phi(r, z, t) = b(r, z, t)\rho^{1/4}$ (see Musielak et al. 1995; Musielak & Ulmschneider 2001; Noble et al. 2003), we obtain

$$\frac{\partial^2 v}{\partial t^2} - c_A^2 \frac{\partial^2 v}{\partial z^2} - c_A^2 \left(\frac{r}{4H}\right) \left[\left(\frac{r}{4H}\right) \frac{\partial^2 v}{\partial r^2} + 2\frac{\partial^2 v}{\partial r \partial z} + \frac{1}{4H} \frac{\partial v}{\partial r}\right] = 0 \ , \qquad (6.9)$$

and

$$\frac{\partial^2 b}{\partial t^2} - c_A^2 \frac{\partial^2 b}{\partial z^2} - c_A^2 \left(\frac{r}{4H}\right) \left[\left(\frac{r}{4H}\right)\frac{\partial^2 b}{\partial r^2} + 2\frac{\partial^2 b}{\partial r \partial z} + \frac{1}{4H}\frac{\partial b}{\partial r}\right] = 0 \ . \tag{6.10}$$

Clearly, the behavior of the transformed wave variables v and b is identical.

To remove the first-order derivatives from the above equations, we use the transformation $d\zeta = (4H/r)dr$, which gives

$$\left(\frac{\partial^2}{\partial t^2} - c_A^2 \frac{\partial^2}{\partial z^2} - c_A^2 \frac{\partial^2}{\partial \zeta^2} - 2c_A^2 \frac{\partial^2}{\partial z \partial \zeta}\right) [v(\zeta, z, t); b(\zeta, z, t)] = 0 \ , \tag{6.11}$$

where $\zeta = 4H \ \ln|r|$. This is the most general equation that describes the propagation of torsional waves along thin and isothermal magnetic flux tubes. The equation shows that there is no cutoff frequency for torsional tube waves.

6.1.5 Dispersion relation

Since all the coefficients in Eq. (6.11) are constant, we make Fourier transforms in time and space, and derive the following dispersion relation

$$\omega^2 = (k_z^2 + 2k_z k_\zeta + k_\zeta^2)c_A^2 \ , \tag{6.12}$$

where ω is the wave frequency and k_z and k_ζ are the z and ζ components of the wave vector $\vec{k}$, respectively. Note that the same dispersion relation is obtained for each wave variable.

Let us define $\kappa = k_z + k_\zeta$ and write

$$\omega^2 = \kappa^2 c_A^2 \ , \tag{6.13}$$

which shows that the propagation of linear torsional Alfvén waves along thin and isothermal magnetic tube waves is not affected by any cutoff frequency.

6.1.6   Other approaches

To demonstrate that the propagation of torsional tube waves is cutoff-free, we used the global coordinate system and the original wave variables v_ϕ and b_ϕ, which were transformed to the new variables v and b. Two different approaches were developed by Ferriz-Mas et al. (1989), who adopted the same coordinate system but used different wave variables, and by Hollweg (1978, 1981, 1992), who chose a local coordinate system and introduced different wave variables (see also Edwin & Roberts 1983 and Poedts et al. 1985). In addition, Noble et al. (2003) considered the global coordinate system and used the wave variables v_ϕ and b_ϕ. However, their assumption that $B_{0r} = 0$ was inconsistent with the solenoidal condition, which makes their claim of the existence of the cutoff frequency for torsional Alfveén waves invalid. In the following, we demonstrate that the momentum and induction equations derived by Ferriz-Mas et al. and Hollweg lead to the same results as those found in this dissertation.

In their work on propagation of waves along thin magnetic flux tubes, Ferriz-Mas et al. (1989) used the global coordinate system and derived the first and second-order equations that describe the propagation of sausage, kink and torsional Alfvén tube waves. In their approach, each wave variable is expanded in a Taylor series and, specifically for torsional tube waves, the new variables $v_{\phi 1}$ and $b_{\phi 1}$, which represent the first order expansion in the series, are introduced. These variables are given by

$$v_{\phi 1}(z,t) = \frac{\partial v_\phi}{\partial r}\Big|_{r=0} \qquad \text{and} \qquad b_{\phi 1}(z,t) = \frac{\partial b_\phi}{\partial r}\Big|_{r=0} . \tag{6.14}$$

Since $v_\phi(r,z,t)|_{r=0} = 0$ and $b_\phi(r,z,t)|_{r=0} = 0$ (see Sec. 3.2), we may use Eq. (6.14) to write $v_\phi(r,z,t) = r v_{\phi 1}(z,t)$ and $b_\phi(r,z,t) = r b_{\phi 1}(z,t)$ in first order. Substituting these new variables into Eqs. (6.5) and (6.6), we obtain

$$\frac{\partial v_{\phi 1}}{\partial t} + \frac{1}{4\pi\rho_0}\left(B'_{0z} b_{\phi 1} - B_{0z}\frac{\partial b_{\phi 1}}{\partial z}\right) = 0 , \tag{6.15}$$

and

$$\frac{\partial b_{\phi 1}}{\partial t} - B_{0z}\frac{\partial v_{\phi 1}}{\partial z} = 0 \; , \tag{6.16}$$

which are the same equations as those obtained by Ferriz-Mas et al. (1989, see their Eqs. 14 and 16; note that our B_{r0} corresponds to their rB_{r1}, and v_z and v_r vanish in our case). Despite the fact that $v_{\phi 1}$ and $b_{\phi 1}$ depend solely on z and t, the above equations are not valid at the tube axis (see discussion above).

The wave equations resulting from the above momentum and induction equations become

$$\frac{\partial^2 v_{\phi 1}}{\partial t^2} - c_A^2\frac{\partial^2 v_{\phi 1}}{\partial z^2} = 0 \; , \tag{6.17}$$

and

$$\frac{\partial^2 b_{\phi 1}}{\partial t^2} - c_A^2\frac{\partial^2 b_{\phi 1}}{\partial z^2} - \frac{c_A^2}{H}\frac{\partial b_{\phi 1}}{\partial z} - \frac{c_A^2}{4H^2}b_{\phi 1} = 0 \; . \tag{6.18}$$

Clearly, the derived wave equations have different forms, which implies that the wave variables $v_{\phi 1}$ and $b_{\phi 1}$ behave differently. To remove the first-order derivative from Eq. (6.18), we use the transformation $b_{\phi 1}(z,t) = \tilde{b}_{\phi 1}(z,t)\rho^{1/2}$, and obtain

$$\frac{\partial^2 \tilde{b}_{\phi 1}}{\partial t^2} - c_A^2\frac{\partial^2 \tilde{b}_{\phi 1}}{\partial z^2} = 0 \; . \tag{6.19}$$

Hence, the behavior of the wave variables v_ϕ and $\tilde{b}_{\phi 1}$ is the same and there is no cutoff frequency that affects the wave propagation. This is an important result as it shows that the non-existence of a cutoff frequency for torsional tube waves is independent of the choice of the wave variables.

Propagation of torsional waves along magnetic flux tubes can also be described by using a local orthogonal curvilinear coordinate system (ξ, θ, s), with s being the length measured along a magnetic field line, θ the azimuthal angle about the axis of symmetry, and ξ a coordinate in the direction $\hat{\xi} = \hat{\theta} \times \hat{s}$. In this case, $\vec{B}_0 = B_{0s}(s)\hat{s}$, $B_{0\xi} = 0$ and $B_{0\theta} = 0$. We also have $\vec{v} = v_\theta(s,t)\hat{\theta}$, $\vec{b} = b_\theta(s,t)\hat{\theta}$ and $R = R(s)$, where R

represents the distance from the magnetic field line to the tube axis. This approach was first considered by Hollweg (1978), who also applied it to solar magnetic flux tubes (see Hollweg 1981, 1992).

Following Hollweg, Jackson, & Galloway (1982), the curvilinear scale factors are $h_\phi = R$ and $h_s = 1$, and we determine h_ξ from the condition $h_\xi \ R \ B_{0s} = $ const, which results from $\nabla \cdot \vec{B}_0 = 0$. To conserve the magnetic flux, we must choose $h_\xi = R$. Using these scale factors, the explicit form of the momentum and induction equations is

$$\frac{\partial}{\partial t}\left(\frac{v_\theta}{R}\right) - \frac{B_{0s}}{4\pi\rho_0 R^2}\frac{\partial}{\partial s}(Rb_\theta) = 0 \ , \tag{6.20}$$

and

$$\frac{\partial}{\partial t}(Rb_\theta) - R^2 B_{0s}\frac{\partial}{\partial s}\left(\frac{v_\theta}{R}\right) = 0 \ . \tag{6.21}$$

It is easy to see that the magnetic field $\vec{B}_0(s)$ in the local coordinate system can be described in the global coordinate system (see Eqs. 6.1 and 6.2) by the $B_{0r}(r,z)$ and $B_{0z}(r,z)$ field components. This means that the following relation must hold between the spatial operators in these two coordinate systems

$$B_{0r}\frac{\partial}{\partial r} + B_{0z}\frac{\partial}{\partial z} = B_{0s}\frac{\partial}{\partial s} \ . \tag{6.22}$$

This relation is consistent with the fact that $\vec{B}_0 \cdot \nabla$ must be the same in the global (the LHS of Eq. 6.22) and local (the RHS of Eq. 6.22) coordinate systems. Moreover, v_ϕ and v_θ are also related, as the former can be treated as a projection of the latter on the ϕ-axis of the global coordinate system. Obviously, the same is true for the wave variables b_ϕ and b_θ.

We follow Hollweg (1978, 1981) and introduce the new variables $x = v_\theta/R$ and $y = Rb_\theta$. The wave equations for these variables are

$$\frac{\partial^2 x}{\partial t^2} - c_A^2\frac{\partial^2 x}{\partial s^2} = 0 \ , \tag{6.23}$$

and

$$\frac{\partial^2 y}{\partial t^2} - \frac{\partial}{\partial s}\left(c_A^2 \frac{\partial y}{\partial s}\right) = 0 \; , \tag{6.24}$$

where in general $c_A = c_A(s)$. However, for thin magnetic flux tubes $c_A = $ const (see Sec. 3.1) and the wave equations become

$$\left(\frac{\partial^2}{\partial t^2} - c_A^2 \frac{\partial^2}{\partial s^2}\right)[x(s,t); y(s,t)] = 0 \; . \tag{6.25}$$

Again, no cutoff frequency exists. It is a significant (but expected) result that this non-existence of a cutoff frequency for torsional tube waves is independent of the choice of the coordinate system and the wave variables.

6.1.7   Implications of the obtained results

We considered the propagation of linear torsional waves along thin and isothermal magnetic flux tubes using the global coordinate system, and derived new wave equations describing this propagation. The derived wave equations were then used to demonstrate that no cutoff frequency exists for these waves, which means that torsional waves of any frequency are freely propagating along the tubes. We also showed that this result is independent of different choices of the coordinate systems and wave variables adopted by Ferriz-Mas et al. (1989) and Hollweg (1978, 1981, 1992).

As first shown by Defouw (1976) for sausage tube modes and by Spruit (1981) for kink tube modes, the propagation of both waves is affected by their corresponding cutoff frequencies. With their cutoff-free propagation, torsional Alfvén modes seem to be exceptional among the tube waves. In general, the existence of cutoff frequencies is caused by either gravity or gradients of the characteristic wave velocities, which result from an inhomogeneity of the background medium. In the cases discussed in this paper, the characteristic wave velocities are constant for all tube modes because of the thin flux tube approximation. Hence, it is gravity which leads to the origin of

the cutoff through either stratification (sausage tube waves) or buoyancy force (kink tube waves).

The fact that stratification leads to a cutoff frequency for acoustic waves propagating in a stratified and isothermal medium was first demonstrated by Lamb (1908, 1911). Since sausage tube waves are essentially acoustic waves guided by the tube magnetic field, and since they propagate in a stratified and isothermal medium inside the tube, it is stratification of the background medium that is responsible for the existence of the cutoff frequency for these waves.

The nature of kink tube waves is significantly different than sausage tube waves and yet it is again gravity that is responsible for the existence of the cutoff frequency for these waves. The main reason is that magnetic tension and buoyancy are the restoring forces for kink tube waves, and that the buoyancy force through its dependence on gravity leads to the cutoff frequency (e.g., Spruit 1982; Hollweg 1985), which is lower than that for sausage tube waves.

Now, despite some similarities between kink and torsional Alfvén tube waves, the main difference is that magnetic tension is the only restoring force for the latter. Since linear torsional tube waves have only purely axisymmetric twists in the ϕ-direction and show no pressure fluctuations, the twists are neither coupled to the gravitational force nor affected by stratification. As a result, no cutoff frequency can exist for linear torsional waves propagating along thin and isothermal magnetic flux tubes.

The cutoff-free propagation of torsional tube waves may have important implications on theories of wave heating of the solar and stellar atmospheres. The theoretical models of stellar chromospheres constructed by Fawzy et al. (2002a,b) are based on the amount of energy carried by acoustic waves and by sausage and kink tube waves; these waves are generated by turbulent motions in the solar and stellar

convection zones. The models point to a missing amount of heating for stars with high levels of activity. It is likely that the energy carried by torsional Alfvén waves could be used, at least partially, to account for these "heating gaps". Since there is no cutoff frequency for torsional tube waves, a broad spectrum of these waves is expected to be generated in the solar and stellar convection zones. The waves of different frequencies of this spectrum may transfer energy to different parts of the solar and stellar atmospheres. Hence, new studies are required to determine the efficiency of generation of torsional tube waves and their dissipation rates.

6.2 Non-isothermal and thin magnetic flux tubes

Our results described above showed that there is no global cutoff frequency for torsional tube waves propagating inside a thin and isothermal magnetic flux tube. From a physical point of view, the cutoff-free propagation of torsional tube waves can be explained by the fact that magnetic tension is the only restoring force for these waves and that neither stratification nor buoyancy force affects their propagation.

We now demonstrate that temperature gradients inside a thin, but *non-isothermal* magnetic flux tube lead to a cutoff frequency for torsional tube waves. We consider a tube that is in thermal equilibrium with the external medium. Since the temperature in the surrounding medium varies with height, our assumption implies that the same temperature gradient must be inside the flux tube. This vertical temperature gradient causes the characteristic speed of torsional tube waves and the pressure and density scale heights to vary with height. Having these physical parameters varying along the tube requires the method describe in Chapter 3 to determine local cutoff frequencies.

We study the effects of different temperature gradients on the local cutoff frequency by considering several power-law temperature models as well as a more real-

istic model of the solar atmosphere developed by Vernazza, Avrett & Loeser (1981).
The cutoff frequency is used to determine the conditions for the propagation of tor-
sional tube waves. The obtained results are also compared to recent observational
data which clearly indicate that torsional tube waves do exist in the solar atmosphere
(e.g., Bonet et al. 2008; Jess et al. 2009). According to Jess et al., there are oscilla-
tions in the solar atmosphere with periods ranging from 126 s to 700 s that can be
identified as a signature of torsional waves propagating along expanding magnetic flux
tubes. We use our theory to determine whether this range of frequencies corresponds
to the propagating torsional tube waves in the solar atmosphere.

6.2.1   Flux tube model and wave equations

We consider an axisymmetric, isolated and vertically oriented magnetic flux
tube whose cross-section is circular. The tube is assumed to be thin (e.g., Spruit
1981; Priest 1982; Roberts 1991; Stix 2004) and embedded in the magnetic-free solar
atmosphere with a vertical gradient of temperature. Since the tube is thin, its in-
ternal structure is assumed to be in thermal equilibrium with the external medium,
which means that the temperature inside and outside the tube is the same at a given
atmospheric height.

To describe the propagation of linear torsional waves inside this non-isothermal
magnetic flux tube, we use the cylindrical coordinate system (r, ϕ, z) and introduce
the wave variables $\vec{v} = v_\phi(r, z, t)\hat{\phi}$ and $\vec{b} = b_\phi(r, z, t)\hat{\phi}$. Following Musielak et al.
(2007), we write the ϕ-component of the linearized equation of motion as

$$\frac{\partial(v_\phi/r)}{\partial t} - \frac{1}{4\pi\rho_o r^2}\left[B_{or}\frac{\partial}{\partial r} + B_{oz}\frac{\partial}{\partial z}\right](rb_\phi) = 0 \ , \tag{6.26}$$

and the ϕ-component of the linearized induction equation as

$$\frac{\partial(rb_\phi)}{\partial t} - r^2\left[B_{or}\frac{\partial}{\partial r} + B_{oz}\frac{\partial}{\partial z}\right](v_\phi/r) = 0 \ , \tag{6.27}$$

where B_{or} and B_{oz} are the radial and vertical components of the tube magnetic field. Since the considered magnetic flux tube is thin, we use the thin flux tube approximation discussed above.

In addition, at $r = R_t$, where R_t is the tube radius, the horizontal pressure balance is satisfied

$$p_o + \frac{B_{oz}^2}{8\pi} = p_e \ , \tag{6.28}$$

with p_e being the gas pressure of the external medium.

We use Eq. (7.93) and take into account the fact that the variables r and z are independent of each other. This allows us to write Eqs. (7.89) and (7.90) as

$$\frac{\partial v_\phi}{\partial t} + \frac{1}{8\pi\rho_o} \left(r\frac{\partial b_\phi}{\partial r} + b_\phi \right) \frac{dB_{oz}}{dz} - \frac{B_{oz}}{4\pi\rho_o} \frac{\partial b_\phi}{\partial z} = 0 \ , \tag{6.29}$$

and

$$\frac{\partial b_\phi}{\partial t} + \frac{1}{2} \left(r\frac{\partial v_\phi}{\partial r} - v_\phi \right) \frac{dB_{oz}}{dz} - B_{oz}\frac{\partial v_\phi}{\partial z} = 0 \ . \tag{6.30}$$

As already mentioned above, the temperature inside the tube is $T_o = T_o(z)$ with $T_o(z) = T_e(z)$ because of the temperature equilibrium between the internal and external media.

Let us introduce the pressure scale height $H_o = H_o(z)$ given by

$$\frac{1}{p_o}\frac{dp_o}{dz} = \frac{1}{\rho_o}\frac{d\rho_o}{dz} + \frac{1}{T_o}\frac{dT_o}{dz} \equiv -\frac{1}{H_o} \ . \tag{6.31}$$

Since $H_o(z)$ is the same as the pressure scale height of the external medium $H_e(z)$, we maye write $H_o(z) = H_e(z) \equiv H(z) = C_s^2(z)/\gamma g$, where $C_s^2(z) \equiv C_{so}^2(z) = C_{se}^2(z)$ is the sound speed, g the gravitational acceleration, and γ the ratio of specific heats, which we assume to be constant. In addition, we introduce the Alfvén speed $C_A(z) = B_{oz}(z)/\sqrt{4\pi\rho_o(z)}$.

Using the horizontal pressure balance and applying the thin flux tube approximation ($r/H << 1$ and $r^2/H^2 << 1$), we obtain $[dB_{oz}(z)/dz]/B_{oz}(z) = -1/2H(z)$

and derive the following wave equations for torsional waves propagating inside the non-isothermal magnetic flux tube

$$\frac{\partial^2 v_\phi}{\partial t^2} - C_A^2 \frac{\partial^2 v_\phi}{\partial z^2} + \frac{C_A^2}{2H} \frac{\partial v_\phi}{\partial z} - \frac{C_A^2}{4H^2}\left(\frac{1}{4} + \frac{dH}{dz}\right) v_\phi = 0 \ , \tag{6.32}$$

and

$$\frac{\partial^2 b_\phi}{\partial t^2} - C_A^2 \frac{\partial^2 b_\phi}{\partial z^2} - \frac{C_A^2}{2H}\left(1 + \frac{4H}{C_A}\frac{dC_A}{dz}\right)\frac{\partial b_\phi}{\partial z} - \frac{C_A^2}{4H^2}\left(\frac{1}{4} + \frac{2H}{C_A}\frac{dC_A}{dz} - \frac{dH}{dz}\right) b_\phi = 0 \ . \tag{6.33}$$

The fact that the wave equations are different for v_ϕ and b_ϕ clearly implies that these wave variables behave differently in the non-isothermal medium and that both wave equations are needed to determine a cutoff frequency. It must also be noted that for an isothermal medium, where C_A and H are constants, Eqs. (7.97) and (6.33) reduce to the wave equations describing the propagation of torsional waves along a thin and isothermal magnetic flux tube is cutoff-free (see above).

6.2.2 Cutoff frequency with local time

In order to cast the above wave equations in their standard forms, we remove the terms with the first-order derivatives by using the following transformations

$$v_\phi(z,t) = v(z,t) \, \exp\left[\frac{1}{4}\int^z \frac{d\tilde{z}}{H}\right] \ , \tag{6.34}$$

and

$$b_\phi(z,t) = b(z,t) \, \exp\left[-\frac{1}{4}\int^z \left(1 + \frac{4H}{C_A}\frac{dC_A}{d\tilde{z}}\right)\frac{d\tilde{z}}{H}\right] \ . \tag{6.35}$$

The resulting wave equations are:

$$\frac{\partial^2 v}{\partial t^2} - C_A^2 \frac{\partial^2 v}{\partial z^2} = 0 \ , \tag{6.36}$$

and

$$\frac{\partial^2 b}{\partial t^2} - C_A^2 \frac{\partial^2 b}{\partial z^2} + \Omega_{crit}^2 b = 0 \ , \tag{6.37}$$

where Ω_{crit} is the critical frequency (Musielak, Fontenla, & Moore, 1992; Musielak et al. 2006) given by

$$\Omega^2_{crit} = C_A \frac{d^2 C_A}{dz^2} \ .$$

(6.38)

Note that the critical frequency for the wave variable v_ϕ is zero.

We make the Fourier transform in time $[v(t,z), b(t,z)] = [\tilde{v}(z), \tilde{b}(z)]e^{-i\omega t}$, where ω is the wave frequency. Then, Eqs (7.12) and (7.13) become

$$\left[\frac{\partial^2}{\partial z^2} + \frac{\omega^2}{C_A^2} \right] \tilde{v}(z) = 0 \ ,$$

(6.39)

and

$$\left[\frac{\partial^2}{\partial z^2} + \frac{\omega^2 - \Omega^2_{crit}}{C_A^2} \right] \tilde{b}(z) = 0 \ .$$

(6.40)

Since the physical parameters in the above equations depend on z, the range of ω that corresponds to propagating wave solutions can be determined by using the oscillation theorem (see Chapter 3). The theorem requires that the equations are compared to Euler's equation, for which the solutions are well-known (again see Chapter 3). As a result of this comparison, the wave propagation conditions and the turning-point frequencies are obtained. There are two conditions that must be obeyed in order to have propagating waves

$$\frac{\omega^2}{C_A^2(z)} > \frac{1}{4z^2} \ ,$$

(6.41)

and

$$\frac{\omega^2 - \Omega^2_{crit}}{C_A^2(z)} > \frac{1}{4z^2} \ .$$

(6.42)

The resulting turning-point frequencies (see Appendices B and C) for v_ϕ and b_ϕ are

$$\Omega^2_{tp,z,v}(z) = \frac{1}{4t_l^2(z)} \ ,$$

(6.43)

and

$$\Omega^2_{tp,z,b}(z) = \Omega^2_{crit}(z) + \frac{1}{4t_l^2(z)} \, , \tag{6.44}$$

where $t_l(z) = z/C_A(z)$ is a quantity with dimension of time, which we call "local time" hereafter, and which will later be compared to the wave travel time along a flux tube. According to the results of Appendix C, solutions of Eqs (7.15) and (7.16) describe propagating waves only if $\omega > \Omega_{tp,z,v}$ and $\omega > \Omega_{tp,z,b}$.

Typically, the larger turning-point frequency is identified as a cutoff frequency (Musielak et al. 2006; Routh et al. 2007). From a physical point of view, this choice guarantees that for any ω larger than the cutoff frequency, both wave variables are always described by the propagating wave solutions. In addition, the cutoff frequency separates the propagating and non-propagating (evanescent) wave solutions. Since the sign of d^2C_A/dz^2 determines the sign of Ω^2_{crit}, the cutoff frequency $\Omega_{cut,z}$ is either

$$\Omega_{cut,z}(z) = \Omega_{tp,z,b}(z) = \sqrt{\Omega^2_{crit}(z) + \frac{1}{4t_l^2(z)}} \, , \tag{6.45}$$

if $d^2C_A/dz^2 > 0$, or

$$\Omega_{cut,z}(z) = \Omega_{tp,z,v}(z) = \frac{1}{2t_l(z)} \, , \tag{6.46}$$

if $d^2C_A/dz^2 \le 0$. To determine the cutoff frequency, a model of the thin and non-isothermal magnetic flux tube has to be specified.

Our results show that the cutoff frequency depends on the local time $t_l(z)$, which is evaluated at each height in the model, and that $t_l(z)$ plays an important role in obtaining the cutoff frequency; only in cases when $\Omega_{crit} >> 1/2t_l$ and the cutoff is given by Eq. (7.21), the effects of t_l become negligible (see Sec. 5 and 6). As already discussed by Musielak et al. (2009) for transverse tube waves, $t_l(z)$ does not represent the actual wave travel time $t_w(z)$ because in order to evaluate the latter the expression $1/C_A(z)$ must be integrated over z in the model. We now introduce a method that allows us to express the cutoff frequency in terms of $t_w(z)$.

6.2.3   Cutoff frequency with actual wave travel time

We begin with the transformation $d\tau = dz/C_A(z)$ and write Eqs (7.97) and (6.33) as

$$\left[\frac{\partial^2}{\partial t^2} - \frac{\partial^2}{\partial \tau^2} + \left(\frac{C_A}{2H} + \frac{C_A'}{C_A}\right)\frac{\partial}{\partial \tau} - \frac{C_A^2}{4H^2}\left(\frac{1}{4} + \frac{H'}{C_A}\right)\right] v_\phi(\tau, t) = 0 \ , \qquad (6.47)$$

and

$$\left[\frac{\partial^2}{\partial t^2} - \frac{\partial^2}{\partial \tau^2} - \left(\frac{C_A}{2H} + \frac{C_A'}{C_A}\right)\frac{\partial}{\partial \tau} - \frac{C_A^2}{4H^2}\left(\frac{1}{4} + \frac{2H}{C_A}\frac{C_A'}{C_A} - \frac{H'}{C_A}\right)\right] b_\phi(\tau, t) = 0 \ , \quad (6.48)$$

where $C_A' = dC_A/d\tau$ and $H' = dH/d\tau$.

To remove the first order derivatives with respect to τ from these wave equations, we use the following transformations

$$v_\phi(\tau, t) = v(\tau, t)\exp\left[\frac{1}{2}\int^\tau \left(\frac{C_A}{2H} + \frac{C_A'}{C_A}\right)d\tilde{\tau}\right] \ , \qquad (6.49)$$

and

$$b_\phi(\tau, t) = b(\tau, t)\exp\left[-\frac{1}{2}\int^\tau \left(\frac{C_A}{2H} + \frac{C_A'}{C_A}\right)d\tilde{\tau}\right] \ , \qquad (6.50)$$

and obtain

$$\left[\frac{\partial^2}{\partial t^2} - \frac{\partial^2}{\partial \tau^2} + \Omega_{cr,v}^2(\tau)\right] v(\tau, t) = 0 \ , \qquad (6.51)$$

and

$$\left[\frac{\partial^2}{\partial t^2} - \frac{\partial^2}{\partial \tau^2} + \Omega_{cr,b}^2(\tau)\right] b(\tau, t) = 0 \ , \qquad (6.52)$$

where

$$\Omega_{cr,v}^2(\tau) = \frac{3}{4}\left(\frac{C_A'}{C_A}\right)^2 - \frac{1}{2}\frac{C_A''}{C_A} \ , \qquad (6.53)$$

and

$$\Omega_{cr,b}^2(\tau) = \frac{1}{2}\frac{C_A''}{C_A} - \frac{1}{4}\left(\frac{C_A'}{C_A}\right)^2 \ , \qquad (6.54)$$

with $C_A'' = d^2C_A/d\tau^2$. Note that $\Omega_{cr,v}$ and $\Omega_{cr,b}$ are known as the critical frequencies (Musielak, Fontenla, & Moore, 1992; Musielak et al. 2006; Routh et al. 2007), and that they are zero if there are no temperature gradients.

We make the Fourier transform in time $[v(\tau, t), b(\tau, t)] = [\tilde{v}(\tau), \tilde{b}(\tau)]e^{-i\omega t}$, where ω is the wave frequency. Then, Eqs (7.104) and (7.105) become

$$\left[\frac{\partial^2}{\partial \tau^2} + \omega^2 - \Omega_{cr,v}^2(\tau)\right] \tilde{v}(\tau) = 0 ,\qquad (6.55)$$

and

$$\left[\frac{\partial^2}{\partial \tau^2} + \omega^2 - \Omega_{cr,b}^2(\tau)\right] \tilde{b}(\tau) = 0 .\qquad (6.56)$$

Applying the oscillation and turning-point theorems (see Appendix B) and the results presented in Appendix C, we obtain the following turning-point frequencies

$$\Omega_{tp,\tau,v}^2(\tau) = \Omega_{cr,v}^2(\tau) + \frac{1}{4\tau^2} ,\qquad (6.57)$$

and

$$\Omega_{tp,\tau,b}^2(\tau) = \Omega_{cr,b}^2(\tau) + \frac{1}{4\tau^2} ,\qquad (6.58)$$

where

$$\tau(z) = \int^z \frac{d\tilde{z}}{C_A(\tilde{z})} + \tau_C ,\qquad (6.59)$$

with τ_C being an integration constant to be evaluated when flux tube models are specified (see Sec. 5). According to Eq. (7.112), the variable $\tau(z)$ is the actual wave travel time $t_w(z)$ from the base of a flux tube model to a given height z. Since $\tau(z) = t_w(z)$, the turning-point frequencies $\Omega_{tp,v}(\tau)$ and $\Omega_{tp,b}(\tau)$ do depend on the actual wave travel time but not on the local time (see Eqs 7.19 and 7.20).

The turning-point frequencies separate the solutions into propagating and non-propagating (evanescent) waves. Since there is a turning-point frequency for each wave variable, only one of them can be the cutoff frequency. We follow Musielak et al. (2006) and Routh et. al. (2007), and identify the largest turning-point frequency as the cutoff frequency. The choice is physically justified by the fact that in order to have propagating torsional tube waves at a given height z, the wave frequency ω

must always be higher than any turning-point frequency at this height; note that as a result of this choice both wave variables are always described by the propagating wave solutions. Thus, we can write

$$\Omega_{cut,\tau}(\tau) = \max[\Omega_{tp,\tau,v}(\tau), \Omega_{tp,\tau,b}(\tau)] \; , \tag{6.60}$$

and use it to determine the cutoff frequency for each τ.

According to Eq. (7.112), the variables τ and z are related to each other. Hence, we may use

$$\frac{1}{C_A}\frac{dC_A}{d\tau} = \frac{dC_A}{dz} \; , \tag{6.61}$$

and

$$\frac{1}{C_A}\frac{d^2C_A}{d\tau^2} = C_A\frac{d^2C_A}{dz^2} + \left(\frac{dC_A}{dz}\right)^2 \; , \tag{6.62}$$

to express the critical frequencies $\Omega^2_{cr,v}(\tau)$ and $\Omega^2_{cr,b}(\tau)$ in terms of z

$$\Omega^2_{cr,v}(z) = \frac{1}{2}\left[\frac{1}{2}\left(\frac{dC_A}{dz}\right)^2 - C_A\frac{d^2C_A}{dz^2}\right] \; , \tag{6.63}$$

and

$$\Omega^2_{cr,b}(z) = \frac{1}{2}\left[\frac{1}{2}\left(\frac{dC_A}{dz}\right)^2 + C_A\frac{d^2C_A}{dz^2}\right] \; . \tag{6.64}$$

The same conversion can be applied to the turning-point frequencies $\Omega^2_{tp,\tau,v}(\tau)$ and $\Omega^2_{tp,\tau,b}(\tau)$, and the results are

$$\Omega^2_{tp,\tau,v}(z) = \Omega^2_{cr,v}(z) + \frac{1}{4}\left[\int^z \frac{d\tilde{z}}{C_A(\tilde{z})} + \tau_C\right]^{-2} \; , \tag{6.65}$$

and

$$\Omega^2_{tp,\tau,b}(z) = \Omega^2_{cr,b}(z) + \frac{1}{4}\left[\int^z \frac{d\tilde{z}}{C_A(\tilde{z})} + \tau_C\right]^{-2} \; , \tag{6.66}$$

with the cutoff frequency given by

$$\Omega_{cut,\tau}(z) = \max[\Omega_{tp,\tau,v}(z), \Omega_{tp,\tau,b}(z)] \; . \tag{6.67}$$

Note that the effects of the wave travel time $t_w(z) = \tau(z)$ on the cutoff frequency are negligible when $\Omega_{cr,v} >> 1/2\tau$ and $\Omega_{cr,b} >> 1/2\tau$, which does occur in some flux tube models.

Specific flux tube models are needed to compare the cutoff frequency $\Omega_{cut,\tau}$ to $\Omega_{cut,z}$ that was obtained in Sec. 3 (see Eqs 7.21 and 7.22). Below we consider some models of a thin and non-isothermal magnetic flux tube, and make a comparison between these two cutoff frequencies.

Finally, we want to point out that when the following condition

$$\frac{1}{2}\left(\frac{dC_A}{dz}\right)^2 = C_A \frac{d^2 C_A}{dz^2} \ , \tag{6.68}$$

is satisfied, $\Omega_{cr,v}(z) = 0$ and $\Omega_{cr,b}(z) = \Omega_{crit}(z)$, where $\Omega_{crit}(z)$ is the critical frequency derived in Sec. 3 (see Eq. 7.14). To satisfy this condition, a solution in the form of a power law, to be compared with the models in the subsequent Sec. 5, must have the form of $C_A(z) = C_{A0}(z/z_0)^2$, where z_0 is a fixed atmospheric height and C_{A0} is the value of C_A at this height.

6.2.4   Specific flux tube models

We now assume that a thin and non-isothermal flux tube is embedded in an atmospheric model with the following temperature distribution (Routh 2006)

$$T_0(z) = T_{00}\xi^m \ , \tag{6.69}$$

where $\xi = z/z_0$ is the distance ratio, with z_0 being a fixed height in the model, and m can be any real number. We define T_{00} to be the temperature at z_0 and take $T_{00} = 5000$ K for all considered models. With $z_0 = 10$ km and $C_A(z_0) = C_{A0} = 10$ km/s, all our calculations begin at $\xi = 1$ and continue up to $\xi = 10$. Taking m to be a positive integer, we plot the Alfvén speed C_A as a function of z in models with m ranging from 1 to 5 in Fig. 6.1.
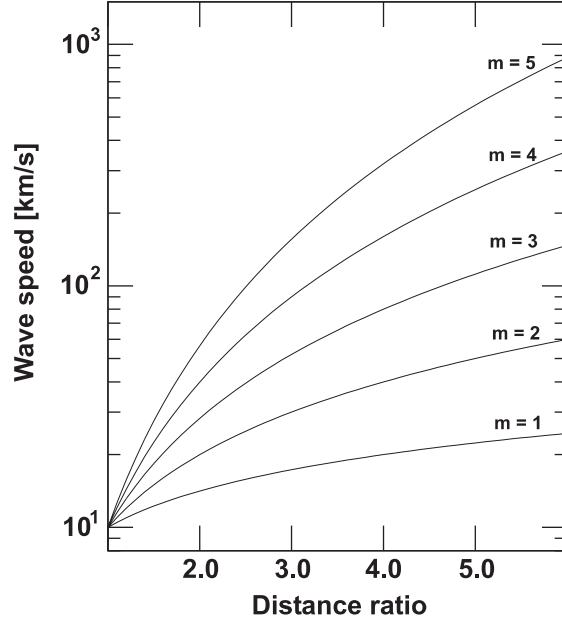
Figure 6.1. Alfvén speed C_A vs. the distance ratio z/z_0 for the power-law temperature models with m ranging from 1 to 5.

We consider two special cases of $m = 1$ and $m = 2$, and one general case of $m > 2$. For each model, we calculate the critical frequencies by using Eqs (6.63) and (6.64), the turning-point frequencies by using Eqs (6.65) and (6.66), and determine the cutoff frequency $\Omega_{cut,\tau}(\xi)$ from the condition given by Eq. (6.67). The calculations of the turning-point frequencies require evaluation of the variable τ, which represents the actual wave travel time t_w. This is done by using Eq. (7.112) in which the integration constant τ_C is evaluated by taking $\tau(\xi = 1) = \tau_0 = z_0/C_{A0}$, where C_{A0} is the value of C_A at z_0; we perform our calculations by taking $z_0 = 10$ km and $C_{A0} = 10$ km/s. Note that the integration constant is evaluated in the same way for all considered power-law models.

For comparison, we also calculate the critical frequency given by Eq. (7.14), and use Eqs (7.21) and (7.22) to determine the cutoff frequency $\Omega_{cut,z}(\xi)$. We now present and discuss the results.

Figure 6.2. Cutoff frequencies $\Omega_{cut,\tau}$ (solid lines) and $\Omega_{cut,z}$ (dashed lines) are plotted versus the distance ratio z/z_0 for the power-law models with $m = 1$ and $m = 2$.

6.2.5 Linear temperature models

For this model $T_0(\xi) = T_{00}\xi$, which gives $C_A(\xi) = C_{A0}\xi^{1/2}$. In this case, the turning-point frequency $\Omega_{tp,\tau,v}$ is always larger than $\Omega_{tp,\tau,b}$, and the cutoff frequency is

$$\Omega_{cut,\tau}(\xi) = \Omega_0 \left[\frac{3}{4} + \frac{\xi}{(2\xi^{1/2} - 1)^2} \right]^{1/2} \xi^{-1/2} , \qquad (6.70)$$

where $\Omega_0 = C_{A0}/2z_0$ has a fixed value at z_o. The plot of the normalized cutoff frequency $[\Omega_{cut,\tau}(\xi)/\Omega_0]$ versus ξ is shown in Fig. 6.2.

Since $d^2C_A/dz^2 < 0$, the cutoff frequency $\Omega_{cut,z}(\xi)$ is given by

$$\Omega_{cut,z}(\xi) = \Omega_0 \xi^{-1/2} , \qquad (6.71)$$

and the ratio of $\Omega_{cut,z}(\xi)/\Omega_0$ is compared to the normalized $\Omega_{cut,\tau}(\xi)$ in Fig. 2.

The comparison shows that $\Omega_{cut,\tau}$ is larger than $\Omega_{cut,z}$ throughout the model. The reason for the difference is the discrepancy between the actual wave travel time
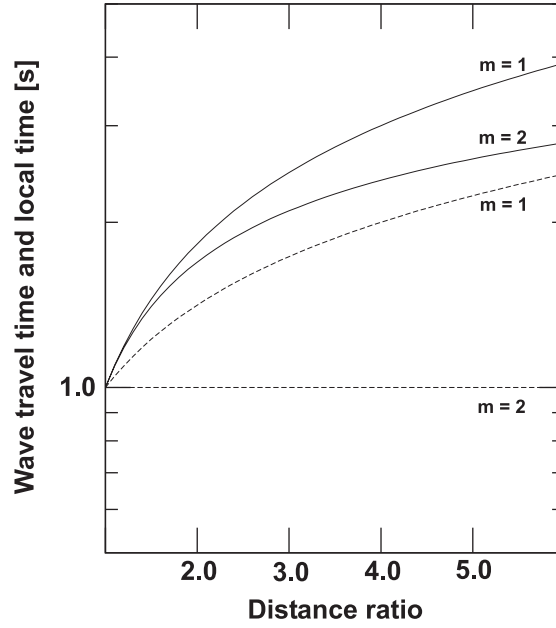
Figure 6.3. The actual wave travel time t_w (solid lines) and the local time t_l (dashed lines) are plotted versus the distance ratio z/z_0 for the power-law models with $m = 1$ and $m = 2$.

t_w, which mainly determines $\Omega_{cut,\tau}$, and the local time t_l, which uniquely establishes the value of $\Omega_{cut,z}$ for this model. The discrepancy between t_w and t_l is shown in Fig. 6.3.

6.2.6 Quadratic temperature models

With $T_0(\xi) = T_{00}\xi^2$, we find $C_A(\xi) = C_{A0}\xi$, which gives the same turning-point frequencies, and the cutoff frequency can be written as

$$\Omega_{cut,\tau}(\xi) = \Omega_0 \left[1 + \frac{1}{(1 + ln\xi)^2}\right]^{1/2} . \tag{6.72}$$

Since $d^2 C_A/dz^2 = 0$, the cutoff frequency $\Omega_{cut,z}(\xi)$ becomes

$$\Omega_{cut,z}(\xi) = \Omega_0 . \tag{6.73}$$

The normalized cutoff frequencies $\Omega_{cut,\tau}(\xi)$ and $\Omega_{cut,z}(\xi)$ are plotted in Fig. 6.2. The difference between these cutoff frequencies are even more prominent than those

found for the model with $m = 1$. The reason is that for the model with $m = 2$, both $\Omega_{cut,\tau}$ and $\Omega_{cut,z}$ are mainly determined by t_l and t_w, respectively, and that in addition $\Omega_{cut,z}$ and t_l are constant (see Figs 6.2 and 6.3).

6.2.7 Other power-law temperature models

We now consider the general case of $T_0(\xi) = T_{00}\xi^m$, where $m > 2$. This gives $C_A(\xi) = C_{A0}\xi^{m/2}$, and among the two turning-point frequencies $\Omega_{tp,\tau,b}$ is always larger than $\Omega_{tp,\tau,v}$. Hence, the cutoff frequency is

$$\Omega_{cut,\tau}(\xi) = \Omega_0 \left[\frac{m(3m-4)}{4}\xi^{m-2} + \frac{(m-2)^2}{(m-2\xi^{(2-m)/2})^2} \right]^{1/2} . \tag{6.74}$$

For this model d^2C_A/dz^2 is positive for all $m > 2$, thus the cutoff frequency $\Omega_{cut,z}(\xi)$ can be written as

$$\Omega_{cut,z}(\xi) = \Omega_0 \left[m(m-2) + 1 \right]^{1/2} \xi^{(m-2)/2} . \tag{6.75}$$

The normalized cutoff frequencies $\Omega_{cut,\tau}(\xi)$ and $\Omega_{cut,z}(\xi)$ are plotted in Fig. 6.4 for $m = 3$, 4 and 5. A surprising result is that the cutoff frequencies are very similar (see Fig. 6.4) despite large discrepancies between the actual wave travel time t_w and the local time t_l (see Fig. 5). This clearly implies that the contributions of t_w and t_l to the cutoffs are small when compared to the contributions of the critical frequencies $\Omega_{cr,b}$ and Ω_{crit}.

Specifically, we can use Eq. (7.47) to determine that the contributions due to Ω_{crit} exceed those due to t_l by a factor of $m(m-2)$, which means that for higher values of m the contributions of t_l are smaller. Very similar results are obtained from Eq. (7.46) for the contributions of $\Omega_{cr,b}$ and t_w. This shows that the critical frequencies play a dominant role in evaluating the cutoff frequencies for the models with $m > 2$. However, the opposite is true for the models with $m = 1$ and $m = 2$, as in these
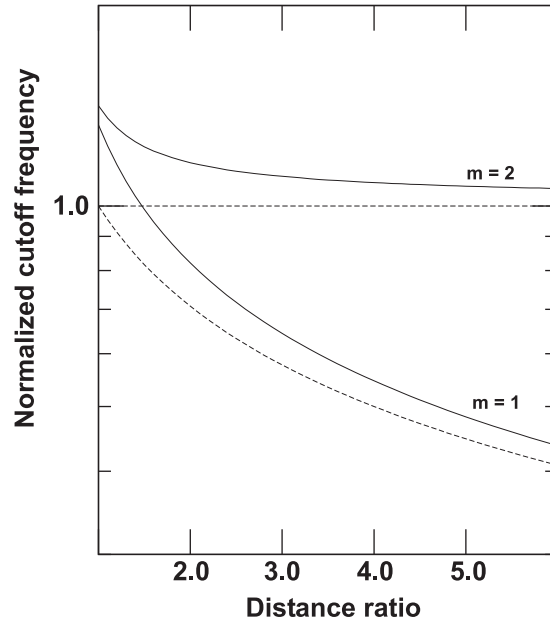
Figure 6.4. Cutoff frequencies $\Omega_{cut,\tau}$ (solid lines) and $\Omega_{cut,z}$ (dashed lines) are plotted versus the distance ratio z/z_0 for the power-law models with $m = 3$, $m = 4$ and $m = 5$.

models the cutoff frequencies were primarily determined by the contributions from t_w and t_l.

Among the three models described here, the model with $m = 4$ plays a special role because this is the only one considered in this paper that satisfies the condition given by Eq. (6.68). As a result, the critical frequencies $\Omega_{cr,b}$ and Ω_{crit} are equal and they dominate the respective contributions from t_w and t_l by a factor of 8 or more. Even so, the cutoff frequencies $\Omega_{cut,\tau}$ and $\Omega_{cut,z}$ are not exactly the same, actually, $\Omega_{cut,z} > \Omega_{cut,\tau}$ everywhere in the model (see Fig. 6.4). Hence, it is the contribution from t_l (see Fig. 6.5) to $\Omega_{cut,z}$ that accounts for these small differences despite the factor 8.

Our results show that the cutoff frequencies $\Omega_{cut,\tau}(\xi)$ and $\Omega_{cut,z}(\xi)$ are not the same in the power-law temperature models and that the values of the cutoffs rapidly

Figure 6.5. The actual wave travel time t_w (solid lines) and the local time t_l (dashed lines) are plotted versus the distance ratio z/z_0 for the power-law models with $m = 3$, $m = 4$ and $m = 5$.

increase when steeper temperature gradients are considered. There are also significant discrepancies between the actual wave travel time t_w and the local time t_l. However, the contributions of t_w and t_l to the respective cutoff frequencies $\Omega_{cut,\tau}(\xi)$ and $\Omega_{cut,z}(\xi)$ are model dependent; the contributions are dominant for the models with $m = 1$ and $m = 2$, and they become small for the models with $m > 2$.

6.2.8 Flux tube embedded in the VAL solar model

We now consider a thin and non-isothermal flux tube that is embedded in the VAL C model of the solar atmosphere (Vernazza et al. 1981), for which the height $z = 0$ corresponds to the unity optical depth and the temperature 6420 K. The model's lowest ($T_{min} = 4170$ K) and highest ($T_{max} = 4.47 \times 10^5$ K) temperatures are located at $z = 515$ km $z = 2543$ km, respectively. The model also extends below the

$z = 0$ height to $z = -206.65$ km, where the temperature is 1.017×10^4 K. We always start our calculations at the height $z = 0$ and continue to $z = 2543$ km.

In our calculations, we first determine the tube magnetic field by using $B_0(z) = B_{00}e^{-z/2H}$, where H is the scale height given by Eq. (7.96) and $B_{00} = B_0(z_0) = 1500$ Gs. Knowing $B_0(z)$, we use the horizontal pressure balance (see Eq. 7.93) to determine the gas pressure $p_0(z)$ inside the tube, and then $\rho_0(z)$. Having obtained $B_0(z)$ and $\rho_0(z)$, we compute the Alfvén speed C_A as a function of z in the model. Comparison of $C_A(z)$ to the sound speed C_s shows that $C_A(z) > C_s(z)$ in the entire model, which means that the plasma-β is lower than 1.

In order to evaluate the cutoff frequencies $\Omega_{cut,\tau}$ and $\Omega_{cut,z}$ (see Eqs 7.113 and 7.21 or 7.22), we must calculate the first and second derivatives of C_A with respect to z. Because the VAL model contains unequally spaced data, the calculations must be performed numerically. We use the method based on the second-order Lagrange polynomial P_2. The resulting cutoff frequencies are plotted in Fig. 6.6, which shows that $\Omega_{cut,z}$ is larger than $\Omega_{cut,\tau}$ in almost the entire model, except in the upper most layers where the cutoffs become practically the same.

To understand the differences between $\Omega_{cut,\tau}$ and $\Omega_{cut,z}$, we plot the local time $t_l(z)$ and the actual wave travel time $t_w(z) = \tau(z)$ in Fig. 7. It is seen that the differences between t_l and t_w are significant in the entire model, and that they are very prominent in the model's upper layers. Based on the comparison of $\Omega_{cut,\tau}$ to $\Omega_{cut,z}$, and t_w to t_l, it is easy to conclude that the contributions of t_w and t_l to the corresponding cutoff frequency are important only in the lower and middle layers of the model, because they must be negligible in the upper most layers. Our results in the model's upper layers must be taken with caution since the thin flux tube approximation breaks down in these atmospheric layers.
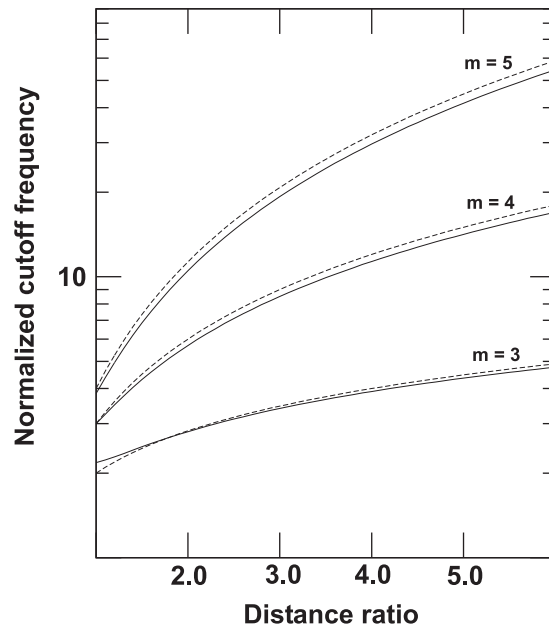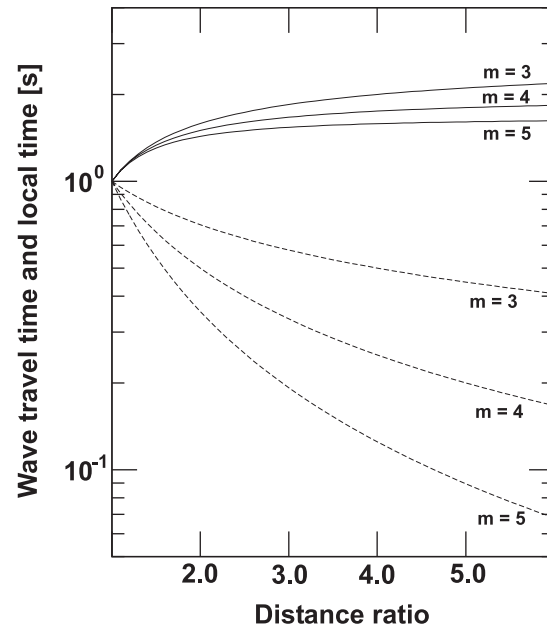
Figure 6.6. Cutoff frequencies $\Omega_{cut,\tau}$ (solid line) and $\Omega_{cut,z}$ (dashed line) are plotted versus height in the VAL C model of the solar atmosphere.
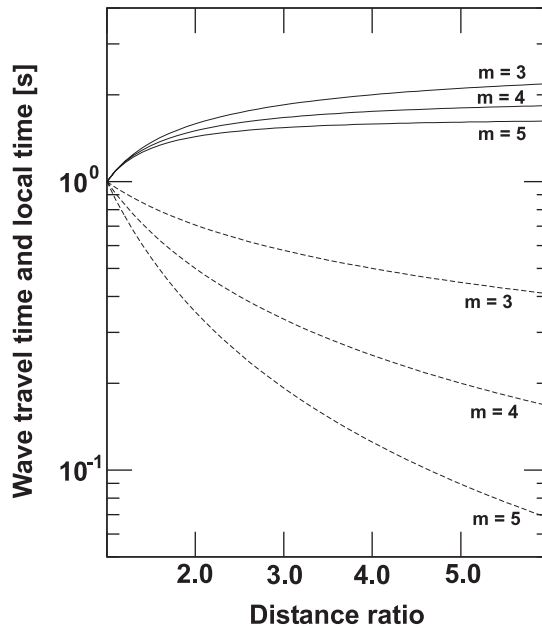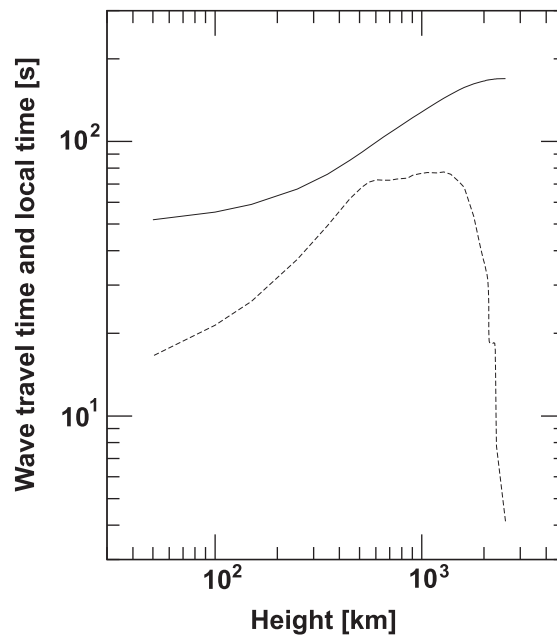

Figure 6.7. The actual wave travel time t_w (solid line) and the local time t_l (dashed line) are plotted versus height in the VAL C model of the solar atmosphere.

6.2.9   Discussion and comparison to observational data

The results presented in the last two sections clearly show that the cutoff frequencies $\Omega_{cut,\tau}$ and $\Omega_{cut,z}$ are not the same in most flux tube models considered in this paper. There are some models in which $\Omega_{cut,z}$ approximates rather well $\Omega_{cut,\tau}$, however, some differences always remain. Based on the fact that $\Omega_{cut,\tau}$ depends on t_w, which is the actual wave travel time, and $\Omega_{cut,z}$ depends on t_l, which is the local time, we consider $\Omega_{cut,\tau}$ to be the true cutoff frequency for torsional waves propagating inside a thin and non-isothermal magnetic flux tube.

An important result is that the true cutoff frequency is a local quantity that varies with height z. From a physical point of view, $\Omega_{cut,\tau}(z)$ represents locally the cutoff frequency in the atmosphere, and torsional waves must have their frequency ω higher than $\Omega_{cut,\tau}$ at a given height in order to reach this height and be propagating waves there. In other words, the cutoff allows us to determine the height in the model at which torsional waves of a given frequency become non-propagating waves.

The effects of different temperature gradients on the true cutoff frequency $\Omega_{cut,\tau}$ were studied in Sec. 5. According to the results, the true cutoff frequency decreases with height when $m = 1$, shows a small decrease near the model's base and then remains practically constant for $m = 2$, and increases with height when $m > 2$; in the latter case, the rate of increase is higher for larger values of m.

Our results obtained for a thin and non-isothermal flux tube embedded in the VAL C model of the solar atmosphere showed that the true cutoff frequency is 0.017 s^{-1} at the base of the model, increases to 0.02 s^{-1} in the middle chromosphere, and to 0.03 s^{-1} in the upper chromosphere. In addition, there is a steep increase of the true cutoff frequency in the upper most chromospheric layers and at the base of the solar transition region; however, these results should be taken with caution because

the thin flux tube approximation is not valid any longer in this part of the VAL C model.

In their recent paper, Jess et al. (2009) reported a detection of torsional tube waves with periods ranging from 126 s to 700 s, which corresponds to wave frequencies ω in the interval $[0.009, 005]$ s^{-1}. Comparison of this wave frequency interval to our theoretical results shows that the detected torsional waves with periods ranging from 126 s to 368 s are propagating waves at the base of the VAL C model. However, in the middle and upper chromosphere, the range's upper limit decreases to 314 s and 209 s, respectively. Hence, the wave period interval corresponding to the propagating detected waves decreases with the atmospheric height. The effect will be important in estimating periods of torsional tube waves that can reach the solar chromosphere and corona.

6.3 Isothermal and thick magnetic flux tube

In a thin flux tube, all magnetic field lines have the same physical properties across the tube, which means that the field has no structure in the horizontal direction. However, at a given height of a thick flux tube, each magnetic field line is characterized by different physical parameters and this leads to different Alfvén velocity for each line (e.g., Hollweg 1981). The results presented below show that the gradients of Alfvén velocity are responsible for the origin of a cutoff frequency for torsional waves propagating along the thick tube. The cutoff frequency that originates as a result of this inhomogeneity is a local quantity, and at a given atmospheric height torsional tube waves must have frequencies higher than the cutoff in order to be propagating waves at this height (Routh et al. 2007).

To determine this new cutoff frequency, the method described in Chapter 3 is used. The resulting cutoff frequency is calculated for specific models of solar magnetic

flux tubes. We discuss the physical meaning of this cutoff and show that in the limit of thin flux tube approximation the cutoff disappears, which is in agreement with the results described at the beginning of this chapter.

6.3.1 Formulation and basic equations

We consider an isolated and vertically oriented magnetic flux tube that is embedded in a magnetic field-free, compressible and isothermal medium that has the same density stratification as the solar atmosphere. The tube is untwisted, has a circular cross-section and is in temperature equilibrium with the external medium. According to Hollweg (1978, 1981, 1992; see also Kudoh & Shibata 1999, and Saito et al. 2001, for more recent work), propagation of torsional Alfvén waves along this flux tube can be described by using an orthogonal curvilinear coordinate system (ξ, θ, s), where s is a parameter along a given magnetic field line, θ is the azimuthal angle about the axis of symmetry, and ξ is a coordinate in the direction $\hat{\xi} = \hat{\theta} \times \hat{s}$. The background magnetic field becomes $\vec{B}_0 = B_{0s}(s)\hat{s}$, with $B_{0\xi} = 0$ and $B_{0\theta} = 0$. Since only linear torsional waves are considered, the pressure and density variations associated with the waves are neglected and the waves are described by $\vec{v} = v_\theta(s,t)\hat{\theta}$ and $\vec{b} = b_\theta(s,t)\hat{\theta}$.

We follow Hollweg, Jackson, & Galloway (1982) and introduce the curvilinear scale factors $h_\phi = R$, where $R = R(s)$ represents distance from the magnetic field line to the tube axis, $h_s = 1$, and $h_\xi = R$, with the latter being determined by the conservation of the magnetic flux. Using these scale factors, the following momentum and induction equations are obtained

$$\frac{\partial}{\partial t}\left(\frac{v_\theta}{R}\right) - \frac{B_{0s}}{4\pi\rho_0 R^2}\frac{\partial}{\partial s}(Rb_\theta) = 0 \ , \tag{6.76}$$

and

$$\frac{\partial}{\partial t}(Rb_\theta) - R^2 B_{0s} \frac{\partial}{\partial s}\left(\frac{v_\theta}{R}\right) = 0 \ . \tag{6.77}$$

These are the basic equations that describe the propagation of torsional waves along the magnetic flux tube embedded in the solar atmosphere.

6.3.2 Wave equations

We now combine Eqs. (6.76) and (6.77) and derive the wave equations for torsional tube waves. Two different sets of wave variables are considered, namely, v_θ and b_θ, and $x \equiv v_\phi/R$ and $y = Rb_\phi$. We selected these variables to study their behavior in the solar atmosphere.

6.3.3 Variables v_θ and b_θ

To derive the wave equations for the variables v_ϕ and b_ϕ, we use the conservation of magnetic flux $\pi R^2(s)B_{0s}(s) = \text{const}$ to express $R(s)$ in terms B_{0s}, and write Eqs. (6.76) and (6.77) as

$$\frac{\partial v_\theta}{\partial t} - \frac{1}{4\pi\rho_0}\left[B_{0s}\frac{\partial b_\theta}{\partial s} - \frac{1}{2}\left(\frac{dB_{0s}}{ds}\right)b_\theta\right] = 0 \ , \tag{6.78}$$

and

$$\frac{\partial b_\theta}{\partial t} - \left[B_{0s}\frac{\partial v_\theta}{\partial s} + \frac{1}{2}\left(\frac{dB_{0s}}{ds}\right)v_\theta\right] = 0 \ . \tag{6.79}$$

The wave equations resulting from the above equations are

$$\frac{\partial^2 v_\theta}{\partial t^2} - c_A^2\frac{\partial^2 v_\theta}{\partial s^2} - \frac{c_A^2}{B_{0s}}\left(\frac{dB_{0s}}{ds}\right)\frac{\partial v_\theta}{\partial s} + c_A^2\left[\frac{1}{4B_{0s}^2}\left(\frac{dB_{0s}}{ds}\right)^2 - \frac{1}{2B_{0s}}\left(\frac{d^2B_{0s}}{ds^2}\right)\right]v_\theta = 0 \ , \tag{6.80}$$

and

$$\frac{\partial^2 b_\theta}{\partial t^2} - c_A^2\frac{\partial^2 b_\theta}{\partial s^2} + c_A^2\left[\frac{1}{B_{0s}}\left(\frac{dB_{0s}}{ds}\right) - \frac{2}{c_A}\left(\frac{dc_A}{ds}\right)\right]\frac{\partial b_\theta}{\partial s}$$

$$+ c_A^2\left[\frac{1}{c_A}\left(\frac{dc_A}{ds}\right)\frac{1}{B_{0s}}\left(\frac{dB_{0s}}{ds}\right) - \frac{3}{4B_{0s}^2}\left(\frac{dB_{0s}}{ds}\right)^2 + \frac{1}{2B_{0s}}\left(\frac{d^2B_{0s}}{ds^2}\right)\right]b_\theta = 0 \ , \tag{6.81}$$

where $c_A(s) = B_{0s}(s)/\sqrt{4\pi\rho_0(s)}$ is the Alfvén velocity along a given magnetic field line. Note that the derived wave equations have different forms, which means that behavior of the wave variables v_ϕ and b_ϕ is not the same.

6.3.4 Hollweg's variables

Another set of wave equations is obtained for the wave variables $x \equiv v_\phi/R$ and $y = Rb_\phi$ originaly introduced by Hollweg (1981, 1992). Using these variables, we write Eqs. (6.76) and (6.77) as

$$\frac{\partial x}{\partial t} - \frac{B_{0s}}{4\pi\rho_0 R^2}\frac{\partial y}{\partial s} = 0 \ , \tag{6.82}$$

and

$$\frac{\partial y}{\partial t} - R^2 B_{0s}\frac{\partial x}{\partial s} = 0 \ . \tag{6.83}$$

Since the condition $B_{0s}R^2(s) = \text{const}$ must be satisfied, the wave equations for x and y are given by

$$\frac{\partial^2 x}{\partial t^2} - c_A^2(s)\frac{\partial^2 x}{\partial s^2} = 0 \ , \tag{6.84}$$

and

$$\frac{\partial^2 y}{\partial t^2} - \frac{\partial}{\partial s}\left[c_A^2(s)\frac{\partial y}{\partial s}\right] = 0 \ . \tag{6.85}$$

Again, the different forms of the derived wave equations reflect the fact that the wave variables x and y behave differently. Comparison of the above wave equations to those derived for the wave variables v_ϕ and b_ϕ (see Eqs. 6.76 and 6.77) clearly shows that each wave variable has different behavior. The comparison also shows that there is advantage in using Hollweg's variables because the wave equations for these variables are much simpler than those obtained for the variables v_ϕ and b_ϕ.

An interesting result is that Eqs. (6.84) and (6.85) are of the same forms as those derived by Musielak et al. (2006, see their Eqs. 5 and 6) in their studies of acoustic waves propagating in a non-isothermal medium.

6.3.5 Klein-Gordon equations

In the derived wave equations, the characteristic wave velocity, c_A, is a function of s. A general method to determine a cutoff frequency for such cases was developed by Musielak et al. (2006). The first step of this method is to transform the wave equations into the corresponding Klein-Gordon equations and then the cutoff frequency is derived by using the oscillation theorem (e.g., Kahn 1990).

6.3.6 Variables v_θ and b_θ

Let us introduce the new variable $d\tau = ds/c_A$ and write Eqs. (6.80) and (6.81) as

$$\frac{\partial^2 v_\theta}{\partial t^2} - \frac{\partial^2 v_\theta}{\partial \tau^2} + \left[\left(\frac{c_A'}{c_A} \right) - \left(\frac{B_{0s}'}{B_{0s}} \right) \right] \frac{\partial v_\theta}{\partial \tau}$$

$$+ \frac{1}{2} \left[\left(\frac{c_A'}{c_A} \right) \left(\frac{B_{0s}'}{B_{0s}} \right) + \frac{1}{2} \left(\frac{B_{0s}'}{B_{0s}} \right)^2 - \left(\frac{B_{0s}''}{B_{0s}} \right) \right] v_\theta = 0 \qquad (6.86)$$

and

$$\frac{\partial^2 b_\theta}{\partial t^2} - \frac{\partial^2 b_\theta}{\partial \tau^2} - \left[\left(\frac{c_A'}{c_A} \right) - \left(\frac{B_{0s}'}{B_{0s}} \right) \right] \frac{\partial b_\theta}{\partial \tau}$$

$$+ \frac{1}{2} \left[\left(\frac{c_A'}{c_A} \right) \left(\frac{B_{0s}'}{B_{0s}} \right) - \frac{3}{2} \left(\frac{B_{0s}'}{B_{0s}} \right)^2 + \left(\frac{B_{0s}''}{B_{0s}} \right) \right] b_\theta = 0 \qquad (6.87)$$

where $c_A' = dc_A/d\tau$, $B_{0s}' = dB_{0s}/d\tau$ and $B_{0s}'' = d^2 B_{0s}/d\tau^2$.

The terms with the first-order derivatives can be removed from these equations by using the following transformations: $v_\theta(t, \tau) = \tilde{v}_\theta(t, \tau)e^{\zeta/2}$ and $b_\theta(t, \tau) = \tilde{b}_\theta(t, \tau) e^{-\zeta/2}$, where $\zeta = \int_{\tau_0}^{\tau} [c_A'(\tilde{\tau})/c_A(\tilde{\tau}) - B_{0s}'(\tilde{\tau})/B_{0s}(\tilde{\tau})] \, d\tilde{\tau}$; note that τ_0 is chosen in such a way that the constant resulting from the lower limit of the integration is zero. The resulting Klein-Gordon equations are

$$\left[\frac{\partial^2}{\partial t^2} - \frac{\partial^2}{\partial \tau^2} + \Omega_{v,b}^2(\tau) \right] [\tilde{v}(t, \tau), \tilde{b}(t, \tau)] = 0 , \qquad (6.88)$$

where Ω_v and Ω_b are known as the critical frequencies (Musielak, Fontenla, & Moore 1992) and are given by

$$\Omega_v^2(\tau) = \frac{3}{4}\left(\frac{c_A'}{c_A}\right)^2 - \frac{1}{2}\left(\frac{c_A''}{c_A}\right) , \tag{6.89}$$

and

$$\Omega_b^2(\tau) = \frac{1}{2}\left(\frac{c_A''}{c_A}\right) - \frac{1}{4}\left(\frac{c_A'}{c_A}\right)^2 , \tag{6.90}$$

where $c_A'' = d^2 c_A/d\tau^2$.

6.3.7 Hollweg's variables

Using $d\tau = ds/c_A$, we write Eqs. (6.84) and (6.85) in the following form:

$$\frac{\partial^2 x}{\partial t^2} - \frac{\partial^2 x}{\partial \tau^2} + \left(\frac{c_A'}{c_A}\right)\frac{\partial x}{\partial \tau} = 0 , \tag{6.91}$$

and

$$\frac{\partial^2 y}{\partial t^2} - \frac{\partial^2 y}{\partial \tau^2} - \left(\frac{c_A'}{c_A}\right)\frac{\partial y}{\partial \tau} = 0 , \tag{6.92}$$

where $c_A' = dc_A/d\tau$.

To remove the first order derivatives from these equations, we use $x(t,\tau) = \tilde{x}(t,\tau)e^{\zeta/2}$ and $y(t,\tau) = \tilde{y}(t,\tau)e^{-\zeta/2}$, where $\zeta = \int_{\tau_0}^{\tau}[c_A'(\tilde{\tau})/c_A(\tilde{\tau})]\ d\tilde{\tau}$; again, τ_0 is chosen so that the lower limit of the integration is zero. Thus, the transformed wave equations become the Klein-Gordon equations

$$\left[\frac{\partial^2}{\partial t^2} - \frac{\partial^2}{\partial \tau^2} + \Omega_{x,y}^2(\tau)\right][\tilde{x}(t,\tau), \tilde{y}(t,\tau)] = 0 , \tag{6.93}$$

where Ω_x and Ω_y are the critical frequencies given by

$$\Omega_x^2(\tau) = \frac{3}{4}\left(\frac{c_A'}{c_A}\right)^2 - \frac{1}{2}\left(\frac{c_A''}{c_A}\right) , \tag{6.94}$$

and

$$\Omega_y^2(\tau) = \frac{1}{2}\left(\frac{c_A''}{c_A}\right) - \frac{1}{4}\left(\frac{c_A'}{c_A}\right)^2 , \tag{6.95}$$

with $c_A'' = d^2 c_A / d\tau^2$.

Comparison of the critical frequencies for the wave variables v_ϕ, b_ϕ, x and y shows that $\Omega_v = \Omega_x$ and $\Omega_b = \Omega_y$. This means that v_ϕ behaves as x and that b_ϕ and y have also the same behavior. Note that along s all wave variables behave differently (see Eqs. 6.80, 6.81, 6.84 and 6.85).

6.3.8   Cutoff frequency

Having derived the critical frequencies for all considered wave variables, we now introduce the so-called turning point frequencies (see Chapter 3). Let us make Fourier transforms in time of Eqs. (6.88) and (6.93), and obtain

$$\left[\frac{d^2}{d\tau^2} + \left(\omega^2 - \Omega_{v,b}^2(\tau) \right) \right] (\tilde{v}, \tilde{b}) = 0 . \tag{6.96}$$

and

$$\left[\frac{d^2}{d\tau^2} + \left(\omega^2 - \Omega_{x,y}^2(\tau) \right) \right] (\tilde{x}, \tilde{y}) = 0 . \tag{6.97}$$

The above equations can now be compared to the Euler equation, for which the solutions are well-known (e.g., Edwards & Penney 1989). We introduce $\Omega_1 = \Omega_v = \Omega_x$ and $\Omega_2 = \Omega_b = \Omega_y$, and define the turning point frequencies Ω_{tp} (see Appendix) as

$$\Omega_{tp,1,2}^2 - \Omega_{1,2}^2 = \frac{1}{4\tau^2} . \tag{6.98}$$

These frequencies separate the solutions into propagating and non-propagating (evanescent) waves. Since there is the turning point frequency for each wave variable, only one of them can be the cutoff frequency. We follow Musielak et al. (2006) and identify the largest turning point frequency as the cutoff frequency. The choice is physically justified by the fact that in order to have propagating torsional tube waves, the wave frequency ω must always be higher than any turning point frequency. In order to determine which turning point freqeuncy is larger, we need to specify a model of magnetic flux tubes embedded in the solar atmosphere.

6.3.9 Conditions for torsional wave propagation

6.3.10 Thin magnetic flux tubes

The structure of a single, thin and isothermal magnetic flux tube embedded in the solar atmosphere is well-known, i.e., the tube magnetic field diverges exponentially with height as a result of the density stratification and, at a given height, the field is uniform in the horizontal direction. Obviously, the validity of this simple flux tube model in the solar atmosphere is restricted to the upper layers of the solar convection zone, the photosphere and the lowest part of the solar chromosphere. According to Priest (1982), Hollweg (1985) and Roberts & Ulmschneider (1997), the thin flux tube approximation becomes invalid approximately 500 km above the solar temperature minimum. Above this height, solar magnetic flux tubes must be treated as wide tubes (see the next subsection).

At the beginning of this chapter, we showed that the propagation of torsional waves along thin and isothermal magnetic flux tubes is cutoff-free. Here, we confirm this result by applying the condition $c_A = $ const, valid for thin and isothermal flux tubes (e.g., Hollweg 1990; Roberts 1991), to Eqs. (6.89), (6.90), (6.94) and (6.95), and obtaining $\Omega_v = \Omega_x = \Omega_b = \Omega_y = 0$. Since all critical frequencies are zero, there is no cutoff frequency for the wave propagation. Note that the same result is obtained when the condition is directly applied to the wave equations given by Eqs. (6.84) and (6.85).

6.3.11 Thick magnetic flux tubes

A single and isothermal magnetic flux tube is considered to be wide when its horizontal magnetic field is non-uniform, which means that each magnetic field line has different physical properties in the horizonatal direction. Let us assume that this tube is approximated by a simple model in which the Alfén velocity varies

exponentially along a given field line; the model was originally considered by Hollweg (1981) and we shall use it here to determine the cutoff frequency for torsional tube waves propagating in this model.

For the exponential model, we have $c_A(s) = c_{A0}e^{s/mh}$, where $c_{A0} = c_A(s = 0)$, m is a positive scaling factor and h is the characteristic scale height; we take $h = H$, with H being the pressure (density) scale height. The reason for choosing different values of m is that, in general, $c_A(s)$ must be different for each magnetic field line. To calculate $\tau(s)$, we use

$$\tau = \int_{s_0}^{s} \frac{d\tilde{s}}{c_A(\tilde{s})} \; , \tag{6.99}$$

and obtain $\tau - \tau_0 = -mH/C_A(s)$; where $\tau_0 = mH/C_A(s_0)$

We write $c_A = mH/(\tau - \tau_0)$ and calculate

$$\left(\frac{c_A'}{c_A}\right)^2 = \frac{1}{(\tau - \tau_0)^2} \qquad \text{and} \qquad \frac{c_A''}{c_A} = \frac{2}{(\tau - \tau_0)^2} \; . \tag{6.100}$$

Now, the turning point frequencies are calculated by using Eq. (6.98) and also Eqs. (6.94) and (6.95), the cutoff frequency becomes $\Omega_{cut} = \Omega_{tp,2}$ as $\Omega_{tp,2}$ is the larger one.

$$\Omega_{cut}(\tau) = \frac{1}{\tau} \qquad \text{or} \qquad \Omega_{cut}(s) = \frac{c_A(s)}{2mH}\left[3 + \frac{\exp{(2s_0/mH)}}{(\exp{(s/mH)} - \exp{(s_0/mH)})^2}\right]^{1/2} \; . \tag{6.101}$$

To calculate the cutoff frequency for solar magnetic flux tubes, we consider a magnetic flux tube with $B_0 = 1500$ G at the atmospheric height $s = 0$, which corresponds to the location in the solar atmosphere where the flux tubes have widened enough, so that c_A is no longer constant but increases exponentially with height. This height level depends on the local magnetic filling factor and typically it should lie at the solar temperature minimum level or in the lowermost chromosphere. As the characteristic temperature for our models, we choose the effective temperature
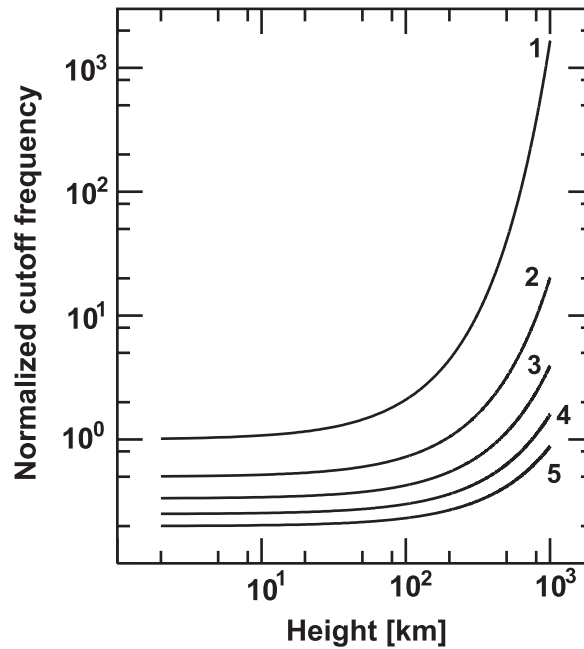
Figure 6.8. The cutoff frequency Ω_{cut}, normalized by c_{A0}/H, is plotted versus s for the exponential model with $m = 1$, 2, 3, 4 and 5 (the labels on the curves). All models are isothermal and the location of the solar temperature minimum is the base of the models.

of the Sun, $T_{eff} = 5770$ K. All considered models are isothermal with T_{eff}. This gives $c_{A0} = 11.0$ km/s and $H = 135$ km. The cutoff frequency Ω_{cut} is plotted as a function of s for different values of m in Fig. 6.8. As expected, the cutoff is much steeper for low values of m. It is also seen that the effect of the cutoff on the wave propagation becomes important at atmospheric heights higher than 100 km above the solar temperature minimum.

Clearly, the cutoff frequency is a local quantity that varies with s in the same way as c_A does. Since Ω_{cut} depends on height, its physical meaning is different than the global cutoff frequencies for longitudinal and transverse tube waves obtained by Defouw (1976) and Spruit (1981), respectively. From a physical point of view, $\Omega_{cut}(s)$ represents locally the cutoff in the atmosphere and torsional tube waves must have their frequency ω higher than Ω_{cut} at a given height in order to reach this height

and be propagating waves at this height. In other words, the cutoff allows us to determine the height s in the model at which torsional waves of a given frequency become non-propagating waves.

6.3.12 Discussion

The results presented in this paper showed that there is no global cutoff frequency for torsional waves propagating along thin and isothermal magnetic flux tubes; the same result was already obtained by Musielak et al. (2007). Since there are global cutoff frequencies for both longitudinal (Defouw 1976) and transverse (Spruit 1981) tube waves, the cutoff-free propagation of torsional tube waves seems to be exceptional. In the following, we discuss the reason for these differences and also present physical arguments that justify the existence of local cutoff frequencies for wide magnetic flux tubes.

From a physical point of view, the existence of cutoff frequencies can be caused either by the effects of gravity, such as density stratification and buoyancy force, or by gradients of the characteristic wave velocities that result from an inhomogeneity of the background medium. As discussed by Musielak et al. (2007), the density stratification of the solar atmosphere is responsible for the existence of the global cutoff frequency for longitudinal tube waves, and the buoyancy force leads to the existence of the global cutoff frequency for transverse tube waves. However, for torsional tube waves the situation is different because the purely axisymmetric twists in the ϕ-direction responsible for the existence of these waves are neither coupled to the gravitational force nor affected by the density stratification. As a result, no cutoff frequency for torsional tube waves can be introduced by the effects of gravity.

As mentioned above, cutoff frequencies can also be introduced by gradients of the characteristic wave velocities (e.g., Musielak et al. 2006). These gradients

are not present in thin and isothermal magnetic flux tubes, since $c_A = $ const (see Sec. 5.1), however, they may dominate the wave propagation in wide flux tubes for which $c_A \neq$ const. In such tubes, different magnetic field lines at a given height have different physical properties and, in addition, each field line is characterized by the Alfvén velocity that varies along the line. These variations of the wave velocity along different field lines lead to the cutoff frequency that becomes a local quantity and has a significantly different physical meaning that the global cutoff. In this paper, we demonstrated how to determine the local cutoff frequency (see Sec. 4) and explained the role played by this frequency in the wave propagation.

CHAPTER 7

PROPAGATION OF TRANSVERSE TUBE WAVES

The results described in Chapter 2 showed that the existence of the global cutoff frequencies for longitudinal and transverse waves is restricted to thin and isothermal magnetic flux tubes. However, our results presented in Chapter 6 demonstrated that the propagation of torsional waves inside such tubes is cutoff-free. In more general cases when the flux tubes are either wide and isothermal, or thin and non-isothermal, or thick and non-isothermal, the resulting cutoff frequencies are local and they depend on atmospheric height (Routh, Musielak & Hammer 2007).

We now use the method described in Chapter 3 to derive the cutoff frequency for transverse waves propagating along a thin and non-isothermal magnetic flux tube embedded in the solar atmosphere. The effects of temperature gradients on the cutoff frequency are studied for several power-law temperature models as well as for the solar atmosphere model given by Vernazza, Avrett & Loeser (1981). New results are also presented for a thick and isothermal magnetic flux tube. The height dependence of the cutoff frequency in these flux tubes models is calculated and it is shown that the value of this cutoff at a given atmospheric height determines the frequency that transverse tube waves must have in order to be propagating at this height. The results are compared to those previously obtained for a thin and isothermal magnetic flux tube. We also briefly discuss implications of our results for the heating of the solar atmosphere and its oscillations.

7.1 Non-isothermal and thin magnetic flux tubes

7.1.1 Flux tube model and governing equations

We consider a thin and non-isothermal magnetic flux tube that is embedded in the solar atmosphere. The tube is assumed to be isolated with its axis oriented vertically along the z-axis, so that gravity $\vec{g} = -g\hat{z}$. The tube density, pressure and temperature are respectively given by $\rho_0 = \rho_0(z)$, $p_0 = p_0(z)$ and $T_0 = T_0(z)$. Since the tube is thin, its magnetic field is approximated by taking $\vec{B}_0 = B_0(z)\vec{\hat{z}}$ (e.g., Priest 1982; Hollweg 1985; Ferriz-Mas et al. 1989; Roberts 1991).

The density, pressure and temperature of the external magnetic-free atmosphere are represented by $\rho_e = \rho_e(z)$, $p_e = p_e(z)$ and $T_e = T_e(z)$, respectively. We assume that the tube is in thermal equilibrium with its surroundings, which means that $T_0(z) = T_e(z) = T(z)$ and that the sound speed inside and outside the tube is the same at each height z, so we can write $c_{s0}(z) = c_{se}(z) = c_s(z)$. Our assumption of thermal equilibrium can be justified by the fact that the considered tube is thin.

Based on this assumption, the pressure scale heights $H_0(z) = c_{s0}^2(z)/\gamma g$ and $H_e(z) = c_{se}^2(z)/\gamma g$, where γ is the ratio of specific heats, are also equal. Hence, we have $H_0(z) = H_e(z) = H(z)$, with $H(z) = c_s^2/\gamma g$.

The gas and magnetic pressure inside the tube is balanced by the gas pressure in the external medium. This is the tube's horizontal pressure balance that must be satisfied at each height z. Typically, the balance is given by

$$p_0(z) + \frac{B_0^2(z)}{8\pi} = p_e(z) \ . \tag{7.1}$$

Let us consider linear oscillations of the tube with the velocity $\vec{v}$ and the magnetic field $\vec{b}$. Taking $\vec{B} = \vec{B}_0 + \vec{b}$, with $|\vec{b}| << |\vec{B}_0|$, the linearized momentum equation describing these oscillations is

$$\rho_0 \frac{\partial \vec{v}}{\partial t} = -\nabla \left(p_0 + \frac{B_0^2}{8\pi} \right) + \rho_0 \vec{g} + \frac{1}{4\pi} \left(\vec{B}_0 \cdot \nabla \right) \vec{B}_0$$

$$+ \frac{1}{4\pi} \left(\vec{B}_0 \cdot \nabla \right) \vec{b} \; . \tag{7.2}$$

Since the tube oscillates, its motion is responsible for generating a flow in the external medium. The equation of motion for this flow is

$$\rho_e \frac{\partial \vec{u}}{\partial t} = -\nabla p_e + \rho_e \vec{g} \; , \tag{7.3}$$

where $\vec{u}$ is the velocity of the external fluid.

We combine Eqs (7.90) and (7.91), and use Eq. (7.89) to obtain

$$\rho_0 \frac{\partial \vec{v}}{\partial t} - \rho_e \frac{\partial \vec{u}}{\partial t} = -(\rho_e - \rho_0)\vec{g} + \frac{1}{4\pi} \left(\vec{B}_0 \cdot \nabla \right) \vec{B}_0$$

$$+ \frac{1}{4\pi} \left(\vec{B}_0 \cdot \nabla \right) \vec{b} \; . \tag{7.4}$$

To describe the propagation of transverse tube waves, we assume that these waves are linear and that they can be represented by the perturbed velocity $\vec{v}(z,t) = v_x(z,t)\vec{x}$ and magnetic field $\vec{b}(z,t) = b_x(z,t)\vec{x}$; note that our restriction to tube oscillations in the x-direction is made without any loss of generality as there is no physical distinction between the x and y directions. Since for purely transverse tube waves the tube cross section remains unchanged, the density and pressure perturbations caused by these waves can be neglected.

With the above assumptions, the horizontal component of Eq. (7.92) becomes

$$\rho_0 \frac{\partial v_x}{\partial t} - \rho_e \frac{\partial u_x}{\partial t} - \frac{B_0}{4\pi} \frac{\partial b_x}{\partial z} = 0 \; . \tag{7.5}$$

Since at the tube boundary $u_x = -v_x$, we write the above equation as

$$\frac{\partial v_x}{\partial t} - \frac{c_k^2}{B_0} \frac{\partial b_x}{\partial z} = 0 \; , \tag{7.6}$$

where

$$c_k(z) = \frac{B_0(z)}{\sqrt{4\pi[\rho_0(z) + \rho_e(z)]}} \; . \tag{7.7}$$

Additional MHD equation that is needed to fully describe the wave propagation is the induction equation

$$\frac{\partial \vec{b}}{\partial t} - \nabla \times (\vec{v} \times \vec{B}_0) = 0. \tag{7.8}$$

The horizontal component of the above equation is

$$\frac{\partial b_x}{\partial t} - B_0 \frac{\partial v_x}{\partial z} = 0 . \tag{7.9}$$

We use the above equations to derive one-dimensional wave equations for the variables $v_x(z,t)$ and $b_x(z,t)$.

7.1.2 Wave equations and conditions for propagating wave solutions

We combine Eqs (7.94) and (7.97), and derive the following wave equations

$$\frac{\partial^2 v_x}{\partial t^2} - c_k^2(z)\frac{\partial^2 v_x}{\partial z^2} + \frac{c_k^2(z)}{2H(z)}\frac{\partial v_x}{\partial z} = 0 , \tag{7.10}$$

and

$$\frac{\partial^2 b_x}{\partial t^2} - c_k^2(z)\frac{\partial^2 b_x}{\partial z^2} - \frac{c_k^2(z)}{2H(z)}\frac{\partial b_x}{\partial z}$$
$$-2c_k(z)\left[\frac{dc_k(z)}{dz}\right]\frac{\partial b_x}{\partial z} = 0 . \tag{7.11}$$

These equations show that the behavior of the wave variables v_x and b_x in time and space depends on the local values of both c_k and H, and that the behavior of b_x is also affected by a gradient of c_k. Since the wave equations have different forms, the behavior of the wave variables v_x and b_x is also different.

To remove the first-order derivatives from the wave equations and write these equations in their standard forms, we use

$$v_x(z,t) = \tilde{v}_x(z,t) \, \exp\left[\frac{1}{4}\int^z \frac{d\tilde{z}}{H}\right] , \tag{7.12}$$

and

$$b_x(z,t) = \tilde{b}_x(z,t) \exp\left[-\frac{1}{4}\int^z \left(\frac{4}{c_k}\frac{dc_k}{d\tilde{z}} + \frac{1}{H}\right) d\tilde{z}\right] . \tag{7.13}$$

The standard forms of the wave equations are

$$\left[\frac{\partial^2}{\partial t^2} - c_k^2(z)\frac{\partial^2}{\partial z^2} + \tilde{\Omega}_{cr,v}^2(z)\right]\tilde{v}_x(z,t) = 0 , \tag{7.14}$$

and

$$\left[\frac{\partial^2}{\partial t^2} - c_k^2(z)\frac{\partial^2}{\partial z^2} + \tilde{\Omega}_{cr,b}^2(z)\right]\tilde{b}_x(z,t) = 0 , \tag{7.15}$$

where

$$\tilde{\Omega}_{cr,v}^2(z) = \Omega_S^2(z)\left(1 + 4\frac{dH}{dz}\right) , \tag{7.16}$$

and

$$\tilde{\Omega}_{cr,b}^2(z) = \Omega_S^2(z)\left(1 - 4\frac{dH}{dz}\right) + 2\Omega_S(z)\frac{dc_k}{dz} + c_k\frac{d^2c_k}{dz^2} \tag{7.17}$$

are the critical frequencies (e.g., Musielak, Fontenla, & Moore, 1992; Musielak et al. 2006), and

$$\Omega_S(z) = \frac{c_k(z)}{4H(z)} . \tag{7.18}$$

In this paper, we shall refer to $\Omega_S(z)$ as Spruit's local cutoff frequency for the reasons described in Chapter 2. In addition, we want to mention that the wave equations written in their standard forms are also called the Klein-Gordon equations (e.g., Rae & Roberts 1982; Musielak et al. 1987, 1995, 2006; Routh et al. 2007).

After making the Fourier transform in time, we obtain

$$\left[\frac{d^2}{dz^2} + \frac{\omega^2 - \tilde{\Omega}_{cr,v}^2(z)}{c_k^2(z)}\right]\tilde{v}_x(z) = 0 , \tag{7.19}$$

and

$$\left[\frac{d^2}{dz^2} + \frac{\omega^2 - \tilde{\Omega}_{cr,b}^2(z)}{c_k^2(z)}\right]\tilde{b}_x(z) = 0 , \tag{7.20}$$

where ω is the wave frequency.

The fact that different solutions of Eqs (7.19) and (7.20) are expected when the sign of the second term changes is well-known (e.g., Murphy 1960). This becomes especially obvious in the simplest case of a thin and isothermal magnetic flux tube for which $c_k = $ const and $H = $ const, and $\tilde{\Omega}_{cr,v} = \tilde{\Omega}_{cr,b} = \Omega_S = c_k/4H = $ const, and the wave equations for $\tilde{v}_x$ and $\tilde{b}_x$ are the same. As shown by Spruit (1981, 1982), the solutions describe propagating waves when $\omega > \Omega_S$ and evanescent waves when $\omega \leq \Omega_S$, with Ω_S being Spruit's global cutoff frequency (see Chapter 2). It must be noted that Ω_S is also the natural frequency of the flux tube; this means that the tube oscillates with its natural frequency when it is perturbed (e.g., Hasan & Kalkofen 1999; Musielak & Ulmschneider 2003).

In the general case of a thin and non-isothermal magnetic flux tube, the situation is more complicated because the physical parameters in Eqs (7.19) and (7.20) depend on z. As a result, the range of ω that corresponds to the propagating wave solutions must be determined by using the oscillation theorem (see Chapter 3) and Euler's equation (see Appendix C). The conditions for the existence of the propagating wave solutions at a given height $z \neq 0$ are

$$\frac{\omega^2 - \tilde{\Omega}_{cr,v}^2(z)}{c_k^2(z)} > \frac{1}{4z^2} \ , \tag{7.21}$$

and

$$\frac{\omega^2 - \tilde{\Omega}_{cr,b}^2(z)}{c_k^2(z)} > \frac{1}{4z^2} \ . \tag{7.22}$$

Using the results of Appendix B, we define the turning-point frequencies

$$\tilde{\Omega}_{tp,v}^2(z) = \tilde{\Omega}_{cr,v}^2(z) + \frac{c_k^2(z)}{4z^2} \ , \tag{7.23}$$

and

$$\tilde{\Omega}_{tp,b}^2(z) = \tilde{\Omega}_{cr,b}^2(z) + \frac{c_k^2(z)}{4z^2} \ , \tag{7.24}$$

and write the conditions for the propagating wave solutions as $\omega > \tilde{\Omega}_{tp,v}$ and $\omega > \tilde{\Omega}_{tp,b}$.

Since the turning-point frequencies separate the propagating and non-propagating wave solutions (see Chapter 3), one of these frequencies must be chosen as a cutoff frequency. According to Musielak et al. (2006), the larger of the turning-point frequencies must be selected as the cutoff because this choice guarantees that the propagating wave solutions are obtained for both wave variables

$$\tilde{\Omega}_{cut}(z) = \max[\tilde{\Omega}_{tp,v}(z), \tilde{\Omega}_{tp,b}(z)] \ . \tag{7.25}$$

However, in order to determine which turning-point frequency is larger, we must have models of thin and non-isothermal magnetic flux tubes.

Before such models are specified, we have to first discuss physical meaning of the terms $c_k^2(z)/2z^2$, which are introduced by the oscillation theorem (see Eqs 7.21 through 7.24). Let us define the local time $t_l(z) = z/c_k(z)$, which is evaluated by making the assumption that transverse tube waves travel the entire distance z along the tube with the same speed c_k whose value is fixed at the height z. Since c_k is a function of z, the correct way to calculate the actual wave travel time $t_w(z)$ along the tube is to integrate $1/c_k(z)$ over z.

From a physical point of view, the conditions for the propagating wave solutions and the turning-point frequencies must be determined by using $t_w(z)$ instead of $t_l(z)$. Such an approach is developed in the next section, where a new variable is defined and the oscillation theorem is used to introduce the actual wave travel time $t_w(z)$.

7.1.3 Transformed wave equations and conditions for wave propagation

Let us introduce a new variable given by

$$d\tau = \frac{dz}{c_k(z)} \ . \tag{7.26}$$

The physical meaning of this variable becomes obvious after both sides of the above equation are integrated. Then, $\tau(z) = t_w(z)$ is the actual wave travel time between a height at which a wave source is located and a given height z along the axis of a magnetic flux tube.

We express Eqs (7.98) and (7.99) in terms of the new variable τ and obtained the following transformed wave equations

$$\left[\frac{\partial^2}{\partial t^2} - \frac{\partial^2}{\partial \tau^2} + \left(\frac{c_k}{2H} + \frac{c'_k}{c_k} \right) \frac{\partial}{\partial \tau} \right] v_x(\tau, t) \; = 0 \; , \tag{7.27}$$

and

$$\left[\frac{\partial^2}{\partial t^2} - \frac{\partial^2}{\partial \tau^2} - \left(\frac{c_k}{2H} + \frac{c'_k}{c_k} \right) \frac{\partial}{\partial \tau} \right] b_x(\tau, t) \; = 0 \; , \tag{7.28}$$

where $c_k = c_k(\tau)$, $H = H(\tau)$ and $c'_k = dc_k/d\tau$.

To convert the transformed wave equations into their standard forms, we use

$$v_x(\tau, t) = v(\tau, t) \exp \left[+\frac{1}{2} \int^\tau \left(\frac{c_k}{2H} + \frac{c'_k}{c_k} \right) d\tilde{\tau} \right] \; , \tag{7.29}$$

and

$$b_x(\tau, t) = b(\tau, t) \exp \left[-\frac{1}{2} \int^\tau \left(\frac{c_k}{2H} + \frac{c'_k}{c_k} \right) d\tilde{\tau} \right] \; , \tag{7.30}$$

and obtain

$$\left[\frac{\partial^2}{\partial t^2} - \frac{\partial^2}{\partial \tau^2} + \Omega^2_{cr,v}(\tau) \right] v(\tau, t) = 0 \; , \tag{7.31}$$

and

$$\left[\frac{\partial^2}{\partial t^2} - \frac{\partial^2}{\partial \tau^2} + \Omega^2_{cr,b}(\tau) \right] b(\tau, t) = 0 \; , \tag{7.32}$$

where

$$\Omega^2_{cr,v}(\tau) = \Omega^2_S(\tau) \left(1 + 4\frac{H'}{c_k} \right) + \frac{1}{2} \left[\frac{3}{2} \left(\frac{c'_k}{c_k} \right)^2 - \frac{c''_k}{c_k} \right] \; , \tag{7.33}$$

and

$$\Omega^2_{cr,b}(\tau) = \Omega^2_S(\tau) \left(1 - 4\frac{H'}{c_k} \right) - \frac{1}{2} \left[\frac{1}{2} \left(\frac{c'_k}{c_k} \right)^2 - \frac{c''_k}{c_k} \right]$$

$$+2\Omega_S(\tau)\left(\frac{c_k'}{c_k}\right) \ , \tag{7.34}$$

with $c_k'' = d^2 c_k/d\tau^2$. The frequencies $\Omega_{cr,v}$ and $\Omega_{cr,b}$ are known as the critical frequencies (Musielak, Fontenla, & Moore, 1992; Musielak et al. 2006).

We make the Fourier transform in time $[v(\tau,t), b(\tau,t)] = [\tilde{v}(\tau), \tilde{b}(\tau)]e^{-i\omega t}$, where ω is the wave frequency, and write Eqs (7.105) and (7.106) as

$$\left[\frac{d^2}{d\tau^2} + \omega^2 - \Omega_{cr,v}^2(\tau)\right]\tilde{v}(\tau) = 0 \ , \tag{7.35}$$

and

$$\left[\frac{d^2}{d\tau^2} + \omega^2 - \Omega_{cr,b}^2(\tau)\right]\tilde{b}(\tau) = 0 \ . \tag{7.36}$$

Using the oscillation theorem (see Chapter 3) and comparing the above equations to Euler's equation (see Chapter 3 again), we obtain the following conditions for the wave propagation

$$\omega^2 - \Omega_{cr,v}^2(\tau) > \frac{1}{4\tau^2} \ , \tag{7.37}$$

and

$$\omega^2 - \Omega_{cr,b}^2(\tau) > \frac{1}{4\tau^2} \ . \tag{7.38}$$

According to the results of Chapter 3, the turning-point frequencies are

$$\Omega_{tp,v}^2(\tau) = \Omega_{cr,v}^2(\tau) + \frac{1}{4\tau^2} \ , \tag{7.39}$$

and

$$\Omega_{tp,b}^2(\tau) = \Omega_{cr,b}^2(\tau) + \frac{1}{4\tau^2} \ . \tag{7.40}$$

Comparison of these wave propagation conditions and turning-point frequencies to those previously obtained shows that now the actual wave travel time is properly accounted for because $\tau(z) = t_w(z)$. This is an important result as it demonstrates that the oscillation theorem only allows introducing the actual wave travel time when the derivations are performed with the τ variable.

7.1.4   Converting τ into z

Having obtained the conditions for the wave propagation (see Eqs 7.111 and 7.112) and the turning-point frequencies (see Eqs 7.113 and 7.114) with the actual wave travel time, we now express them in terms of the z variable; this requires converting τ to z.

We begin with the critical frequencies $\Omega_{cr,v}(\tau)$ and $\Omega_{cr,b}(\tau)$ given by Eqs (7.107) and (7.108). Using the following expressions

$$\frac{1}{c_k}\frac{dc_k}{d\tau} = \frac{dc_k}{dz} \ , \tag{7.41}$$

$$\frac{1}{c_k}\frac{d^2c_k}{d\tau^2} = c_k\frac{d^2c_k}{dz^2} + \left(\frac{dc_k}{dz}\right)^2 \ , \tag{7.42}$$

and

$$\frac{1}{c_k}\frac{dH}{d\tau} = \frac{dH}{dz} \ , \tag{7.43}$$

we obtain

$$\Omega^2_{cr,v}(z) = \Omega^2_S(z)\left[1 + 4\frac{dH}{dz}\right] + \frac{1}{2}\left[\frac{1}{2}\left(\frac{dc_k}{dz}\right)^2 - c_k\frac{d^2c_k}{dz^2}\right] \tag{7.44}$$

and

$$\Omega^2_b(z) = \Omega^2_S(z)\left[1 - 4\frac{dH}{dz}\right] + \frac{1}{2}\left[\frac{1}{2}\left(\frac{dc_k}{dz}\right)^2 + c_k\frac{d^2c_k}{dz^2}\right]$$
$$+ 2\Omega_S(z)\frac{dc_k}{dz} \ . \tag{7.45}$$

Comparison of $\Omega_{cr,v}(z)$ and $\Omega_{cr,b}(z)$ to $\tilde{\Omega}_{cr,v}(z)$ and $\tilde{\Omega}_{cr,b}(z)$ obtained above shows differences between the corresponding critical frequencies. An interesting result is that these differences could potentially be eliminated by constructing a flux tube model that would satisfy the following condition

$$\frac{1}{2}\left(\frac{dc_k}{dz}\right)^2 = c_k\frac{d^2c_k}{dz} \ . \tag{7.46}$$

Such simple model can indeed be constructed by assuming that $c_k(z) \sim z^2$, however, other flux tube models with temperature distributions described by elementary mathematical functions, including the exponential function, do not satisfy this condition. The same is true for more realistic models of the solar atmosphere, such as the VAL C model considered below.

Having obtained the critical frequencies $\Omega_{cr,v}(z)$ and $\Omega_{cr,b}(z)$, we can now express the conditions for the wave propagation and the turning-point frequencies as functions of z. This requires $\tau(z)$, which can be evaluated from

$$\tau(z) = \int^z \frac{d\tilde{z}}{c_k(\tilde{z})} + \tau_C , \tag{7.47}$$

where τ_C is an integration constant to be evaluated when flux tube models are specified.

The conditions for the wave propagation can be written as

$$\left[\omega^2 - \Omega_{cr,b}^2(z)\right] > \frac{1}{4}\left[\int^z \frac{d\tilde{z}}{c_k(\tilde{z})} + \tau_C\right]^{-2} , \tag{7.48}$$

and

$$\left[\omega^2 - \Omega_{cr,b}^2(z)\right] > \frac{1}{4}\left[\int^z \frac{d\tilde{z}}{c_k(\tilde{z})} + \tau_C\right]^{-2} . \tag{7.49}$$

The turning-point frequencies are

$$\Omega_{tp,v}^2(z) = \Omega_{cr,v}^2(z) + \frac{1}{4}\left[\int^z \frac{d\tilde{z}}{c_k(\tilde{z})} + \tau_C\right]^{-2} , \tag{7.50}$$

and

$$\Omega_{tp,b}^2(z) = \Omega_{cr,b}^2(z) + \frac{1}{4}\left[\int^z \frac{d\tilde{z}}{c_k(\tilde{z})} + \tau_C\right]^{-2} . \tag{7.51}$$

Clearly, the conditions for the wave propagation and the turning-point frequencies given above are different than those obtained in Sec. 3. Since $\Omega_{tp,v}(z)$ and $\Omega_{tp,b}(z)$ account for the actual wave travel time, we use these turning-point frequencies to determine the cutoff frequency for transverse tube waves.

7.1.5 The cutoff frequency

We follow Musielak et al. (2006) and take the larger of the two turning-point frequency as the cutoff frequencies Ω_{cut}. As shown in Sec. 7, the selection process is independent of the variable used. This means that we may consider either

$$\Omega_{cut}(\tau) = \max[\Omega_{tp,v}(\tau), \Omega_{tp,b}(\tau)] \ . \tag{7.52}$$

or

$$\Omega_{cut}(z) = \max[\Omega_{tp,v}(z), \Omega_{tp,b}(z)] \ . \tag{7.53}$$

Our selection of Ω_{cut} is physically justified by the fact that in order to have propagating transverse tube waves, the wave frequency ω must always be higher than any turning-point frequency. In other words, the choice guarantees that the propagating wave solutions are obtained for both wave variables, and that the cutoff frequency does separate the propagating and non-propagating wave solutions. Hence, the condition for propagating waves is $\omega > \Omega_{cut}$. Based on our definition of the turning-point frequencies, the condition for non-propagating (evanescent) waves is $\omega \leq \Omega_{cut}$.

The above results show that the cutoff frequency can only be determined when we know which turning-point frequency is larger; obviously this depends on models of thin and non-isothermal flux tubes. In addition, one must keep in mind that the conditions given by Eqs (7.52) and (7.53) must be checked at each height because in some regions along the tube $\Omega_{tp,v}$ could be larger than $\Omega_{tp,v}$, however, the opposite could be true in other regions.

7.1.6 Models with power-law temperature distributions

Let us consider the following temperature distribution inside the tube (Subramaniam 2006)

$$T_0(z) = T_{00}\xi^m , \qquad (7.54)$$

where $\xi = z/z_0$ is the distance ratio, with z_0 being a fixed height in the model, T_{00} is the temperature at z_0, and m can be any real number. Note that in all power-law models a wave source is located at $\xi = 1$, which means that in all calculations $\xi \geq 1$. In addition, for all models $z_0 = 10$ km, $T_{00} = 5000$ K, $c_{k0} = 10$ km/s, and for gravity we take its solar value. The resulting temperature distributions for m being a positive integer that ranges from 1 to 5 are presented in Fig. 4.1.

7.1.7 Case of m = 1

To describe the process of deriving a local cutoff frequency, we begin with the simplest case of $m = 1$, which corresponds to the temperature varying linearly with ξ. We calculate ρ_0, p_0, B_0 and c_k as functions of ξ, and use Eq. (7.47) to obtain

$$\tau(\xi) = 2\frac{z_0}{c_{k0}}\xi^{1/2} + \tau_C , \qquad (7.55)$$

where c_{k0} is the value of c_k at z_0 and τ_C is the integration constant. To determine this constant, we assume that $\tau(\xi = 1) = \tau_0 \equiv z_0/c_{k0}$, which gives $\tau_C = -\tau_0$ and

$$\tau(\xi) = \tau_0(2\xi^{1/2} - 1) . \qquad (7.56)$$

Knowing τ as a function of ξ, we calculate

$$\xi(\tau) = \frac{1}{4}\left(\frac{\tau + \tau_0}{\tau_0}\right)^2 , \qquad (7.57)$$

$$c_k(\tau) = \frac{1}{2}c_{k0}\left(\frac{\tau + \tau_0}{\tau_0}\right) \qquad (7.58)$$

and

$$H(\tau) = \frac{1}{4} H_{00} \left(\frac{\tau + \tau_0}{\tau_0} \right)^2 , \tag{7.59}$$

where H_{00} is the value of the tube scale height at z_0.

Now, we use Eqs (7.58) and (7.59) to determine the turning-point frequencies, which become

$$\Omega^2_{tp,v}(\tau) = \frac{1}{4} \left[\left(\frac{z_0}{H_{00}} \right)^2 + \frac{4z_0}{H_{00}} + 3 \right] \frac{1}{(\tau + \tau_0)^2} + \frac{1}{4\tau^2} , \tag{7.60}$$

and

$$\Omega^2_{tp,b}(\tau) = \frac{1}{4} \left[\left(\frac{z_0}{H_{00}} \right)^2 - 1 \right] \frac{1}{(\tau + \tau_0)^2} + \frac{1}{4\tau^2} . \tag{7.61}$$

We identify the larger turning-point frequency as the cutoff frequency. Inspection of the above equations shows that $\Omega^2_{tp,v}$ is larger than $\Omega^2_{tp,b}$, which means that the local cutoff frequency is $\Omega_{cut}(\tau) = \Omega_{tp,v}(\tau)$ or

$$\Omega_{cut}(\tau) = \frac{1}{2} \left[\left(\frac{z_0}{H_{00}} \right)^2 + \frac{4z_0}{H_{00}} + f_1(\tau) \right]^{1/2} \frac{1}{(\tau + \tau_0)} , \tag{7.62}$$

where

$$f_1(t) = \frac{4\tau^2 + 2\tau\tau_0 + \tau_0^2}{\tau^2} . \tag{7.63}$$

It is important to point out that the above process of deriving the cutoff frequency can also be done by using directly the ξ variable, and that the result is the same. To demonstrate this, we use Eq. (7.56) to express the turning-point frequencies given by Eqs. (7.60) and (7.61) in terms ξ. This gives

$$\Omega^2_{tp,v}(\xi) = \Omega_0^2 \left[1 + \frac{4H_{00}}{z_0} + \left(\frac{H_{00}}{z_0} \right)^2 g_1(\xi) \right] \xi^{-1} , \tag{7.64}$$

where $\Omega_0 = c_{k0}/4H_{00}$ and

$$g_1(\xi) = \frac{16\xi - 12\xi^{1/2} + 3}{(2\xi^{1/2} - 1)^2} , \tag{7.65}$$

and

$$\Omega_{tp,b}^2(\xi) = \Omega_0^2 \left[1 - \left(\frac{H_{00}}{z_0} \right)^2 (1 - g_2(\xi)) \right] \xi^{-1} , \tag{7.66}$$

where

$$g_2(\xi) = \frac{4\xi}{(2\xi^{1/2} - 1)^2} . \tag{7.67}$$

The difference between the turning-point frequencies is

$$\frac{\Omega_{tp,v}^2(\xi) - \Omega_{tp,b}^2(\xi)}{\Omega_0^2} = 4 \left(\frac{H_{00}}{z_0} \right) \left[1 + \left(\frac{H_{00}}{z_0} \right) \right] \xi^{-1} , \tag{7.68}$$

which shows that $\Omega_{tp,v}^2(\xi)$ is always larger than $\Omega_{tp,b}^2(\xi)$. Hence our choice of $\Omega_{tp,v}$ as the cutoff frequency is the same. Thus, we write $\Omega_{cut}(\xi) = \Omega_{tp,v}(\xi)$ and

$$\Omega_{cut}(\xi) = \Omega_0 \left[1 + \frac{4H_{00}}{z_0} + \left(\frac{H_{00}}{z_0} \right)^2 g_1(\xi) \right]^{1/2} \xi^{-1/2} , \tag{7.69}$$

which is the same result as that given by Eq. (7.64).

Finally, the same cutoff frequency is obtained when Eqs (7.50) and (7.51) are directly used with the z variable being replaced by ξ.

The local cutoff frequency Ω_{cut} is plotted as a function of ξ in Fig. 7.1. It is seen that the cutoff frequency decreases with the atmospheric height in the model with $m = 1$.

7.1.8   Case of m = 2

Since the procedure to obtain the cutoff frequency for $m = 2$ is the same as that described above for $m = 1$, we only write the resulting equations. In this case, $\tau(\xi)$ is given by

$$\tau(\xi) = \frac{z_0}{c_{k0}} \ln\xi + \tau_C , \tag{7.70}$$

where τ_C is the integration constant determined from the assumption that $\tau(\xi = 1) = \tau_0 \equiv z_0/c_{k0}$. This gives $\tau_C = \tau_0$ and
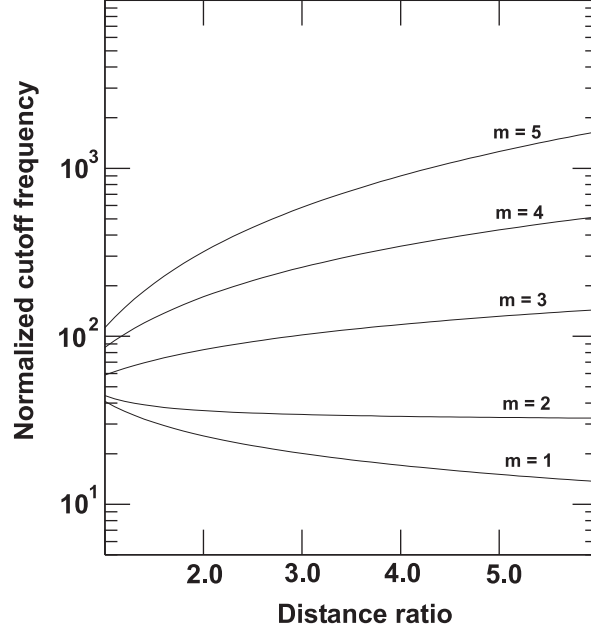
$$\tau(\xi) = \tau_0(\ln\xi + 1) . \tag{7.71}$$

Figure 7.1. The normalized cutoff frequency Ω_{cut}/Ω_0 vs. the distance ratio z/z_0.

Now, ξ as a function of τ can also be calculated and the result is

$$\xi(\tau) = e^{\tau/\tau_0 - 1} , \tag{7.72}$$

which can be used to evaluate $c_k(\tau)$ and $H(\tau)$, and to obtain the critical and turning-point frequencies. We introduce $\kappa = 1 - \tau/\tau_0$ and write the turning-point frequencies as

$$\Omega_{tp,v}^2(\tau) = \frac{1}{4}\left[\left(\frac{z_0}{2H_{00}}\right)^2 e^{2\kappa} + \frac{2z_0}{H_{00}}e^{\kappa} + 1\right]\frac{1}{\tau_0^2} + \frac{1}{4\tau^2} \tag{7.73}$$

and

$$\Omega_{tp,b}^2(\tau) = \frac{1}{4}\left[\left(\frac{z_0}{2H_{00}}\right)^2 e^{2\kappa} + 1\right]\frac{1}{\tau_0^2} + \frac{1}{4\tau^2} . \tag{7.74}$$

Since $\Omega_{tp,v}^2(\tau)$ is always larger than $\Omega_{tp,b}^2(\tau)$, we have $\Omega_{cut}(\tau) = \Omega_{tp,v}(\tau)$ and

$$\Omega_{cut}(\tau) = \frac{1}{2\tau_0}\left[\left(\frac{z_0}{2H_{00}}\right)^2 e^{2\kappa} + \frac{2z_0}{H_{00}}e^{\kappa} + f_2(\tau)\right]^{1/2} , \tag{7.75}$$

where

$$f_2(\tau) = 1 + \frac{\tau_0^2}{\tau^2} . \tag{7.76}$$

We now use Eq. (7.72) and calculate $\Omega_{cut}(\xi)$, which becomes

$$\Omega_{cut}(\xi) = \Omega_0 \left[\xi^{-2} + \frac{8H_{00}}{z_0} \xi^{-1} + \left(\frac{2H_{00}}{z_0} \right)^2 g_3(\xi) \right]^{1/2} \tag{7.77}$$

where

$$g_3(\xi) = 1 + \frac{1}{(1 + ln\xi)^2} \ . \tag{7.78}$$

The plot of this cutoff frequency in Fig. 7.1 shows that it is practically constant throughout the temperature model with $m = 2$.

7.1.9   Cases with $m > 2$

In this general case of $m > 2$, we obtain

$$\tau(\xi) = \frac{z_0}{c_{k0}} \left(1 - \frac{m}{2} \right)^{-1} \xi^{1-m/2} + \tau_C \ , \tag{7.79}$$

where the integration constant τ_C is evaluated by taking $\tau(\xi = 1) = \tau_0 \equiv z_0/c_{k0}$; note that our choice of τ_0 gives the same physical parameters at $z = z_0$ for all the power-law models. After evaluating τ_C, we write

$$\tau(\xi) = \tau_0 \left(\frac{m}{m-2} \right) \left[1 - \frac{2}{m} \xi^{(2-m)/2} \right] \ , \tag{7.80}$$

and

$$\xi(\tau) = \left[\frac{2\tau - m(\tau - \tau_0)}{2\tau_0} \right]^{2/(2-m)} . \tag{7.81}$$

Using Eq. (7.81), we calculate $c_k(\tau)$ and $H(\tau)$, and then the critical and turning-point frequencies. The latter can be written as

$$\Omega_{tp,v}^2(\tau) = \Omega_0^2 \left[\frac{2\tau - m(\tau - \tau_0)}{2\tau_0} \right]^{2m/(m-2)}$$

$$+ \Omega_0 \frac{2m}{2\tau - m(\tau - \tau_0)} \left[\frac{2\tau - m(\tau - \tau_0)}{2\tau_0} \right]^{m/(m-2)}$$

$$+ \frac{(4 - m)m}{4[2\tau - m(\tau - \tau_0)]^2} + \frac{1}{4\tau^2} \ , \tag{7.82}$$

and

$$\Omega^2_{tp,b}(\tau) = \Omega_0^2 \left[\frac{2\tau - m(\tau - \tau_0)}{2\tau_0} \right]^{2m/(m-2)}$$

$$+ \frac{(3m-4)m}{4[2\tau - m(\tau - \tau_0)]^2} + \frac{1}{4\tau^2} . \tag{7.83}$$

To determine the local cutoff frequency, we use Eq. (7.80) and write Eqs (7.82) and (7.83) as

$$\Omega^2_{tp,v}(\xi) = \Omega_0^2 \left[4m \left(\frac{H_{00}}{z_0} \right) \xi^{-1} + m(4-m) \left(\frac{H_{00}}{z_0} \right)^2 \xi^{m-2} \right.$$

$$\left. + \xi^{-m} + 4 \left(\frac{m-2}{m} \right)^2 \left(\frac{H_{00}}{z_0} \right)^2 g_4(\xi) \right] , \tag{7.84}$$

where

$$g_4(\xi) = \left(1 - \frac{2}{m} \xi^{1-m/2} \right)^{-2} , \tag{7.85}$$

and

$$\Omega^2_{tp,b}(\xi) = \Omega_0^2 \left[\xi^{-m} + m(3m-4) \left(\frac{H_{00}}{z_0} \right)^2 \xi^{m-2} \right.$$

$$\left. + 4 \left(\frac{m-2}{m} \right)^2 \left(\frac{H_{00}}{z_0} \right)^2 g_4(\xi) \right] . \tag{7.86}$$

We now calculate the difference between these turning-point frequencies and obtain

$$\frac{\Omega^2_{tp,v}(\xi) - \Omega^2_{tp,b}(\xi)}{\Omega_0^2} = 4m \left(\frac{H_{00}}{z_0} \right) \left[1 - (m-2)\xi^{m-1} \right.$$

$$\left. \times \left(\frac{H_{00}}{z_0} \right) \right] \xi^{-1} . \tag{7.87}$$

Since $m > 2$ and $\xi > 1$, $\Omega^2_{tp,b}$ is larger than $\Omega^2_{tp,v}$ if $H_{00} > z_0$. Hence for $H_{00} > z_0$, the local cutoff frequency is $\Omega_{cut}(\xi) = \Omega_{tp,b}(\xi)$ or

$$\Omega_{cut}(\xi) = \Omega_0 \left[\xi^{-m} + m(3m-4) \left(\frac{H_{00}}{z_0} \right)^2 \xi^{m-2} \right.$$

$$\left. + 4 \left(\frac{m-2}{m} \right)^2 \left(\frac{H_{00}}{z_0} \right)^2 g_4(\xi) \right]^{1/2} . \tag{7.88}$$

The cutoff frequency calculated for the power-law temperature models with $m = 3$, 4 and 5 is plotted versus the distance ratio in Fig. 7.1. It is seen that this cutoff frequency always increases with the atmospheric height in the models with $m > 2$ and that its increase is much faster for higher values of m.

7.1.10 Discussion

The effects of different temperature gradients on the cutoff frequency for transverse tube waves are presented in Fig. 2. Since the cutoff frequency is a local quantity, its value at a given atmospheric height determines frequency that the waves must have in order to propagating waves at this height. Our results demonstrate that the conditions for the wave propagation strongly depend on the temperature gradients.

If the temperature increases linearly with height ($m = 1$), the cutoff frequency reaches the maximum at $z = z_0$ and then decreases with height. For the temperature gradient with $m = 2$, the cutoff frequency remains practically constant with height. However, the cutoff frequency always increases with height in the temperature models with $m \geq 3$; the higher the value of m, the steeper the increase of the local cutoff frequency with height is observed (see also Subramaniam 2006).

The main purpose of using the power-law temperature models was to demonstrate the dependence of the local cutoff frequency on the increasing steepness of the temperature models. Obviously, the power-law models do not properly describe the temperature gradients in the solar atmosphere. Therefore, we now consider a more realistic model of the solar atmosphere.

7.1.11 Applications to the solar atmosphere:

VAL model of the solar atmosphere

We now assume that a thin flux tube tube is embedded in the VAL C model of the solar atmosphere (Vernazza et al. 1981). In this model, the height $z = 0$ corresponds to unity optical depth at 500 nm, where the temperature is 6420 K. At the height $z = 2543$ km the temperature reaches 4.47×10^5 K; the temperature minimum $T_{min} = 4170$ K is located at $z = 515$ km. Actually, the model also extends to deeper photospheric layers with $z = -206.65$ km and the temperature 1.017×10^4 K. All our calculations begin at the height $z = 0$ and continue to $z = 2543$ km.

To calculate the characteristic wave speed c_k as a function of z, we have to know the magnetic field $B_0(z)$. Since the latter is not given in the VAL C model, we evaluate $B_0(z)$ from the horizontal pressure balance calculated at each height z and starting with the value $B_0(z_0) = 1500$ Gs (see Eq. 7.89). In Fig. 7.2, we plot $c_k(z)$ and for comparison the sound speed c_s versus atmospheric height in the model. The results show that c_k is smaller than c_s in almost the entire model except in the upper chromosphere and lower transition region, where c_k becomes comparable to, or even slightly larger than c_s.

Our results showed the role played by the local time $t_l(z) = z/c_k(z)$ in obtaining the cutoff frequency $\tilde{\Omega}_{cut}(z)$. Similarly, we derived the cutoff frequency $\Omega_{cut}(z)$ and demonstrated that it depends on the actual wave travel time t_w, which is the same as τ. In order to calculate τ, we use Eq. (7.47) and evaluate the integration constant τ_C by taking $\tau_C = \tau(z = 0) = \tau_0$. Since the VAL C model extends below the height $z = 0$, it is reasonable to assume that transverse tube waves enter the atmosphere at the model base located at $z = -206.65$ km. Hence, τ_0 is the actual wave travel time between the model base and $z = 0$. The distance $\Delta z = 206.65$ km is also added to the value of z used to evaluate the local time $t_l(z)$.
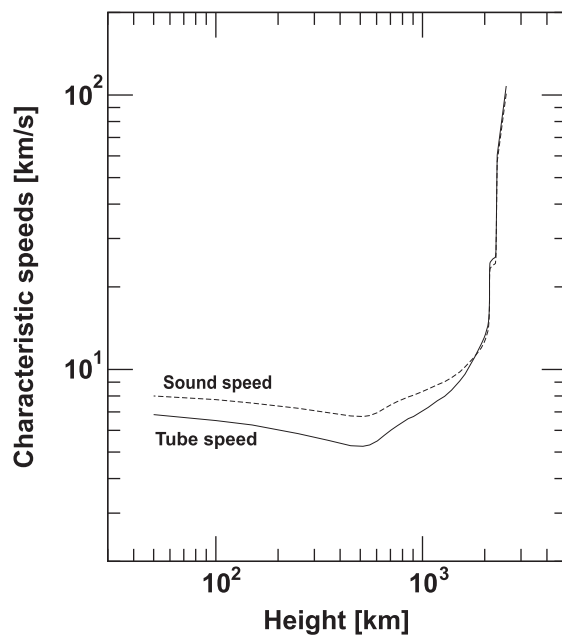
Figure 7.2. The characteristic tube speed c_k and the sound speed c_s vs. height.
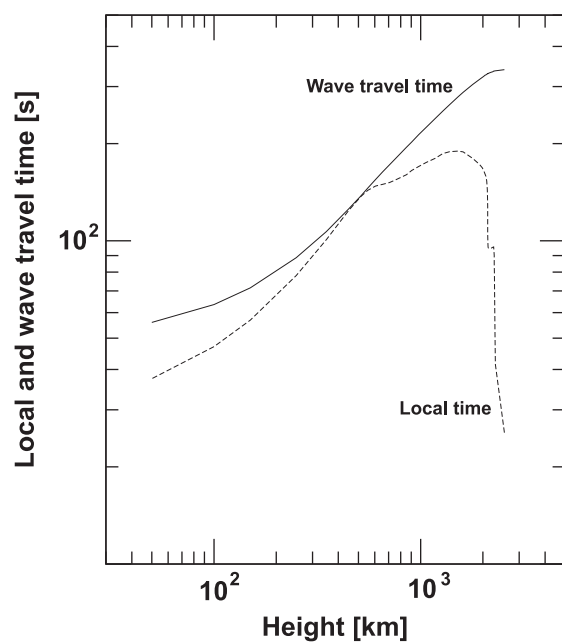

Figure 7.3. The local time $t_l = z/c_k$ and the actual wave travel time $t_w = \tau$ vs. height.

The local time $t_l(z)$ and the actual wave travel time $t_w(z) = \tau(z)$ are plotted versus height in Fig. 4. The results show that there are significant differences between these two times in the lower and upper parts of the VAL C model. However, there is a narrow region in the middle chromosphere where t_l approximates t_w rather well. As a result, in this region $\tilde{\Omega}_{cut}(z) \approx \Omega_{cut}(z)$ but differences between the two cutoffs remain in the other regions of the model. This clearly demonstrates the limitation of the approach based on the local time $t_l(z)$.

It must also be noted that the solid line in Fig. 7.3 depicts τ as a function of z in the VAL C model. Having obtained $\tau(z)$, it is easy to determine $z(\tau)$ and then evaluate the τ-dependence of all physical parameters of the tube.

To determine the cutoff frequency $\Omega_{cut}(z)$ in the VAL C model, we have to know which turning-point frequency is larger (see Sec. 6). Hence, both $\Omega_{tp,v}(z)$ and $\Omega_{tp,b}(z)$ given by Eqs (7.50) and (7.51) must be calculated and the larger one has to be selected as $\Omega_{cut}(z)$. To perform these calculations, we must evaluate the first derivative of c_k and H, and the second derivative of c_k. The calculations have to be done numerically because the model contains unequally spaced data. We tested three different numerical methods and obtained similar results. However, the method based on the second-order Lagrange polynomial P_2 gave more 'smooth' variations of these derivatives with height than the other methods. Therefore, we use this method to calculate the cutoff frequency for the VAL C model.

The results of our calculations show that the values of the turning-point frequencies in the VAL C model are comparable, and that in the upper photosphere $\Omega_{tp,v}(z)$ is slightly larger than $\Omega_{tp,b}(z)$, however, the opposite is true in the lower and middle chromosphere. There is one region in the upper chromosphere where $\Omega_{tp,v}(z)$ dominates, and another one where $\Omega_{tp,b}(z)$ is larger. Similar situation is at the base of the solar transition region. By selecting the larger turning-point frequency, we obtain
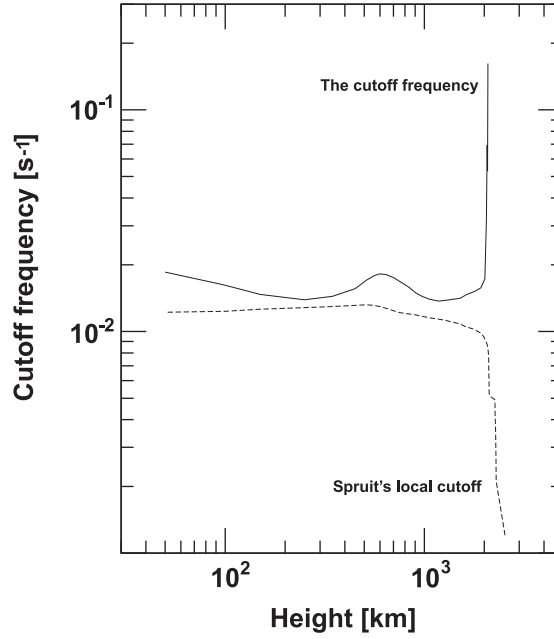
Figure 7.4. The cutoff Ω_{cut} and Spruit's local cutoff $\Omega_S = c_k/4H$ vs. height.

the cutoff frequency Ω_{cut} and plot it versus height in the VAL C model (see Fig. 7.4). Since the value of Ω_{cut} is different at each atmospheric height, the wave frequency ω must be higher than the cutoff at a given height z in order to have propagating transverse tube waves at this height.

Since Ω_{cut} depends on Ω_S (see Eqs 7.50 and 7.51, and also Eq. 7.53), the contributions to Ω_{cut} by the gradients of c_k and H can be estimated by comparing these two quantities. In Fig. 5, we plot Spruit's local cutoff frequency $\Omega_S(z) = c_k(z)/4H(z)$ versus height in the model (see Eq. 7.18). Comparison of Ω_{cut} to Ω_S shows that the former always exceeds the latter, which means that the contributions due to the gradients are not negligible. The differences between Ω_{cut} and Ω_S are especially prominent in the upper parts of the model. However, the results obtained for the upper atmosphere must be taken with caution because the thin flux tube

approximation, which is the basis for the results presented in this paper and for Spruit's results as well, is not longer valid at those heights.

We considered here an isolated magnetic flux tube. Therefore, the tube magnetic field expands exponentially with height in the VAL C model. As a result of this expansion, the thin flux tube approximation breaks down in the upper atmospheric layers. To determine the approximate behavior of the cutoffs in these layers, the calculations were extended up to the uppermost layers in the model. This is beyond the formal limit of validity of our analytical results. Nevertheless, the presented results demonstrate that the temperature gradient in the upper solar chromosphere and in the solar transition region will have a major influence on the propagation of transverse tube waves.

The increase of temperature with height in the VAL C model requires atmospheric heating that is typically identified with acoustic and flux tube waves, including transverse tube waves, or with phenomena related to magnetic reconnection (e.g., Priest 1982; Narain & Ulmschneider 1996; Ulmschneider & Musielak 2003). Our results presented in Fig. 5 give constraints on the range of frequencies of transverse tube waves that are propagating in different parts of the solar atmosphere. The constraints can be used to determine the role of transverse tube waves in the atmospheric heating.

As discussed by Hasan & Kalkofen (1999), Musielak & Ulmschneider (2003) and Hasan (2003), transverse tube waves may be responsible for excitation of solar atmospheric oscillations observed in magnetically active regions outside of sunspots. The results obtained in this paper can be used to determine the natural frequency of the solar atmosphere inside thin and non-isothermal magnetic flux tubes and the effects of temperature gradients on the solar atmospheric oscillations.

7.2 Isothermal and thick magnetic flux tube

The main purpose of this chapter is to determine the conditions for propagation of linear transverse waves along an isolated and isothermal magnetic flux tube that is considered here to be thick. In a thin flux tube, all magnetic-field lines have the same physical properties across the tube, which means that the field has no structure in the horizontal direction. However, at a given height of a wide flux tube, each magnetic field line is characterized by different physical parameters and this leads to different wave velocity for each line (e.g., Hollweg, 1981). In addition, there is a gradient of wave velocity along each field line and this results in a cutoff frequency, which is determined here by using the method described in Chapter 3. The cutoff frequency is calculated for specific models of solar magnetic flux tubes. We discuss the physical meaning of this cutoff and show that in the limit of the thin flux tube approximation the cutoff becomes Spruit's global cutoff frequency.

7.2.1 Derivation of basic equations

We consider an isolated and vertically-oriented magnetic-flux tube that is embedded in a magnetic-field-free, compressible, and isothermal medium that has the same density stratification as the solar atmosphere. The tube is untwisted, has a circular cross section, and is in temperature equilibrium with the external medium.

We use a two-dimensional coordinate system $(\hat{s}, \hat{n})$ where s is a parameter along the magnetic field line and $\hat{n}$ is a unit vector along the perpendicular to the tangent vector $\hat{s}$.

The tube is assumed to be isolated with its axis oriented vertically along the z-axis, so that gravity $\vec{g} = -g\hat{z}$. The tube magnetic field is given by $\vec{B}_0 = B_0(s)\vec{\hat{s}}$.

The density, pressure of the external magnetic-free atmosphere are represented by $\rho_e = \rho_e(z)$, $p_e = p_e(z)$ respectively. We assume that the tube is in thermal equilibrium with its surroundings.

Based on this assumption, the pressure scale heights $H_0(z) = c_{s0}^2(z)/\gamma g$ and $H_e(z) = c_{se}^2(z)/\gamma g$, where γ is the ratio of specific heats, are also equal. Hence, we have $H_0(z) = H_e(z) = H(z)$, with $H(z) = c_s^2/\gamma g$.

The gas and magnetic pressure inside the tube is balanced by the gas pressure in the external medium. This is the tube's horizontal pressure balance that must be satisfied at each height z. Typically, the balance is given by

$$p + \frac{B^2}{8\pi} = p_e \ . \tag{7.89}$$

Note: you can choose any magnetic field line inside the tube as $p_1 + \frac{B_1^2}{8\pi} = p_2^2 + \frac{B_2^2}{8\pi}$ =..... $p_n + \frac{B_n^2}{8\pi} = p_e$ where $1, 2, ...n$ the number of lines from the center of the tube and n refers to the edge.

Let us consider linear oscillations of the tube with the velocity $\vec{v}$ and the magnetic field $\vec{b}$. Taking $\vec{B} = \vec{B}_0 + \vec{b}$, with $|\vec{b}| << |\vec{B}_0|$, the linearized momentum equation describing these oscillations is

$$\rho_0 \frac{\partial \vec{v}}{\partial t} = -\nabla \left(p_0 + \frac{B_0^2}{8\pi} \right) + \rho_0 \vec{g} + \frac{1}{4\pi} \left(\vec{B} \cdot \nabla \right) \vec{B} \tag{7.90}$$

Since the tube oscillates, its motion is responsible for generating a flow in the external medium. The equation of motion for this flow is

$$\rho_e \frac{\partial \vec{u}}{\partial t} = -\nabla p_e + \rho_e \vec{g} \ , \tag{7.91}$$

where $\vec{u}$ is the velocity of the external fluid.

We combine Eqs (7.90) and (7.91), and use Eq. (7.89) to obtain

$$\rho_0 \frac{\partial \vec{v}}{\partial t} - \rho_e \frac{\partial \vec{u}}{\partial t} = -(\rho_e - \rho_0)\vec{g} + \frac{1}{4\pi} \left(\vec{B} \cdot \nabla \right) \vec{B} \tag{7.92}$$

To describe the propagation of transverse tube waves, we assume that these waves are linear and that they can be represented by the perturbed velocity $\vec{v}(s,t) = v_n(z,t)\vec{\hat{n}}$ and magnetic field $\vec{b}(s,t) = b_n(n,t)\vec{\hat{n}}$. Since for purely transverse tube waves the tube cross section remains unchanged, the density and pressure perturbations caused by these waves can be neglected.

With the above assumptions, the horizontal component of Eq. (7.92) becomes

$$\rho_0\frac{\partial v_n}{\partial t} - \rho_e\frac{\partial u_n}{\partial t} - (\rho_o - \rho_e)(\hat{s} \times \vec{g}) \times \hat{s} - \frac{1}{4\pi}[\left(\vec{B} \cdot \nabla\right)\vec{B}]_\perp = 0 . \tag{7.93}$$

Since at the tube boundary $u_n = -v_n$, we write the above equation as

$$(\rho_0 + \rho_e)\frac{\partial v_n}{\partial t} - (\rho_0 - \rho_e)(\hat{s} \times \vec{g}) \times \hat{s} - \frac{1}{4\pi}[\left(\vec{B} \cdot \nabla\right)\vec{B}]_\perp = 0 , \tag{7.94}$$

Now $\left(\vec{B} \cdot \nabla\right)\vec{B} = \left((\vec{B}_0 + \vec{b}) \cdot \nabla\right)(\vec{B}_0 + \vec{b}) = B_o\frac{\partial}{\partial s}(B_o\hat{s}) + B_o\frac{\partial b}{\partial s}\hat{n}$

With $B_o\frac{\partial}{\partial s}(B_o\hat{s}) = \frac{1}{2}\hat{s}\frac{\partial}{\partial s}B_o^2 + B_o^2\frac{\partial}{\partial s}\hat{s}$ (Spruit, 1980)

Here $\frac{\partial}{\partial s}\hat{s} \equiv \hat{k}$ is the curvature of the magnetic field line which is directed towards the center of curvature.

Now perpendicular to the tube the balance is between buoyancy and curvature. So $(\rho_0 - \rho_e)(\hat{s} \times \vec{g}) \times \hat{s} + \frac{1}{4\pi}B_o^2\hat{k} = 0$.

Thus Eq.(7.94) becomes

$$\frac{(\rho_0 + \rho_e)\partial v_n}{\partial t - \frac{1}{4\pi}B_o\frac{\partial b}{\partial s}} = 0. \tag{7.95}$$

Additional MHD equation that is needed to fully describe the wave propagation is the induction equation

$$\frac{\partial \vec{b}}{\partial t} - \nabla \times (\vec{v} \times \vec{B}_0) = 0. \tag{7.96}$$

The horizontal component of the above equation is

$$\frac{\partial b_n}{\partial t} - B_0\frac{\partial v_n}{\partial s} = 0 . \tag{7.97}$$

We use the above equations to derive one-dimensional wave equations for the variables $v_n(s,t)$ and $b_n(s,t)$.

7.2.2 Wave equations and conditions for propagating wave solutions

We combine Eqs (7.95) and (7.97), and derive the following wave equations

$$\frac{\partial^2 v_n}{\partial t^2} - c_k^2(s)\frac{\partial^2 v_n}{\partial s^2} - c_k^2(s)\left(\frac{B_o'}{B_o}\right)\frac{\partial v_n}{\partial s} = 0 \ , \tag{7.98}$$

and

$$\frac{\partial^2 b_n}{\partial t^2} - c_k^2(s)\frac{\partial^2 b_s}{\partial s^2} - c_k^2(s)\left[2\frac{c_k'}{c_k} - \frac{B_o'}{B_o}\right]\frac{\partial b}{\partial s} = 0 \ . \tag{7.99}$$

These equations show that the behavior of the wave variables v_n and b_n in time and space depends on the local values of both c_k and gradient B_o, and that the behavior of b_n is also affected by a gradient of c_k. Since the wave equations have different forms, the behavior of the wave variables v_n and b_n is also different.

7.2.3 Transformed wave equations and conditions for wave propagation

Let us introduce a new variable given by

$$d\tau = \frac{ds}{c_k(s)} \ . \tag{7.100}$$

We express Eqs (7.98) and (7.99) in terms of the new variable τ and obtained the following transformed wave equations

$$\left[\frac{\partial^2}{\partial t^2} - \frac{\partial^2}{\partial \tau^2} + \left(\frac{c_k'}{c_k} - \frac{B_o'}{B_o}\right)\frac{\partial}{\partial \tau}\right]v_n(\tau, t) = 0 \ , \tag{7.101}$$

and

$$\left[\frac{\partial^2}{\partial t^2} - \frac{\partial^2}{\partial \tau^2} - \left(\frac{c_k'}{c_k} - \frac{B_o'}{B_o}\right)\frac{\partial}{\partial \tau}\right]b_n(\tau, t) = 0 \ , \tag{7.102}$$

where $c_k = c_k(\tau)$, $H = H(\tau)$ and $c_k' = dc_k/d\tau$.

To write the transformed wave equations into their standard forms, we use

$$v_n(\tau, t) = v(\tau, t) \exp\left[+\frac{1}{2}\int^\tau \left(\frac{c_k'}{c_k} - \frac{B_o'}{B_o}\right) d\tau\right] , \qquad (7.103)$$

and

$$b_n(\tau, t) = b(\tau, t) \exp\left[-\frac{1}{2}\int^\tau \left(\frac{c_k'}{c_k} - \frac{B_o'}{B_o}\right) d\tau\right] , \qquad (7.104)$$

and obtain

$$\left[\frac{\partial^2}{\partial t^2} - \frac{\partial^2}{\partial \tau^2} + \Omega_{cr,v}^2(\tau)\right] v(\tau, t) = 0 , \qquad (7.105)$$

and

$$\left[\frac{\partial^2}{\partial t^2} - \frac{\partial^2}{\partial \tau^2} + \Omega_{cr,b}^2(\tau)\right] b(\tau, t) = 0 , \qquad (7.106)$$

where

$$\Omega_{cr,v}^2(\tau) = \frac{3}{4}\left(\frac{c_k'}{c_k}\right)^2 - \frac{1}{2}\left(\frac{c_k'}{c_k}\right)\left(\frac{B_o'}{B_o}\right) - \frac{1}{4}\left(\frac{B_o'}{B_o}\right)^2 - \frac{1}{2}\frac{c_k''}{c_k} + \frac{1}{2}\left(\frac{B_o''}{B_o}\right) , \qquad (7.107)$$

and

$$\Omega_{cr,b}^2(\tau) = -\frac{1}{4}\left(\frac{c_k'}{c_k}\right)^2 - \frac{1}{2}\left(\frac{c_k'}{c_k}\right)\left(\frac{B_o'}{B_o}\right) + \frac{3}{4}\left(\frac{B_o'}{B_o}\right)^2 + \frac{1}{2}\frac{c_k''}{c_k} - \frac{1}{2}\left(\frac{B_o''}{B_o}\right) , \qquad (7.108)$$

with $c_k'' = d^2 c_k / d\tau^2$. The frequencies $\Omega_{cr,v}$ and $\Omega_{cr,b}$ are known as the critical frequencies (Musielak, Fontenla, & Moore, 1992; Musielak et al. 2006). Note that in the thin flux tube limit the critical frequencies become

$$\Omega_{u,thin}^2(\tau) = -\frac{1}{4}\left(\frac{B_o'}{B_o}\right)^2 + \frac{1}{2}\frac{B_o''}{B_o} \text{ and } \Omega_{b,thin}^2(\tau) = \frac{3}{4}\left(\frac{B_o'}{B_o}\right)^2 - \frac{1}{2}\frac{B_o''}{B_o}.$$

Now for thin flux tubes $B_o = B_{oo}\exp(-z/2H)$ (see Chapter 6). Thus we obtain $\Omega_{u,thin}^2 = \Omega_{b,thin}^2 = c_k^2/16H^2$, which is Spruit's cutoff frequency.

We make the Fourier transform in time and write Eqs (7.105) and (7.106) as

$$\left[\frac{d^2}{d\tau^2} + \omega^2 - \Omega_{cr,v}^2(\tau)\right] v(\tau) = 0 , \qquad (7.109)$$

and

$$\left[\frac{d^2}{d\tau^2} + \omega^2 - \Omega_{cr,b}^2(\tau)\right] v(\tau) = 0 . \qquad (7.110)$$

Using the oscillation theorem (see Chapter 3) and comparing the above equations to Euler's equation (see Chapter 3), we obtain the following conditions for the wave propagation

$$\omega^2 - \Omega_{cr,v}^2(\tau) > \frac{1}{4\tau^2} \ , \tag{7.111}$$

and

$$\omega^2 - \Omega_{cr,b}^2(\tau) > \frac{1}{4\tau^2} \ . \tag{7.112}$$

According to the results of Appendix B, the turning-point frequencies are

$$\Omega_{tp,v}^2(\tau) = \Omega_{cr,v}^2(\tau) + \frac{1}{4\tau^2} \ , \tag{7.113}$$

and

$$\Omega_{tp,b}^2(\tau) = \Omega_{cr,b}^2(\tau) + \frac{1}{4\tau^2} \ . \tag{7.114}$$

We choose the cutoff as the largest among the turning point frequencies.

7.2.4 Exponential model

A single and isothermal magnetic-flux tube is considered to be wide when its horizontal magnetic field is nonuniform, which means that each magnetic-field line has different physical properties in the horizontal direction. Let us assume that this tube is approximated by a simple model in which the Alfvn velocity varies exponentially along a given field line; the model was originally considered by Hollweg (1981), and we shall use it here to determine the cutoff frequency for transverse tube waves propagating in this model.

We have $c_k = c_{koo}e^{s/H_c}$ and $B_o = B_{oo}e^{-s/H_B}$, where H_c and H_B are the characteristic scale heights of transverse wave velocity c_k and magnetic field B_o respectively.

To calculate $\tau(s)$, we use

$$d\tau = \int_s^{s_o} \frac{ds}{c_k(s)} \tag{7.115}$$

and obtain $\tau = -\frac{H_c}{c_k(s)} + \tau_o$ where τ_o is a integration constant and its value is $H_c/c_k(s_o)$.

Now the critical frequencies are calculated by using Equations (7.107) and (7.108), and we obtain

$$\Omega_u^2(\tau) = \frac{1}{4(\tau - \tau_o)^2}\left[\frac{H_c^2}{H_B^2} - 1\right] ,\tag{7.116}$$

and

$$\Omega_b^2(\tau) = \frac{1}{(\tau - \tau_o)^2}\left[\frac{1}{4}\frac{H_c^2}{H_B^2} + \frac{H_c}{H_B} + \frac{3}{4}\right] .\tag{7.117}$$

As Ωb^2 is larger than Ωu^2 we take the cutoff as $\Omega_{cutoff} = \Omega_{tp,b}$ where $\Omega_{tp,b}$ is the turning point frequency for b. So $\Omega_{cutoff}^2(\tau) = \Omega_b^2 + \frac{1}{4\tau^2}$ or

$$\Omega_{cutoff}^2(s) = \frac{c_k^2(s)}{H_c^2}\left(\frac{3}{4} + \frac{H_c}{H_B} + \frac{H_C^2}{4H_B^2}\right) + \frac{1}{4}\frac{c_k^2(s_o)}{[c_k(s) - c_k(s_o)]^2} .\tag{7.118}$$

Now we can take $H_c = mH_p$ and $H_B = nH_p$ where m,n are integers and H_p is the pressure scale height. Here $m \neq n$ as otherwise there will be no density gradient which is not the case for stratified atmosphere.

Now $c_k^2 = B_o^2/4\pi\rho_o$. Differentiating both sides with respect to s we get

$$-\frac{1}{H_c} + \frac{1}{H_B} = -\frac{1}{2}\frac{(\rho_o + \rho_e)'}{(\rho_o + \rho_e)} .\tag{7.119}$$

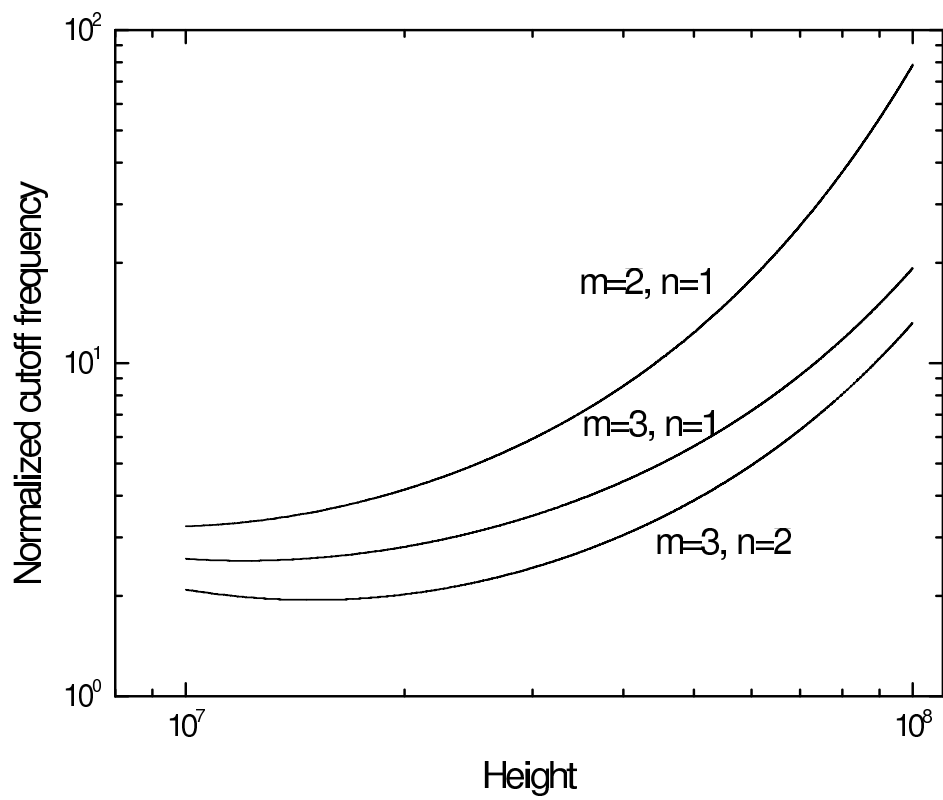From the above equation we can see that $H_c > H_B$ i.e. $m > n$ as the right hand side is always positive.

Figure 7.5. Normalized cutoff frequencies vs. the distance.

CHAPTER 8

SUMMARY AND FUTURE WORK

To establish theoretical bases for studying the propagation and generation of waves in the solar atmosphere, a general method to determine cutoff frequencies for waves propagating in inhomogeneous media was developed and apply to different wave motions observed in the solar atmosphere. Specifically, the cutoff frequencies for acoustic waves propagating in the non-isothermal solar atmosphere, and for torsional and transverse waves propagating along non-isothermal (thin and thick) magnetic flux tubes. Moreover, the method was also used to extent the original Lighthill theory of sound generation to a non-isothermal medium. The results obtained in this PhD dissertation shed a new light on the problem of heating and excitation of oscillations in the inhomogeneous solar atmosphere.

One of the most important results of this PhD dissertation is the extension of the concept of cutoff frequency to inhomogeneous atmospheres. To achieve this, a general method to determine the cutoff frequency is described. The method is based on integral transformations that give new forms of wave equations, and it uses the oscillation and turning-point theorems to obtain the cutoff frequency without formally solving the wave equations. The main result is that the derived cutoff frequency is a local quantity and that its value at a given atmospheric height determines the frequency that waves must have in order to be propagating at this height.

To determine the propagation conditions for acoustic waves in the non-isothermal solar atmosphere described by the semi-empirical VAL C model, the method was used to obtain the resulting acoustic cutoff frequency. This new cutoff frequency general-

128

ized Lamb's acoustic cutoff frequency that was obtained for an isothermal atmosphere. In Lamb's approach, the cutoff frequency was defined as the ratio of sound speed to twice density (pressure) scale height and it was the same in the entire isothermal atmosphere. However, the new cutoff depends on gradients of the sound speed and, as a result, it is a local quantity. Acoustic waves freely propagating through the solar atmosphere described by the VAL C model excite atmospheric oscillations with the frequency that coincides with this local acoustic cutoff frequency.

The original Lighthill theory of sound generation was developed for an uniform medium. To determine the effects of temperature gradients on the rate of the acoustic wave generation in Lighthill's theory, the method was used to extend Lighthill's theory to a non-isothermal medium. The model of this medium was assumed to be simple enough so that that analytical solutions were obtained. The solutions were then used to study the effects caused by one specific temperature gradient on the wave generation. The results obtained in this PhD dissertation showed that a temperature gradient in the region of wave generation is responsible for the origin of the monopole and dipole sources of acoustic emission, and that the acoustic cutoff frequency arose as a result of the temperature gradient.

Studies of torsional tube waves propagating inside non-isothermal thin and isothermal thick magnetic flux tubes showed that gradients of temperature and magnetic fields were responsible for the origin of cutoff frequencies for these waves. The fact that the propagation of torsional waves along a thin and isothermal flux tube was cutoff-free was also demonstrated. An important result is that the cutoff frequencies are local quantities, which means that torsional tube waves must have their frequencies higher than these cutoffs at a given height in the solar atmosphere given by the VAL C model in order to reach this height and be propagating waves at the height. Comparison of the obtained results to the observational data showed that

the detected torsional waves with periods in the interval $[126, 368]$ s were propagating waves at the base of the solar atmosphere model, and that in the middle and upper chromosphere the interval became $[126, 314]$ s and $[126, 208]$ s, respectively. This decrease in the wave period interval restricts periods of torsional tube waves that can effectively carry their energy to the solar chromosphere and corona.

The method was also used to the local cutoff frequency for transverse waves propagating along non-isothermal thin and isothermal thick magnetic flux tubes. The obtained results extend Spruit's global cutoff frequency to these inhomogeneous flux tubes. The resulting local cutoff frequency was calculated as a function of height in the VAL C model and compared it to Spruit's cutoff frequency that was treated as a height-dependent quantity. The comparison showed that the local cutoff always exceeded Spruit's cutoff and that the differences were especially prominent in the upper parts of the model, where the thin flux tube approximation may not valid any longer. On the other hand, the differences in the solar photosphere, where the thin flux tube approximation is valid, may be important for the energy carried by transverse tube waves from the solar convection zone, where the waves are generated, to the overlying solar atmosphere, where the wave energy is deposited.

The cutoff frequencies for transverse and torsional tube waves calculated for the VAL C model give constraints on the range of frequencies of these waves that are propagating in different parts of the solar atmosphere. Using these constraints, one can determine the role played by transverse and torsional tube waves in the heating of the solar atmosphere. Therefore, the results obtained in this PhD dissertation can be used to determine the natural frequency of the solar atmosphere inside thin and non-isothermal flux tubes and the effects of temperature gradients on the excitation of atmospheric oscillations inside non-isothermal thin and isothermal thick solar magnetic flux tubes.

8.1 Future Work

The effects of the temperature gradient on the propagation conditions for longitudinal tube waves are being now studied as an extension of the work described in this PhD dissertation.

Theoretical models of the solar atmosphere require the input of the acoustic and magnetic wave energy fluxes produced by the solar convective motions. The so-called "heating gaps" discovered by Fawzy et al. (2002a, b, c) require additional sources of mechanical energy. One possible source is the energy carried by torsional tube waves. We are developing a general theory describing the interaction between a thin magnetic flux tube with the external turbulent flows and calculating the resulting wave energy fluxes. These fluxes can be used in theoretical models of the solar chromosphere.

APPENDIX A

CALCULATION OF SOURCE FUNCTION

$$S_{turb}(\omega, k_i) = \frac{-1}{(2\pi)^4} \int (\rho_0 u_i u_j)(\frac{\partial^2}{\partial \tau_i \partial \tau_j} + c'_{si}\frac{\partial}{\partial \tau_j})e^{I_c}e^{-i(\omega t - k_i \tau_i)}d^3\tau_i\, dt$$

$$= \frac{-1}{(2\pi)^4} \int (\rho_0 u_i u_j)f(\tau_i, t)d^3\tau_i\, dt \tag{A.1}$$

$$f(t, \tau_i) = (\frac{\partial^2}{\partial \tau_i \partial \tau_j} + c'_{si}\frac{\partial}{\partial \tau_j})e^{I_c}e^{-i(\omega t - k_i \tau_i)}$$

$$= [-k_i k_j + i\frac{1}{2}k_j c'_{si} + i\frac{1}{2}k_i c'_{sj} + \frac{1}{4}c'_{si}c'_{sj} + c'_{si}ik_j + \frac{1}{2}c'_{si}c'_{sj}]e^{I_c}e^{-i(\omega t - k_i \tau_i)}$$

$$= [-k_i k_j + \frac{3}{4}c'_{si}c'_{sj} + i(\frac{1}{2}k_i c'_{sj} + \frac{3}{2}k_j c'_{si})]e^{I_c}e^{-i(\omega t - k_i \tau_i)} \tag{A.2}$$

Substituting Eq. (A.2) into Eq. (A.1) results in

$$S_{turb}(\omega, k_i) = \frac{1}{(2\pi)^4} \int \{k_i k_j - \frac{3}{4}c'_{si}c'_{sj} - i[\frac{1}{2}c'_{sj}k_i + \frac{3}{2}c'_{si}k_j]\}(e^{I_c}\rho_0 u_i u_j)$$

$$e^{-i(\omega t - k_i \tau_i)}d^3\tau_i\, dt$$

Comparing the last Eq. with the following Eq

$$S_{turb}(\omega, k_i) = \frac{1}{(2\pi)^4} \int S_{turb}(t, \tau_i)e^{-i(\omega t - k_i \tau_i)}d^3\tau_i\, dt$$

results in

$$S_{turb}(t, \tau_i) = \{k_i k_j - \frac{3}{4}c'_{si}c'_{sj} - i[\frac{1}{2}c'_{sj}k_i + \frac{3}{2}c'_{si}k_j]\}(e^{I_c}\rho_0 u_i u_j)$$

APPENDIX B

CALCULATION OF THE EMITTED FLUX

Time averaging of the flux requires the frequency of both factors, $\vec{p}$ and $\vec{u}$, to be the same. Hence $k_i' = k_i'' = k_i$. Substituting (5.29) into (5.28) and performing the required algebra, the Flux turns out to be:

$$\vec{F}(k_i) = \lim_{T \to \infty} \frac{1}{T} \int_{-T/2}^{T/2} dt \frac{1}{\rho_0 c_s} \int \frac{k_i}{\omega''} \frac{S_{turb}(\omega', k_i) S_1^*(\omega'', k_i) e^{i(\omega'-\omega'')t} \, d^6 k_i d\omega' d\omega''}{\{-\omega'^2 + k_i^2 + \Omega_i^2\}\{-\omega''^2 + k_i^2 + \Omega_i^2\}}$$

where the "*" denotes a conjugate. Using $\int_{-\infty}^{\infty} e^{i(\omega'-\omega'')t} dt = 2\pi \delta(\omega' - \omega'')$ to integrate by time, the equation is reduced to:

$$\vec{F}(k_i) = \lim_{T \to \infty} \frac{2\pi}{T} \frac{1}{\rho_0 c_s} \int (\frac{k_i}{\omega''}) \frac{S_{turb}(\omega', k_i) S_{turb}^*(\omega'', k_i) \delta(\omega' - \omega'') d^6 k_i \, d\omega' d\omega''}{\{-\omega'^2 + k_i^2 + \Omega_i^2\}\{-\omega''^2 + k_i^2 + \Omega_i^2\}}$$

Integrating by $d\omega''$ and using $\vec{F}(k_i) = \int \vec{F}(\omega', k_i) d\omega'$, the expression for $\vec{F}(\tau_i)$ is evaluated as:

$$\vec{F}(\omega, k_i) = \lim_{T \to \infty} \frac{2\pi}{T} \frac{1}{\rho_0 c_s} \int (\frac{k_i}{\omega}) \frac{S_{turb}(\omega, k_i) S_{turb}^*(\omega, k_i) d^3 k_i d^3 k_i}{\{-\omega^2 + k_i^2 + \Omega_i^2\}\{-\omega^2 + k_i^2 + \Omega_i^2\}}. \tag{B.1}$$

B.1   Appendix C

Eq. (5.38) can then be rewritten by letting $wv = k_i u_i = k_1 u_1 + k_2 u_2 + k_3 u_3$.

$$\Upsilon(\tau_i, t) = w^4 < v'^2 v''^2 > -3\Omega_0^2 w^2 < v'^2 u_3''^2 > -3\Omega_0^2 w^2 < v''^2 u_3'^2 >$$

$$+9\Omega_0^4 < u_3'^2 u_3''^2 > +16\Omega_0^2 w^2 < v'v'' u_3' u_3'' >$$

Making use of (5.39), each term in the above equation can be simplified as shown in the next five equations. The resulting spectral efficiency turns out to be (5.40) after taking $< v'u_3'' >^2 = < v''u_3' >^2$.

$$< v'v'v''v'' >= 2 < v'v'' >^2$$

$$< v'v'u_3''u_3'' >= 2 < v'u_3'' >^2$$

$$< v''v''u_3'u_3' >= 2 < v''u_3' >^2$$

$$< u_3'u_3'u_3''u_3'' >= 2 < u_3'u_3'' >^2$$

$$< v'v''u_3'u_3'' >=< v'v'' >< u_3'u_3'' > + < v'u_3'' >^2$$

REFERENCES

[1] J. L. Linsky, *Mechanisms of Chromospheric and Coronal Heating.* Springer, 1991.

[2] P. Foukal, *Solar Astrophysics.*

[3] R. G. Athay, *Multiwavelength Astrophysics.*

[4] L. Golub, *Mechanisms of Chromospheric and Coronal Heating.*

[5] L. Golub and J. M. Pasachoff, *The Solar Corona.*

[6] M. Stix, *The Sun: An Introduction.*

[7] C. J. Schrijver and A. M. Title, *AP. J.*, vol. L165, p. 597, 2003.

[8] L. S. Anderson and R. G. Athay, *AP. J.*, vol. 211, p. 336, 1989.

[9] E. R. Priest, J. F. Heyvaerts, and A. M. Title, *AP. J.*, vol. 533, p. 576, 2002.

[10] E. N. Parker, *Cosmic Magnetic Fields: Their Origin and Their Activity.*

[11] E. R. Priest, *Solar Magnetohydrodynamics.*

[12] S. K. Solanki, *Space Sci. Rev.*, vol. 1, p. 63, 1993.

[13] S. H. Saar, "Stellar surface structure," *ASP Conf. Ser.*, pp. 154–211, 1996.

[14] ——, "Cool stars, stellar systems, and the sun," *ASP Conf. Ser.*, pp. 154–321, 1998.

[15] R. Cameron and D. Galloway, *MNRAS*, vol. 358, p. 1025, 2005.

[16] U. Narain and P. Ulmschneider, *Space Sci. Rev.*, vol. 453, p. 75, 1996.

[17] P. Ulmschneider and Z. E. Musielak, *ASP Conf. Ser.*, pp. 286–363, 2003.

[18] Z. E. Musielak, R. Rosner, R. F. Stein, and P. Ulmschneider, *Ap. J.*, vol. 423, p. 474, 1994.

[19] M. Cuntz, P. Ulmschneider, and Z. E. Musielak, *Ap. J.*, vol. L117, p. 493, 1998.

136

[20] M. Cuntz, W. Rammacher, P. Ulmschneider, Z. E. Musielak, and S. H. Saar, *Ap. J.*, vol. 522, p. 1050, 1999.

[21] P. Ulmschneider, D. Fawzy, Z. E. Musielak, and K. Stepien, *Ap. J.*, vol. L1673, p. 559, 2001.

[22] D. Fawzy, W. Rammacher, P. Ulmschneider, Z. E. Musielak, and K. Stepien, *Astron. Astrophys.*, vol. 386, p. 971, 2002a.

[23] D. Fawzy, P. Ulmschneider, K. Stepien, and Z. E. M. W. Rammacher, *Astron. Astrophys.*, vol. 386, p. 983, 2002b.

[24] J. A. Bonet, I. Marquez, J. S. Almeida, I. Cabello, and V. Domingo, *Ap. J.*, vol. 431, p. 687, 2008.

[25] D. B. Jess, M. Mathioudakis, R. Erdelyi, P. J. Crokett, F. P. Keenan, and D. J. Christian, *Science*, vol. 323, p. 1582, 2009.

[26] S. Wedemeyer-Bohm, O. Steiner, J. Bruls, W. Rammacher, and Coimbra, *Solar Physics Meeting on Physics of Chromospheric Plasmas*, 2007.

[27] C. J. Schrijver, A. M. Title, A. A. van Ballegooijen, H. J. Hagenaaar, and R. A. Shine, *AP. J.*, vol. 424, p. 487, 1997.

[28] E. R. Priest, D. W. Longcope, and J. F. Heyvaerts, *AP. J.*, vol. 624, p. 1057, 2005.

[29] T. M. Brown, B. M. Mihalas, and J. Rhodes, *Physics of the Sun*, vol. 1, p. 177, 1987.

[30] R. G. M. Rutten and H. Uitenbroek, *Sol. Phys.*, vol. 15, p. 134, 1991.

[31] B. W. Lites, R. J. Rutten, and W. Kalkofen, *Ap. J.*, vol. 345, p. 414, 1993.

[32] W. Kalkofen, *Ap. J.*, vol. L145, p. 486, 1997.

[33] W. Curdt and P. Heinzel, *Ap. J.*, vol. L95, p. 503, 1998.

[34] R. T. J. McAteer, P. T. Gallagher, D. R. Williams, M. Mathioudakis, D. S. Bloomfield, K. J. H. Phillips, and F. P. Keenan, *Ap. J.*, vol. 587, p. 806, 2003.

[35] D. E. McKenzie and D. J. Mullan, *Sol. Phys.*, pp. 127–176, 1997.

[36] T. Kudoh and K. Shibata, *Ap. J.*, vol. 493, p. 514, 1999.

[37] B. D. Pontieu, R. Erdelyi, and A. G. D. Wijn, *Ap. J.*, vol. L63, p. 595, 2003.

[38] B. D. Pontieu, R. Erdelyi, and I. D. Moortel, *Ap. J.*, vol. L61, p. 624, 2005.

[39] B. Roberts, *Geophys. Astrophys. Fluid Dynamics*, vol. 62, p. 83, 1991.

[40] T. Saito, T. Kudoh, and K. Shibata, *Ap.J.*, vol. 554, p. 1151, 2001.

[41] S. S. Hasan, *Advances in Space Research*, vol. 42, p. 86, 2008.

[42] B. Fleck and F. Schmitz, *Astron. Astrophys.*, vol. 235, p. 250, 1991.

[43] H. Lamb, *Proc.London Math. Soc.*, vol. 7, p. 122, 1909.

[44] W. Kalkofen, P. Rossi, G. Bodo, and S. Massaglia, *Astron. Astrophys.*, vol. 284, p. 976, 1994.

[45] M. V. Uexkull and F. Kneer, *Astron. Astrophys.*, vol. 252, p. 294, 1995.

[46] M. Carlsson and R. F. Stein, *Ap. J.*, vol. 481, p. 500, 1997.

[47] K. Wilhelm and W. Kalkofen, *Astron. Astrophys.*, vol. 408, p. 1137, 2003.

[48] Z. E. Musielak and P. Ulmschneider, *Astron. Astrophys.*, vol. 725, p. 400, 2003a.

[49] S. S. Hasan and W. Kalkofen, *Ap.J.*, vol. 519, p. 899, 1999.

[50] Z. E. Musielak and P. Ulmschneider, *Astron. Astrophys.*, vol. 406, p. 1057, 2003b.

[51] J. E. Vernazza, E. H. Avrett, and R. Loeser, *Ap. J.*, vol. 45, p. 635, 1981.

[52] M. J. Lighthill, *Proc. Roy. Soc.*, vol. A211, p. 564, 1952.

[53] R. F. Stein, *Solar Phys.*, vol. 2, p. 385, 1967.

[54] H. Lamb, *Hydrodynamics.*

[55] F. Schmitz and B. Fleck, *Astron. Astrophys.*, vol. 337, p. 487, 1998.

[56] G. B. Whitman, *Linear and Nonlinear Waves.* New York: Wiley, 1974.

[57] H. C. Spruit, *Astron. Astrophys.*, vol. 98, p. 155, 1981.

[58] ——, *Sol. Phys.*, vol. 3, p. 75, 1982.

[59] R. J. Defouw, *Ap. J.*, vol. 209, p. 226, 1976.

[60] I. C. Rae and B. Roberts, *Ap.J.*, vol. 256, p. 761, 1982.

[61] Z. E. Musielak, R. Rosner, H. P. Gail, and P. Ulmschneider, *Ap. J.*, vol. 44, p. 865, 1995.

[62] J. V. Hollweg, *Advances in Space Plasma Physics*, p. 77, 1985.

[63] ——, "Physics of magnetic flux ropes," *Geophys. Monograph*, vol. 58, p. 23, 1990.

[64] A. Ferriz-Mas, M. Schüssler, and V. Anton, *Astron. Astrophys.*, vol. 210, p. 425, 1989.

[65] A. Ferriz-Mas and M. Schüssler, *Ap. J.*, vol. 433, p. 852, 1994.

[66] S. S. Hasan, *Lectures Notes in Physics*, vol. 619, p. 173, 2003.

[67] M. Noble, Z. E. Musielak, and P. Ulmschneider, *Astron. Astrophys.*, vol. 409, pp. 1085–1095, 2003.

[68] J. V. Hollweg, *Sol. Phys.*, vol. 56, p. 305, 1978.

[69] ——, *Sol. Phys.*, vol. 21, p. 70, 1981.

[70] ——, *Ap. J.*, vol. 389, p. 731, 1992.

BIOGRAPHICAL STATEMENT

Swati Routh is originally from India. Since her junior high school days she set her mind upon studying Physics and decided to pursue Astrophysics as a career in college. After completing Masters in Physics from University of Calcutta in India Swati joined as junior research fellow at S.N.Bose Center for Basic Sciences in Calcutta, India. However she set her sight on serious research in theoretical Astrophysics and decided to go to US for further education. In 2004 Swati came to University of Texas at Arlington, USA, to pursue her goal. She finished MS majoring in physics with a thesis on solar physics,having worked under the advisement of Dr.Zdzislaw Musielak. During her time as MS/PhD student she has published several important papers on Solar and stellar physics. She was awarded by the College of Science for outstanding academic achievement in 2005 through 2007. She is also recipient of the John D. McNutt Memorial Scholarship by the Department of Physics for 2005-2006. Swati has been a Deans Honor student and was also awarded for excellence in research in 2009. Finally she defended her doctoral dissertation in November 09 and is awaiting her diploma. Her current research interest is theoretical study of magnetical wave phenomena in solar and stellar atmosphere. Swati will soon begin post doctoral assignment at JILA,University of Colorado at Boulder where she will be working with the Juri Toomre Group. Swati has several refereed and non-refereed publication in reputed scientific journals and conferences. Beyond graduate school she wishes to engage in cutting edge research in Solar Physics and Astrophysics.